PROCEEDINGS

OF THE

INDIAN NATIONAL SCIENCE ACADEMY

(*Formerly* NATIONAL INSTITUTE OF SCIENCES OF INDIA)

PART A — PHYSICAL SCIENCES

No 4 — July 1970 — Vol 36

INDIAN NATIONAL SCIENCE ACADEMY
NEW DELHI

Price : Rupees Eleven and Ninety Paise

P 270

Issued 28 December 1970

Council of the Indian National Science Academy, 1970

President:

Dr. Atma Ram, D.Sc., *New Delhi.*

Vice-Presidents:

Dr. R. K. Asundi, Ph.D., *Bombay.*
Dr. K. Ramiah, D.Sc., *Bhubaneswar.*

Treasurer:

Prof. S. Rangaswami, Ph.D., *Delhi.*

Foreign Secretary:

Prof. A. G. Jhingran, Ph.D., *Delhi.*

Secretaries:

Dr. B. D. Nag Chaudhuri, Ph.D., *New Delhi.*
Dr. M. S. Swaminathan, Ph.D., *New Delhi.*

Editor of Publications:

Prof. B. R. Seshachar, D.Sc., *Delhi.*

Members of Council:

Prof. S. V. Anantakrishnan, Ph.D., *Madras.*
Prof. F. C. Auluck, Ph.D., D.Sc., *Delhi.*
Prof. P. L. Bhatnagar, D.Phil., D.Sc., *Jaipur.*
Prof. R. N. Chaudhuri, M.B., F.R.C.P., *Calcutta.*
Dr. N. N. Das Gupta, Ph.D., *Calcutta.*
Dr. S. Datta, D.Sc., *Calcutta.*
Dr. M. L. Dhar, Ph.D., *Lucknow.*
Prof. N. R. Dhar, D.Sc., *Allahabad.*
Dr. C. Gopalan. Ph.D., *Hyderabad.*
Dr. K. Jacob, D.Sc., *New Delhi.*
Prof. P. K. Kichlu, D.Sc., *New Delhi.*
Dr. A. Lahiri, Ph.D., *Dhanbad.*
Dr. P. N. Mehra, D.Sc., *Chandigarh.*
Prof. R. S. Mishra, Ph.D., D.Sc., *Varanasi.*
Dr. N. K. Panikkar, D.Sc., *Panaji (Goa).*
Dr. Bhrahm Prakash, Ph.D., D.Sc., *Bombay.*
Dr. J. C. Ray, M.D., *Calcutta.*
Dr. S. S. Shrikhande, Ph.D., *Bombay.*
Prof. S. M. Sircar, Ph.D., *Calcutta.*
Prof. C. V. Subramanian, Ph.D., D.Sc., *Madras.*
Dr. M. J. Thirumalachar, Ph.D., D.Sc., *Poona.*
Prof. T. R. Seshadri, Ph.D., F.R.S., *Delhi* (*Past President*, ex-officio).

MERCUROMETRIC INVESTIGATIONS FOR BASE-METAL EXPLORATION AND THE ANALYTICAL TECHNIQUES

by SACHINATH MITRA,* *Resources Division, Planning Commission, New Delhi 1*

(Communicated by M. S. Krishnan, F.N.I.)

(*Received 28 February 1970*)

Mercury occurs as trace element in almost all rocks, and because of its chalcophile nature it occurs as a common associate of the base metals and this property has effectively been exploited in the exploration of these metals. Mercury having far greater dispersion than the base metals is used as an indicator element in the geochemical exploration programme. In this paper earlier works on mercurometric studies done at several places in the world, particularly in the U.S.S.R. and the U.S.A., have been reviewed along with the geochemical property of mercury.

The author undertook investigations in this line on the Cu-Pb-Zn-Sn mineralized area of Devonshire lying between Bodmin Moor and the Dartmoor granites. A fair pattern of mercury dispersion in the stream sediments observed following the E–W. base metal mineralization. Values as high as 7 ppm were observed near the mineralized zones. The agricultural soils, however, of the West Devon gave values of 5–15 ppm to another group of workers.

For the analyses an ultraviolet absorption meter of the Imperial College was used and the precision of the analyses and the problems of error as developed into for the effects of various factors such as sampling technique, personnel, day temperature, voltage, storage time, etc., were determined.

Precision of the analyses was determined analysing twelve test samples of the U.S.G.S. and the accuracy of assaying was in the 7–8% range at 95% confidence level. Experiments on the quantum of mercury liberation with temperature were also carried out.

A circular averaging technique akin to the rolling mean was designed by the author in making the Hg-dispersion map of the area, which very effectively eliminated the geochemical 'noise' and also the local 'drifts'. A study of the general trend relation of the Hg-dispersion in stream sediments with respect to the geology of the area reveals that an anomalous zone runs almost E–W. roughly parallel to the Cu-Pb-Zu-Sn mineralization; but an over-all drift of the broad anomaly towards the north has become conspicuous. This drift is postulated by the author as due to solifluxion since the Pleistocene or a little earlier.

Mercury rarely forms large deposits and common rocks apparently do not contain any mercury mineral. Its presence, however, in different rocks has been proved beyond doubt and the average content in g/ton has been calculated as below (Table I).

---

* On leave from Jadavpur University, Calcutta 32.

TABLE I

	Hg, g/ton
Igneous rocks	
Gabbro (Stock and Cucuel 1934) ..	0·079
Gabbro (Preuss 1941)	0·1
Basic effusives (Saukov 1946)	0·09
Granite (Stock and Cucuel 1934) ..	0·058
Granite (Preuss 1941)	0·01
Acid intrusives (Saukov 1946)	0·064
Sedimentary rocks	
Sandstone, average (Preuss 1941) ..	0·1
Sandstone (Stock and Cucuel 1934) ..	0·033
Shales, average (Stock and Cucuel 1934) ..	0·51
Shales, average (Preuss 1941)	0·30
Limestones (Stock and Cucuel 1934) ..	0·033

(Source: Rankama and Sahama (1950))

Geochemically mercury maintains a chalcophile character. The chalcophile nature of mercury, according to Fersman, is indicated by its position among the elements of the sulphide deposits and by its atomic volume curve. At magmatic temperatures, according to Goldschmidt (1954), the redox potential of the ferrous iron in magmas, in most cases, is sufficient to transform mercury compounds into mercury and thus force the metal into gaseous exhalation products, where it can again combine with sulphur.

Besides native mercury and sulphide of mercury as cinnabar, selenide, tiemannite and telluride, coloradoite have been found in nature mainly with the concentration of selenium and tellurium connected with gold deposits. Silver and palladium amalgams have also been observed in nature. Mercury is one of the most typical telemagmatic metals. The sulpho-salts of arsenic and antimony tetrahedrite, with up to 17% Hg, may sometimes contain

TABLE II

	No. of samples	Range ppm	Average ppm	Median ppm
Sphalerite ..	11	5–3400	690	150
Galena ..	10	0·5–200	39	2
Pyrite ..	3	0·5–10	4	3
Bournonite ..	5	0·1–5	2·2	2
Barite ..	7	0·03–4	2	2
Siderite ..	4	0·01–5	1·7	0·8
Calcite ..	12	0·01–6	0·8	0·3
Ores ..	1662	4·4–200	64	40
Normal rocks ..		0·03–0·1	0·06	

(Ref. : Hawkes and Williston 1962)

considerable amounts of mercury. Livingstonite, HgS, $2Sb_2S_3$, is sometimes associated with sulpho-salts. The oxide HgO (montroydite) and a number of selenides, halogenides and oxy-chlorides of mercury occur as minerals. A study of the contents of mercury in the minerals of the lead-zinc ores from Central Asia (Fergana Karatau and Lyakan lead-zinc districts, Turkestan) reveals a considerable range of values with high mean and median values of mercury (Table II).

According to Saukov (1946), mercury, as Hg^{2+} ion (radius 1·12 kX), may replace Ca^{2+} (radius 1·06 kX), although this diadochy is very limited. Another possibility is the $Hg^{2+}—Ba^{2+}$ diadochy, which explains the presence of mercury in concentration up to 0·5% Hg in barytes.

Table I shows that shales contain a greater amount of mercury than igneous rocks. Goldschmidt (1954) assumed that Hg like B, S and Cl has been introduced into the sea by volcanism. The cycle of mercury in the crust of the earth is assumed to be as shown in Fig. 1.

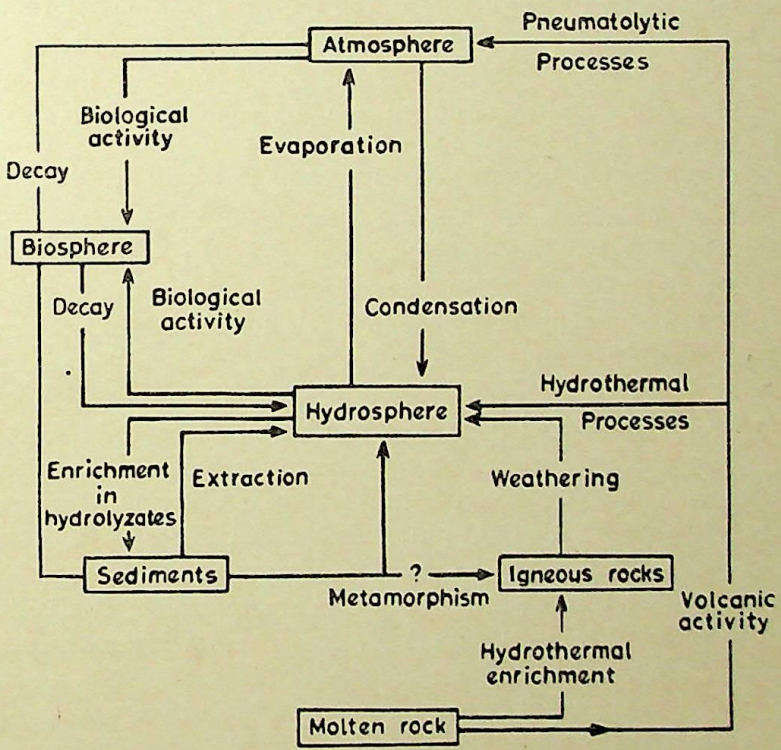

FIG. 1. Geochemical cycle of mercury.

Although mercury belongs to the Group IIB of the periodic table, together with zinc and cadmium, its chemical properties differ considerably from others. It is the only metal which is liquid at normal temperature,

while its volatility is unparalleled by any other metallic element. Table III shows a comparative assessment of the vapour pressures of magnesium, zinc, cadmium and mercury at 200 °C and 600 °C.

TABLE III

Temp. °C	Vapour pressure			
	Mg	Zn	Cd	Hg
200	10^{-5} mm	2×10^{-5} mm	3×10^{-4} mm	28 mm
600	7 mm	12 mm	80 mm	16,500 mm

(After Sidgwick 1950)

At considerably low temperatures the v.p. of mercury is 800–1,000 times greater than that of lead or zinc compounds. At 204 °C the v.p. of mercury is 200 mm Hg std, and at 357 °C it is 760 mm, the pressure of PbS is only 1 mm Hg std at 487 °C.

Due to this high vapour pressure of mercury (and also its compounds) under hydrothermal conditions the surrounding country rock is deeply permeated by mercury with the formation of a primary dispersion halo, which sometimes extends hundreds of metres beyond the limits of the ore body. Saukov asserted the strong chalcophilic character of mercury as propounded by Goldschmidt (1937) and he demonstrated that the majority of polymetallic sulphide mineral deposits contain mercury much above the Clarke values; moreover, the mercury content in these minerals increases during the transition from hypothermal to mesothermal deposits and reaches the maximum in epithermal deposits.

Saukov (1946) showed that Hg contents of the following deposits increase systematically with decreasing intensity of genetic conditions: magmatic rocks (77 ppb); pegmatites (n ppb to $n\times10$ ppb); pneumatolytic deposits ($n\times10$ ppb to $n\times100$ ppb); mesothermal deposits ($n\times100$ ppb to n ppm); and epithermal deposits (n ppm to n per cent).

Ozerova (1962) has found by field and geochemical studies that Hg anomalies in rocks of mineral deposits, formed at the highest temperatures and pressures, are most weakly developed, and the anomalies associated with deposits formed at successively lower temperatures and pressures are progressively more strongly developed; rocks of epithermal deposits of mercury show the highest Hg contents.

In the U.S.S.R. Furzov (1958) collected and analysed nearly 500 samples from the Achisai lead-zinc deposits. Most of the samples contained less mercury than could be detected by the test employed (0·3 ppm). Mercury haloes were also detected in the bed rocks of barren limestones, overlying a blind lead-zinc

ore deposit. Peak anomaly values varied from 1·2 ppm to 6·5 ppm. Mercury anomalies were also detected where no lead or zinc haloes were found, suggesting gaseous transportation of mercury through the host rock. The mercury anomaly detected in the soils overlying the blind ore was much lower.

Sergeyev (1957) detected haloes, having peaks of 30 ppm, over a polymetallic ore deposit. It has been suggested by some authors (Ginzburg 1960, Furzov 1958) that the mercury content of a mineral is a function of the temperature of deposition (more explicitly so in the case of sphalerite).

The work of Furzov (1958) and Grip (1948) indicates that rather more mercury is present in most hydrothermal ore deposits than in unmineralized rocks. In most cases, mercury content of sulphide ores is of the order of n ppm to $n \times 10^2$ ppm, whereas most rocks contain only 0·5 ppm or less (Table I and Table II).

In several Swedish ore deposits the concentration of mercury in the ore appears to be related to the zinc content. The results of many ore deposits including Boliden (Grip 1948) of North Sweden show that, if they are divided into zinc-bearing and non-zinc-bearing deposits, the ores of the former are found to be higher in mercury than those of the latter.

Ozerova (1959) studied the primary dispersion haloes of mercury on the lead-zinc deposits of the Turkestan mountain range. The primary haloes over the deposits show ten times as high values as those from the barren zones. The dispersion is also ten times larger than the actually mineralized area. He used spectrograph and stressed that the sensitivity should be as much to detect values of $(1–2) \times 10^{-6}$% Hg.

These observations were supplemented by Ginzburg (1960) on the presence of mercury haloes in the pyrite deposits in S. Urals, and by later workers such as Hawkes and Williston (1962), James and Webb (1964), Friedrich and Hawkes (1966), Warren *et al.* (1966), Mitra and Webb (1967). Ginzburg (1960) in his book refers to an early investigation carried on by Uchaly *et al.* on mercury dispersions around pyritic bodies in South Urals.

In the northern part of the silver-producing Pachuca-Real del Monte district, Mexico, soils over the mineralized veins, which are shallow in depth, contain 250 to 1,900 ppb of Hg in contrast to the background of 50 ppb. In southern areas, the soil over the veins, buried deeper than 120 m, contain 150–600 ppb of Hg with the projection of peaks corresponding to the surface projection of vein structures (Friedrich and Hawkes 1966). Here, however, the wall-rock immediately adjoining the Hg-rich silver ore in Mina Purisima shows no enrichment in Hg, suggesting that the Hg-content of residual soil, but not of the unweathered rock, can be used as a guide to blind ore deposits. This is contrary to the earlier observation of Furzov (1958) on Achisi lead-zinc deposits, where the mercury anomalies in soil were much less conspicuous than those in the overlying barren limestone.

Stream sediment survey (Mitra and Webb 1967) of 300 sq. miles between Dartmoor granite and Bodmin Moor granite in Devon reveals a fair pattern of Hg related to the East-West base metal mineralization in this terrain. The Hg values are surprisingly high ranging up to about 7 ppm. Prof. Warren and his colleagues at the University of British Columbia have detected 5–15 ppm Hg in the agricultural soils from West Devon (personal communication to Dr. J. S. Webb). It is believed that the stream sediment pattern for Hg is least affected by agricultural contamination. The accuracy of the analyses and the problem of treatment of the samples collected have been treated in the latter pages.

In British Columbia the peak values of Hg in soils, studied in the vicinity of Au, Mo and base-metal deposits, range from 0·05–0·25 ppm, reaching in a few places to 2 ppm. Around mercury deposit the value ranges from 1 to 10 ppm or more. The background values are less than 0·05 ppm (Warren *et al.* 1966).

Analytical Techniques for Mercurometric Investigations and Problems of Error

Researches in the applications of mercury as a pathfinder in geochemical prospecting necessitated devising instruments for rapid determination of very small quantities of mercury. The analytical techniques that are generally employed for mercury analysis are: (1) colorimetry, (2) spectrometry and (3) ultraviolet absorption.

Ward and Bailey (1960) developed colorimetric method based on dithizone procedure. This method was good enough for ranges above 1 ppm but fails in accuracy in cases where the critical region lies in the region of 0·01–0·1 ppm. The spectrographic technique developed by Sergeyev (1957) for mercurometric investigations is rapid and has a better sensitivity of 0·02 ppm; it is not, however, found suitable for the direct analysis of mercury in vapour phase.

In the early sixties S. H. Williston of Cordero Mining Corporation constructed an instrument to determine the concentration of mercury vapour in air by the absorption of ultraviolet light with a specific frequency. To avoid the high level of background 'noise' and drift, caused by the fluctuations in lamp intensity or variation in voltage across the photo-cells, he used double beams. The same lamp illuminates the photo-cell through a chamber containing a non-absorbing gas, e.g. nitrogen. James and Webb (1964), with the consent of Williston developed a twin-cell system at the Royal School of Mines. The details of the description and operation of the instrument are given in the paper of James and Webb (1964). In the instrument air or vapour sample is pumped in and dehydrated by passing through silica gel. The dehydrated air is bifurcated and allowed to pass to the sample chambers (placed between the

photo-cells and the UV lamp). One half of the air passes through glass wool and the other half through palladium chloride, the latter completely demercurifies the air. The two photo-cells at the extremes of the reference chamber are illuminated by UV lamp, placed at the centre. The lamp radiates 2537 Å, which shows maximum absorption of mercury. Lamps made slightly of impure silica such as Vycor or other materials are recommended because pure fused silica permits transmission of wavelengths below 200 Å, which causes formation of ozone from atmospheric oxygen. Ozone, being a strong absorbent of UV at this range, is highly undesirable.

Kokshoy *et al.* (1967) modified the mercury vapour meter described by James and Webb, in that air was demercurified and dried before passing over the sample and no silica gel was in the flow path beyond the R.F. induction heating coil containing the sample (Fig. 2). According to them, water vapour evolved from the heated samples did not affect the estimation. The present author, however, noted that moisture does absorb a certain amount of U.V. of the specified wavelength.

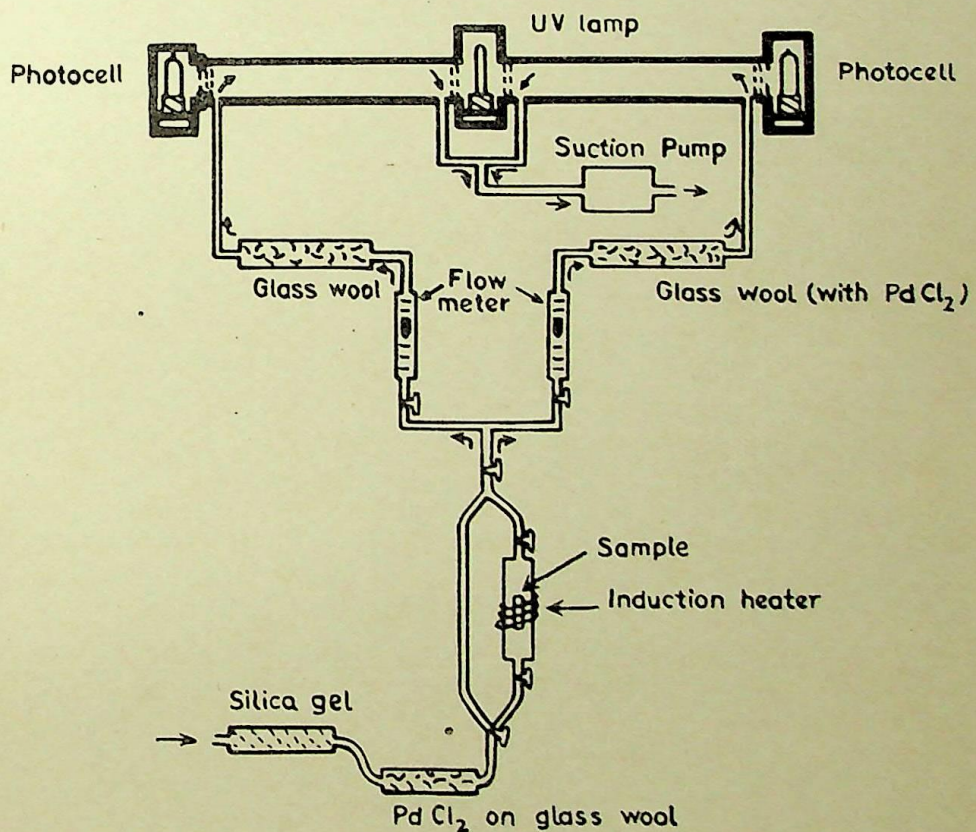

FIG. 2. Mercury absorption meter.

The usual procedure adopted by the author for the mercurometric investigation of the mineralizations of base metals (of copper, lead and zinc), around Dartmoor granite in Devon, included heating the samples at about 200 mA to 300 mA (i.e. 550 °C to over 800 °C) for about 30 seconds.

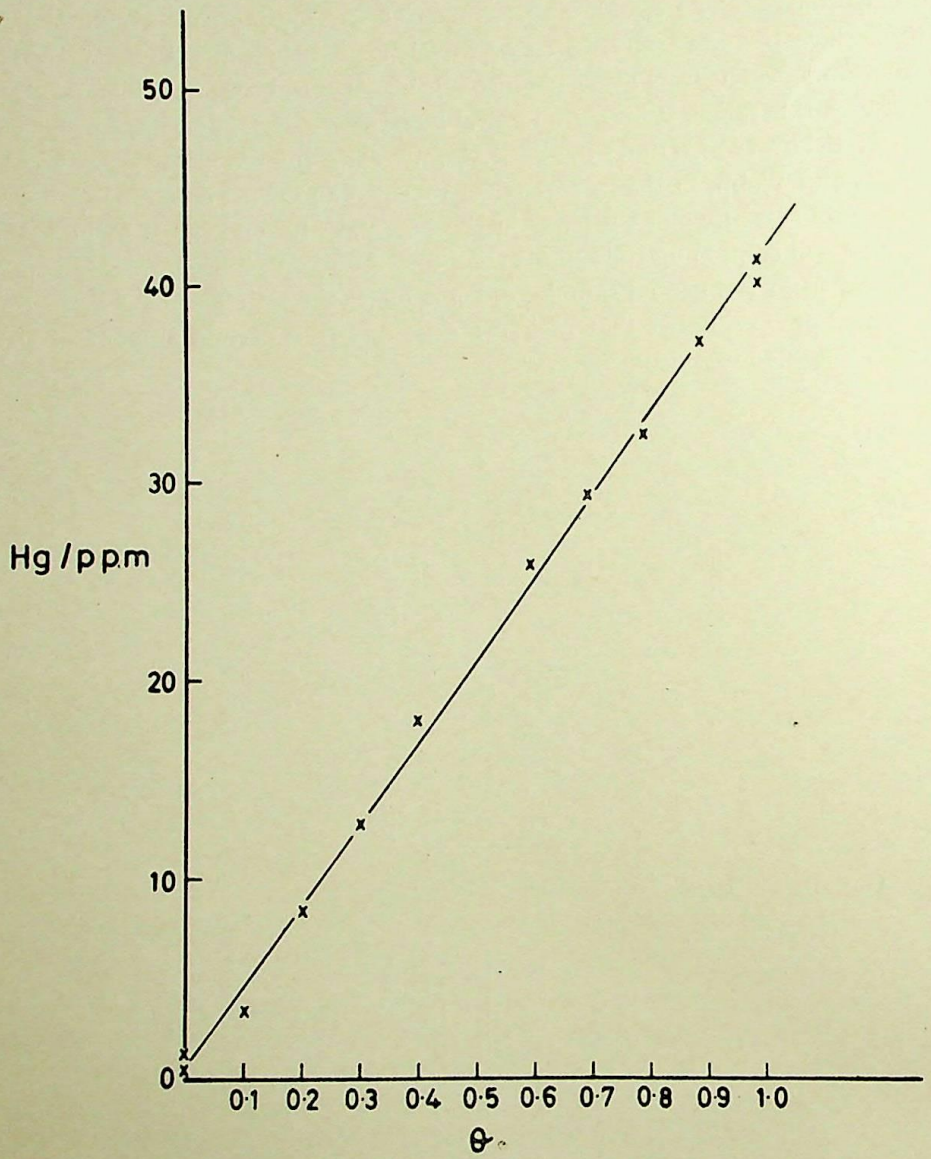

Fig. 3. Analytical precision curve as determined by the analyses of the standard samples containing HgS in linear proportions.

$$\left(\theta = \frac{\text{wt. of standard of highest Hg-content}}{\text{wt. of standard of lowest Hg-content}}\right)$$

The precision of analysis by the author was determined by using duplicate sample analyses (at 30 mA) of a set of twelve test samples of the U.S.G.S. (James 1963 and James and Webb 1964), having two high and low values mixed in known linear proportions. A modified technique of Craven (1954) was employed to test the accuracy of assaying and the result came out to be in the 7–8% range at 95% confidence level (Appendix A, Appendix B and Fig. 3). Reheating of the samples after first treatment at 300 mA (i.e. above 800 °C) for 30 sec showed no indications of mercury. Presence of mercury, however, was detected after heating at 200 mA as used by Kokshoy *et al.* (1967). To check the variation in the mercury vapour pressure during an investigation, due to variation in temperature (Table IV) and other unknown causes, test samples of mercury vapour of known Hg-content were injected to enable calibration of the instrument.

TABLE IV

Mercury contents of air saturated with mercury vapour at different temperatures

°C	γ-Hg/ml	°C	γ-Hg/ml	°C	γ-Hg/ml	°C	γ-Hg/ml
−30	0·00006						
−29	0·00007	−9	0·00084	11	0·0061	31	0·0320
−28	0·00008	−8	0·00093	12	0·0067	32	0·0345
−27	0·000092	−7	0·00104	13	0·0073	33	0·0370
−26	0·000105	−6	0·00116	14	0·0080	34	0·0400
−25	0·00012	−5	0·00130	15	0·0087	35	0·0430
−24	0·00014	−4	0·00145	16	0·0095	36	0·0465
−23	0·00016	−3	0·00162	17	0·0105	37	0·0500
−22	0·000185	−2	0·00180	18	0·0115	38	0·0545
−21	0·00021	−1	0·00200	19	0·0125	39	0·0570
−20	0·000235	0	0·00220	20	0·0135	40	0·0630
−19	0·00026	1	0·0024	21	0·0145	41	0·0680
−18	0·00029	2	0·0026	22	0·0156	42	0·0730
−17	0·00033	3	0·0029	23	0·0170	43	0·0780
−16	0·00037	4	0·0032	24	0·0185	44	0·0830
−15	0·00042	5	0·0035	25	0·0200	45	0·0890
−14	0·00047	6	0·0038	26	0·0215	46	0·0960
−13	0·00053	7	0·0042	27	0·0232	47	0·1030
−12	0·00060	8	0·0046	28	0·0249	48	0·1110
−11	0·00067	9	0·0050	29	0·0267	49	0·1190
−10	0·00075	10	0·0055	30	0·0295	50	0·1280

Initially, readings for calibration were taken thrice before the analyses and thrice after a continuous series of analyses. Calibration curve prepared from the average of these readings was used. After a standard calibration curve (which is found to approximate closely the calculated regression line $mV = 15381{\cdot}98\,\gamma\ Hg + 151{\cdot}67$) was prepared from the data of six calibrations,

prepared on different days, the successive calibrations were done by constructing parallel lines through the mean mV recorded by injecting 10 cc of mercury vapour. One such calibration line was regarded to be valid for 10 successive analyses involving about half hour. A more generalized calibration line passing through the origin of mV—γ Hg coordinates could be prepared having greater amount of correlation coefficient (amounting to 0·9790) compared to the line mentioned above which has a coefficient of correlation 0·9295. These generalized working curves show very low standard error in the estimate of Hg-content (0·0403 and 0·0222 respectively). Strong linear regression is also apparent from Fig. 4, where four correlation data are plotted. The curvilinearity at the upper part of the curve as noted by Kokshoy (1965) may be due to the loss during handling of larger volume of test samples.

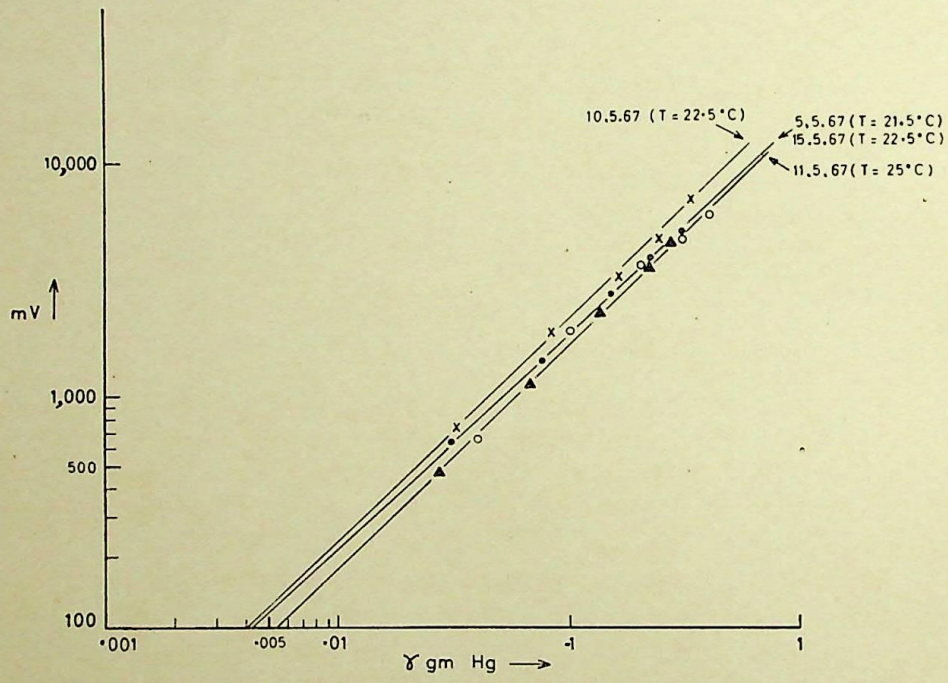

FIG. 4. Calibration curves for γ-gm of mercury and different mV's at different temperatures of some days.

Due to constant shifts in the position of calibration line during the day, analytical errors creep in. These deviations go to be incorporated in the present error. As an experiment for testing such error, analyses of two sets of stream samples collected by two teams in different periods from the same streams in Devon were analysed by two analysts (S.M. and A.D.) using this instrument. There was a slight difference in handling. The latter used two

calibration lines for the whole set of analyses and followed the method described. Table V shows the results obtained (collections I and II correspond to the same stream but not always the same location).

TABLE V

Collection I			Collection II		
Sample No.	S.M. (in ppm)	A.D. (in ppm)	Sample No.	S.M. (in ppm)	A.D. (in ppm)
I (1)	0·53	0·41	II (1)	0·53	0·18
I (2)	0·49	0·36	II (2)	0·23	0·23
I (3)	0·33	0·19	II (3)	0·25	0·11
I (4)	2·04	1·72	II (4)	0·66	0·47
I (5)	1·06	0·98	II (5)	0·69	0·50
I (6)	0·53	0·73	II (6)	0·31	0·12
I (7)	0·58	0·40	II (7)	0·67	0·29
I (8)	0·31	0·18	II (8)	0·31	0·18
I (9)	0·87	0·60	II (9)	0·67	0·46
I (10)	0·32	0·27	II (10)	0·67	0·45
I (11)	0·64	0·51	II (11)	0·55	0·45
I (12)	0·61	0·36	II (12)	0·68	0·42
I (13)	0·80	0·48	II (13)	0·35	0·30
I (14)	0·51	0·43	II (14)	0·33	0·10
I (15)	0·54	0·40	II (15)	0·61	0·36
I (16)	0·35	0·32	II (16)	0·40	0·24
I (17)	0·93	0·90	II (17)	1·09	0·80
I (18)	0·78	0·37	II (18)	0·37	0·18
I (19)	0·97	0·55	II (19)	0·32	0·26
I (20)	1·03	0·50	II (20)	0·33	0·20

The 'errors' or differences in the two sets of paired values may be caused by: (1) sampling error (between two sets) and (2) analytical error (between pairs).

The sampling 'error' is due to (*a*) the difference in the sample values themselves and (*b*) difference in the treatment of the samples during and after collection.

Treatment of the samples after collection is particularly important; this might cause considerable change in the Hg-content. The time of heating of the wet samples for drying after the collection is normally prescribed as 24 hours and the temperature of the hot plate is supposed to be over 40 °C. Variation in temperature and time of heating may cause deviation in Hg-content, as observed. Higher temperature causes greater loss in Hg-content (mercury from the samples is slowly volatilized at temperatures lower than 40 °C). Again, the quantity of samples under drying, the size-fraction and the difference in the content of the Hg-bearing minerals affect the observed Hg-values. Two equal samples containing the same amount of total mercury

will yield different values after the same heating if they contain different proportions of chlorides, sulphates, sulphides, etc. Experiments by Kokshoy *et al.* (1967) showed that native mercury and mercury chlorides ($HgCl_2$ and Hg_2Cl_2) liberate detectable quantities of mercury at less than 80 °C with complete liberation occurring below 250 °C. Mercury sulphide and oxide did not liberate a detectable amount of mercury until the temperature had reached 210 °C and 270 °C, respectively. They stated that complete extraction was obtained at 340 °C and 535 °C respectively (Fig. 5). But, as already noted, the author observed that until the temperature is nearly 800 °C (for samples of 80 mesh) the maximum liberation is not assured.* That size-fraction

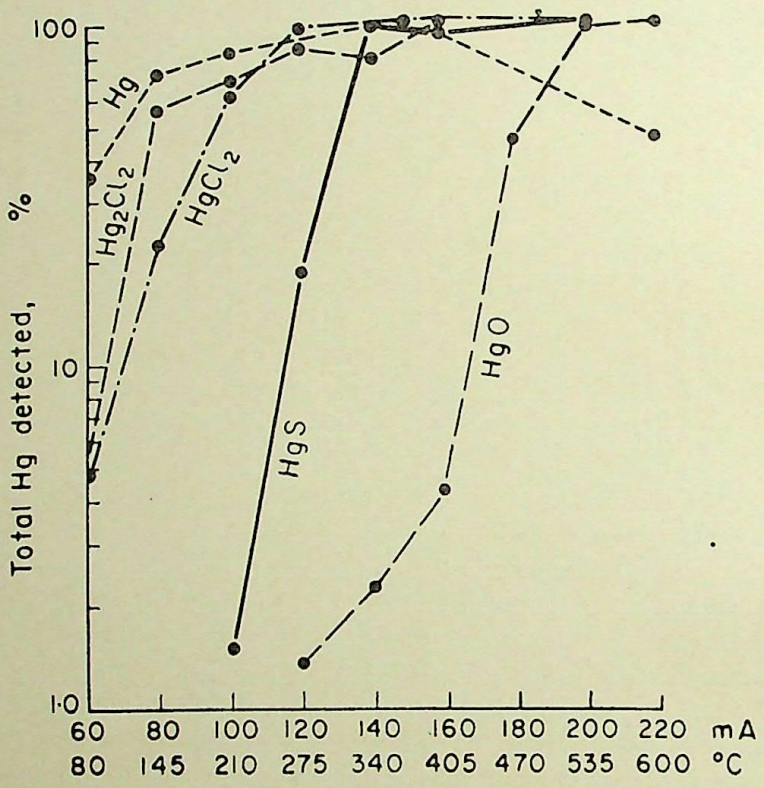

FIG. 5. Comparison of effect of temperature on liberation of mercury from selected compounds (samples heated for 30 sec) (Kokshoy *et al.*, 1967).

* To determine the optimum temperature of heating for drying the field samples, the author started investigation with two soil samples for the present area collected wet in the field and preserved in double layered polythene bags. Several fractions of the samples were dried at different temperatures (22 °C (room temperature), 30 °C, 45 °C, 60 °C, 100 °C and 450 °C). A general loss in Hg-content was noted but due to contamination from the furnace at certain stages the experiment could not be satisfactorily completed before the departure of the author from I.C. (in September 1967). From over-all consideration it is, however, suggested that the mercury samples after collection should be dried at room temperature, or by passing dry air over the samples as mentioned by Kokshoy *et al.* (1967).

is an important factor affecting liberation was noted by previous workers and 80-mesh samples for soil and stream sediments were recommended. Of course, the size-fraction, required for a set of samples, is determined by the mineralogy as well as the distribution of mercury in other minerals.

Regarding the distribution of mercury in different sulphide minerals Sergeyev (1957) reported that for the 14 basic sulphides, e.g. molybdenite, pyrrhotite, pyrite, sphalerite, galena, chalcopyrite, tetrahedrite, bornite, bournonite, chalcocite, marcasite, antimonite, realgar, orpiment, the mercury values range between 10^{-4} and 10^{-2}%, varying as a function of the type of the mineral and the region from which they were collected. For example, tetrahedrite ores of Nikolayevsk deposit in the Altay region contain up to $4{\cdot}2\times10^{-3}$% of Hg; while certain ores of Caucasus contain up to 10^{-2}%. Investigation of Novokhatskü and Kalinin (1952) revealed that copper minerals contain up to $1{\cdot}5\times10^{-1}$% of mercury and the sphalerite contains mercury in quantities of the order of 1×10^{-3}%, reaching in minerals of low temperature deposits as much as $(1{\cdot}5\text{–}2)\times10^{-2}$%.

Besides the consideration of mineralogy and treatment in the field the other factor affecting change in Hg-values in samples is storage, as noted by Kokshoy *et al.* (1967). They reported the effect of storage leading to increase in Hg values of samples having initially low Hg, when those were stored for a long time in association with high Hg-samples. Detectable mercury content of a sample originally containing 220 ppb Hg was increased by 25%, when stored for 30 days at room temperature in the same box with samples containing 8000 ppb Hg. However, this storage effect should be negligible in the present case since the 'high' samples are not so high as Kokshoy *et al.* used in their studies, although the period of storage in this case was considerably more (about 4 years) than that studied by them.

The technique which could be used to prepare a geochemical map from the data obtained from such treated stream-sediment samples is to prepare a ratioing map or a standard deviation map in place of a map prepared from the values of the contents, the 'exact' quantity of which may be uncertain. Ratioing of the data by the mean of the background in such cases would evade the problem of representing the exact ppm values but could at the same time indicate the 'highs' and 'lows' in the manner as the 'exact' data would indicate. In the geochemical investigation of the Hg-dispersion in Devonshire between Dartmoor and Bodmin granite (*see* map, Fig. 6) with stream-sediment samples (—80 mesh) of density of one sample per square mile over a region of 300 sq. miles a similar technique akin to the rolling mean was used to delineate the trend of variation of Hg in the stream-sediments in this area. The area was divided in one mile grids, and circles were drawn at each corner with radius one mile, the average of all points lying on and within the circles was plotted at the centre. By this the 'noise' of the whole area was much reduced and a

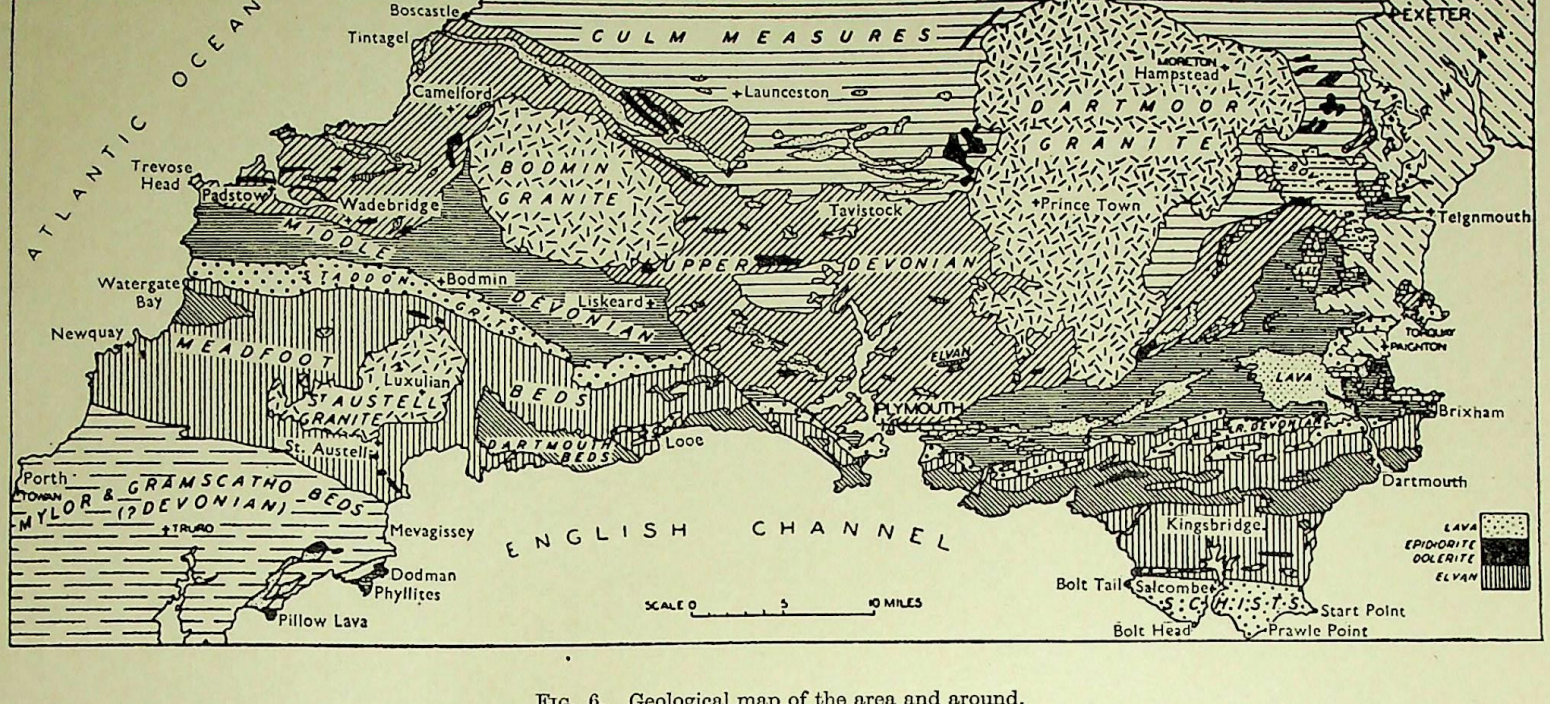

FIG. 6. Geological map of the area and around.

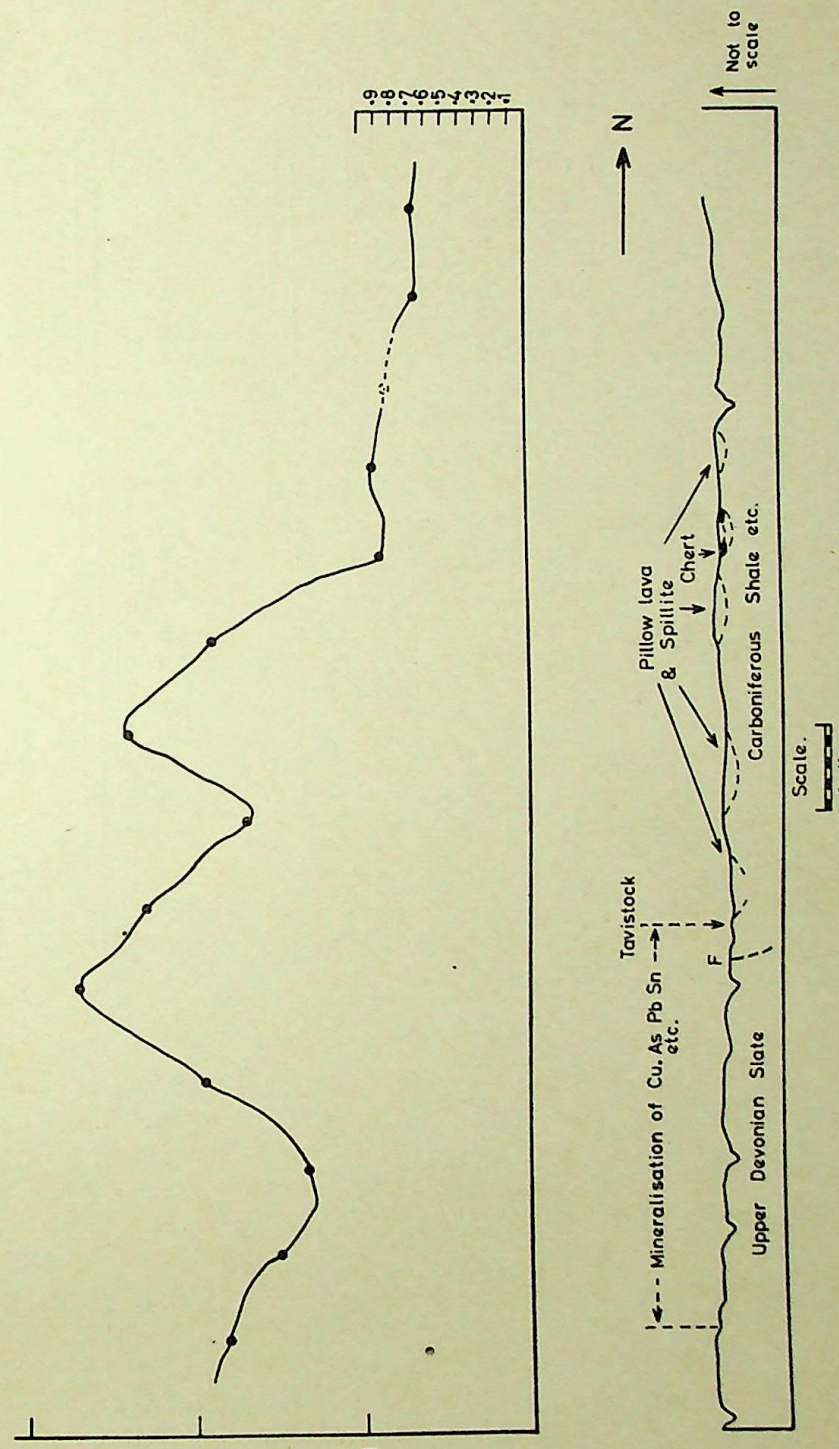

FIG. 7. Secondary dispersion of mercury (in ppm) in stream-sediments over a N–S profile through Tavistock.

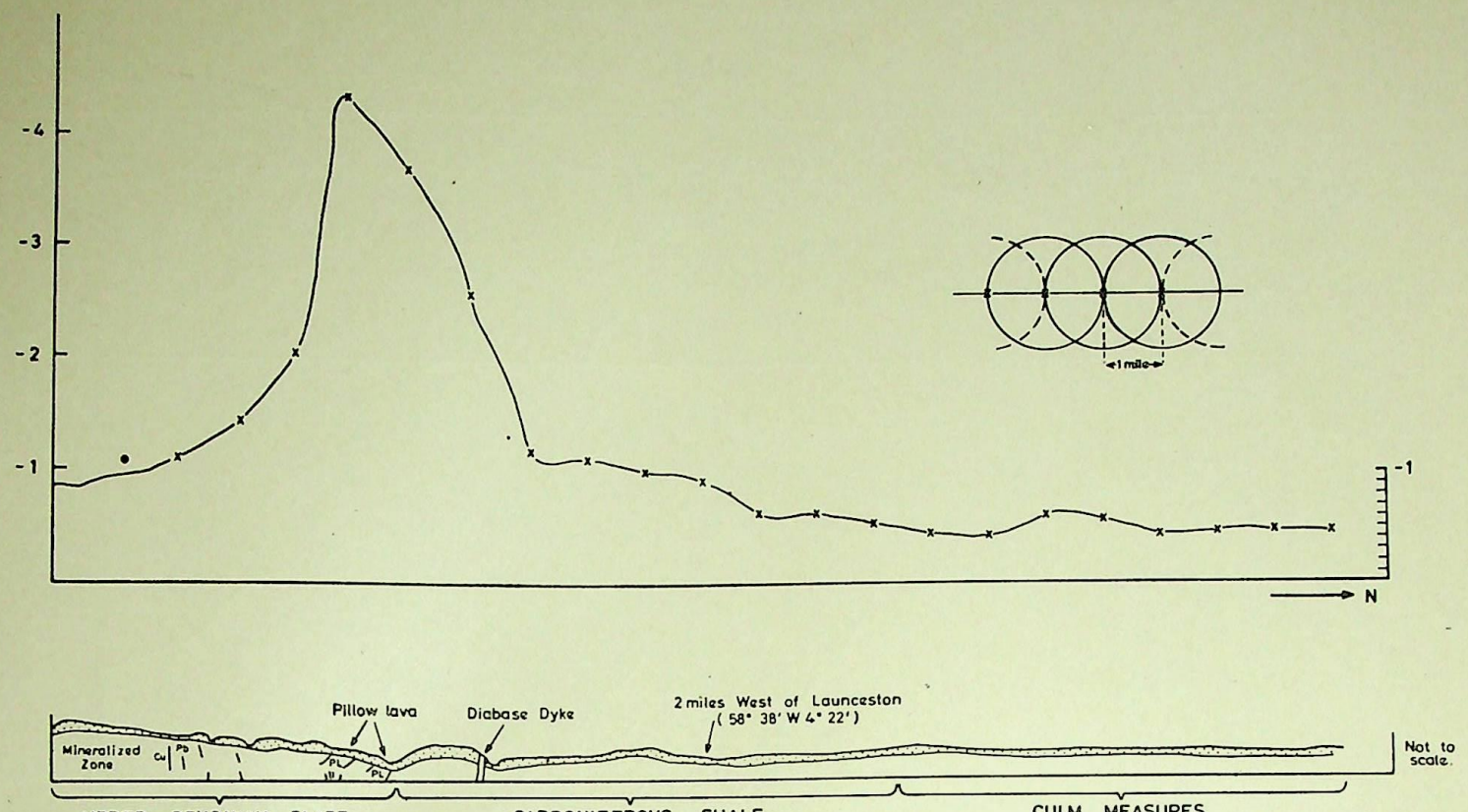

FIG. 8. The mean dispersion pattern of mercury (in ppm) over a N–S traverse running 2 miles west of Launceston (*see* map). The average sample values over an area of 3·14 (approx.) sq miles are plotted at the centre of the area as shown in the insertion.

general northerly and southerly slope from the central area became apparent (Fig. 7).

A study of the general trend relation of the Hg-dispersion in stream sediments with respect to the geology of the area reveals that anomalous zone runs almost E–W., roughly parallel to the Cu-Pb-Zn-Sn mineralized zone. But a general shift of the anomaly peaks towards the north became apparent. Two N–S. profiles, one without using circular rolling mean and the other using it, are shown in Figs. 7 and 8, drawn through Tavistock and two miles west of Launceston. These profiles show the northerly shift of the anomaly peaks from the zone of mineralization. Geologically the area was never glaciated and the migration towards the north may be due to solifluxion since the Pleistocene or earlier.

Acknowledgements

The author expresses his sincere thanks to Nuffield Foundation for the financial assistance. He is thankful to Dr. J. S. Webb for the introduction of the work and the facilities he provided during the course of the author's work at his laboratory. Thanks are also due to Dr. Newman, Dr. J. S. Tooms, Dr. P. M. Bradshaw and Dr. I. Nichols for their help, suggestions and criticisms during the work.

The author also expresses his gratitude to Mr. Roy Phillips and Prof. G. M. Brown for their kind permission to carry out a part of the work at the Dept. of Geology, Durham University. Thanks are also due to Dr. J. Aucott and Miss M. Lumley, both of the above University, for their help in computer programming and for drawing the diagrams respectively. Kind thanks are expressed to the late Prof. M. S. Krishnan, F.N.I., for communicating the paper. Constant and untiring help in the part of the work often continued at home was rendered by Ashima, my wife.

References

Craven, C. A. U. (1954). Statistical estimation of the accuracy of assaying. *Trans. Inst. Min. Metall.*, 63, 551–63.

Friedrich, G. H., and Hawkes, H. E. (1966). Mercury as an ore guide in the Pachuca-Real del Monte district, Hidalgo, Mexico. *Econ. Geol.*, 61, No. 4.

Furzov, V. Z. (1958). Haloes of dispersed mercury as prospecting guides at the Achisai lead-zinc deposits. *Geokhemiya*, 3, 338.

Ginzburg, I. I. (1960). Principles of Geochemical Prospecting (translation). Pergamon Press, London.

Goldschmidt, V. M. (1937). The principles of distribution of chemical elements in minerals and rocks. *Journ. Chem. Soc.* (London), pp. 655–73.

————(1954). Geochemistry. Oxford University Press, London.

Grip, E. (1948). On the occurrence of mercury in Boliden and in some other sulphide deposits in North Sweden. *Sver. geol. Unders. Arsbok*, 42, No. 8, ser. C, 499.

Hawkes, H. E., and Williston, S. H. (1962). Mercury vapour as a guide to lead-zinc-silver deposits. *Min. Congr. J.*, December.

James, C. H. (1963). A review of the geochemistry of mercury and its application to geochemical prospecting. *Geochemical Prospecting Research Centre, Imperial College. Tech. Comm.* No. 41.

James, C. H., and Webb, J. S. (1964). Sensitive mercury vapour meter for use in geochemical prospecting. *Trans. Instn. Min. Metall.*, 73, pt. 9, 1963–64.

Kokshoy, M. (1965). Ph.D. thesis, London University.

Kokshoy, M., Bradshaw, P. M., and Tooms, J. S. (1967). Notes on the determination of mercury in geological samples. *Trans. Inst. Min. Metall.*, 76, Sec. B, 121–24.

Mitra, S., and Webb, J. S. (1967). Mercury in south-west England. *Trans. Inst. Min. Metall.*, 76, Sec. B, 180.

Novokhatskü, M. P., and Kalinin, S. K. (1952). O soderzhanü ftora v nekotorykh Sul'fidnykh mineralakh. *Vest. Akad, Nauk Kazakh SSR*, no. 9.

Ozerova, N. A. (1959). On the use of primary dispersion haloes of quicksilver in search for lead-zinc deposits (in Russian): *Geokhimiya*, pp. 638–45.

————(1962). Primary dispersion halo of mercury. *Proc. Geol. Ore Deposits, Petrog. Min. and Geochem.* (Chikrov Inst., IGEM), No. 72, Questions of Geochemistry, Pt. 4., Acad. Sci., U.S.S.R., Acad. Sci. Press, Moscow, U.S.S.R.

Preuss, E. (1941). Beiträge zur spektralanalytischen Methodik II. Bastimmung von Zn, Cd, Hg, In, Tl, Ge, Sn, Pb, Sb and Bi durch fraktionierte Destillation. *Z. angew. Min.*, 3, 8.

Rankama, K., and Sahama Th. (1950). Geochemistry. Chicago University Press, Chicago.

Saukov, A. A. (1946). 'Geokhimiya rtuti' (Geochemistry of mercury). Tr. AN U.S.S.R. Academy of Sciences (Mining of Geochemistry series), No. 17.

Sergeyev, Ye. A. (1957). Methodology of Mercurometric Investigations. Proc. of the 1st All Union Conference on Geochemical Prospecting for Ore Deposits Service. (Ed. V. I. Krasnikov) University of Alabama.

Sidgwick, N. V. (1950). The Chemical Elements and their Compounds, Vol. 2. Oxford University Press, London.

Stock, A., and Cucuel, F. (1934). Die Verbreitung des Quecksilber. *Naturweissenschaft.*, 22, 390–93.

Ward, F. N., and Bailey, E. H. (1960). Camp and sample-site determination of traces of mercury in soils and rocks. *Trans. Am. Inst. Min. Engrs.*, 217, 343–50.

Warren, H. V., Delavault, R. E., and Barakso, J. (1966). Some observations on the geochemistry of mercury as applied in prospecting. *Econ. Geol.*, 61, No. 6, 1010–28.

Appendix A

Mercury analyses using mercury vapour meter*

Sample mark	Tube No.	Wt. of sample	mV recorded	γgm/Hg†	ppm Hg	Average ppm Hg
J	J_1	0·0196	210	0·0095	0·4845	0·5714
	J_2	0·0202	230	0·0133	0·6584	
A	A_1	0·0199	250	0·0180	0·9045	0·8111
	A_2	0·0202	300	0·0145	0·7178	
G	G_1	0·0206	1040	0·0630	3·0582	3·3057
	G_2	0·0197	1110	0·0700	3·5533	
E	E_1	0·0201	2210	0·1550	7·7114	8·2973
	E_2	0·0197	2450	0·1750	8·8832	
I	I_1	0·0193	3400	0·2650	13·7330	12·7710
	I_2	0·0199	3100	0·2350	11·8090	
D	D_1	0·0185	4150	0·3350	18·1081	17·8550
	D_2	0·0196	4250	0·3450	17·6020	
B	B_1	0·0199	5850	0·5100	25·6280	25·6853
	B_2	0·0202	6000	0·5200	25·7426	
F	F_1	0·0199	–	–	–	29·2307
	F_2	0·0195	6500	0·5700	29·2307	
K	K_1	0·0205	7250	0·6450	31·4630	32·1888
	K_2	0·0199	7350	0·6550	32·9146	
H	H_1	0·0201	8200	0·7500	37·3134	36·7336
	H_2	0·0195	7800	0·7050	36·1538	
C	C_1	0·0205	8900	0·8300	40·4878	39·5738
	C_2	0·0194	8200	0·7500	38·6598	
L	L_1	0·0203	9050	0·8420	41·0000	41·0000
	L_2	–	–	–	–	

* Analyses in duplicate were done of a series of eight mixtures (G, E, I, D, B, F, K and H) of the two set of samples (one set of two samples contain the same high Hg-content, viz. L and C; and the other two contain the same low amount), mixed in linear proportions (viz. the sample G has A or G : C or L :: 0·1; and E has A or G : C or L :: 0·2 and so on, ultimately, H has A or G : C or L :: 0·9).

† Calculated from the calibrations.

Appendix B

*Analytical reliability test**

θ	Sample No.	Analytical Result ppm	Calculated Result	Difference	Differences greater than σ	Differences greater than 2σ
0	J	0·5714	0·6032	−0·0318	×	×
0	A	0·8111	0·6032	+0·2079	×	×
0·1	G	3·306	4·576	−1·270	√	×
0·2	E	8·297	8·630	−0·333	×	×
0·3	I	12·771	12·642	+0·129	×	×
0·4	D	17·855	16·656	+1·199	√	×
0·6	B	25·685	24·682	+1·003	√	×
0·7	F	29·231	28·695	+0·536	×	×
0·8	K	32·189	32·708	−0·519	×	×
0·9	H	36·734	37·264	−0·530	×	×
1·0	C	39·574	40·7341	−1·160	√	×
1·0	L	41·000	40·7341	+0·266	×	×

$\Sigma(A-\hat{A})^2 = 6{\cdot}4818$

$\Sigma A = 248{\cdot}0237$ Calc. High = 40·7341

$\Sigma A\theta = 188{\cdot}2212$ Calc. Low = 0·6032

$\Sigma A\lambda = 59{\cdot}8025$ Mean = 20·6687

$\Sigma A\theta\, \Sigma\theta\lambda = 263{\cdot}5097$ No. of samples = 12

$\Sigma A\, \Sigma\theta\lambda = 83{\cdot}7235$ Variance .. 0·64818

Standard deviation .. 0·805

Mean accuracy $\left(\frac{2\times \text{ Standard deviation } \times 100}{\text{Mean}}\right)$ .. 7·79%

* Made after a modified technique of C. A. U. Craven (1954).

SUITABILITY OF SALINE WATER AS A RECLAIMANT FOR ALKALI SOILS OF UTTAR PRADESH

S. G. Misra *and* D. P. Sharma, *Agricultural Chemistry Section, Department of Chemistry, University of Allahabad, Allahabad*

(Communicated by S. P. Raychaudhuri, F.N.I.)

(*Received 10 July 1969; after revision 13 February 1970*)

Repeated leachings of saline alkali, alkali and saline soils with water containing excess of Ca^{2+} over Na^{+} and Na^{+} over Ca^{2+} showed that increasing ratios of Ca/Na helped in replacing Na^{+} from the exchange complex by Ca^{2+} ions and the *p*H of the leachates gradually fell off. The saline soil presented an exceptional case because the changes were not very spectacular. However, there was regular increase in exchangeable Ca and simultaneous decrease in exchangeable Na of all the soils leached.

On increasing the proportion of Na^{+} in comparison to Ca^{2+} in leaching water, no change in exchangeable calcium of the soils took place so long as the ratio of Na/Ca was kept within the range of 1 to 4 but, as soon as it became 5, the exchangeable Ca^{2+} decreased.

There was an increase in soluble CO_3^{2-} as Na^{+} was increased in leaching water but the amount of HCO_3^{-} decreased. The electrical conductivity had a tendency to decrease first and then increase. In saline soil, no soluble CO_3^{2-} was detected but HCO_3^{-} increased.

Reclaiming saline-alkali and alkali soils is rather difficult than reclaiming saline soils because the former involves not only leaching out soluble salts, but also replacing exchangeable sodium from the exchange-complex. Hence, while developing only reclamative measure for such soils, a greater emphasis has to be placed upon supplying Ca^{2+} to exchange with Na^{+} in the exchange-complex. It has been shown by Bower and Reeve (1960) that transmission rate of water through sodic* soils depends very markedly upon the electrolyte concentration of water. When a sodic soil is leached with water of low salt content, the permeability may decrease to a value that practically prevents completeness of the reclamative process, but by increasing electrolyte concentration the transmission rate may be markedly increased. The effect on the transmission rate of water was also demonstrated by Fireman and Bodman (1940), Fireman (1944), Christiansen (1947) and others. More recently, Quirk and Schofield (1955) published qualitative data on the effect of electrolyte concentration on soil permeability and pointed out the advantages of high salt water for reclamation processes.

* Bower and Reeve used the term sodic soil for alkali soils.

The desirability of water used for reclamation depends mainly on its easy transmission through the soil regardless whether calcium has been added to or is originally present in the soil, otherwise reclamation will not be effective. Although gypsum has been used as an amendment, it has not been effective in maintaining high permeability, because of its low solubility. Cation exchange equilibrium theory indicates, however, that the use of high salt water such as sea water may be entirely possible for the replacement of Na^+ and reclamation of alkali soils. It is, therefore, proposed that saline water can be used with advantage.

Since such waters contain Ca^{2+} and Na^+ ions in different ratios, it was considered worth while to leach the saline and alkali soils with mixed salts of calcium and sodium. Thus, by finding out the minimum proportions of Ca^{2+} in conjunction with Na^+, the safe levels of the latter can be predicted in irrigational waters and thus the soils can be prevented from further deterioration.

Large tracts of salt-affected soils are found in several parts of Uttar Pradesh, but no efforts have been made to reclaim these soils through leaching techniques. Taking into consideration the beneficial effects of leaching over other methods of reclamation, the present investigation regarding the reclamation of saline and alkali soils was undertaken using a series of leachings with neutral salt solutions.

Experimental Procedure

Seven soil profiles were collected from different places of Allahabad and Fatehpur districts of U.P. The soils fall into three classes—(1) saline type, e.g. Ghurpur profile (GP), (2) saline-alkali type, e.g. Handia (HP), Katoghan (KP) and Soraon (SP) profiles and (3) nonsaline-alkali type, e.g. Phulpur (PP), Meja (MP) and Chial (CP) profiles. Out of the above profiles, the first layer from each profile has been used in the present investigation and their chemical characteristics are given in Table I (each layer being represented by GP1, HP1, KP1, SP1, PP1, MP1, CP1).

*p*H of the original soils was determined in 1 : 2·5 soil : water ratio (Jackson 1962). Electrical conductivity (EC) was determined in 1 : 1 soil : water extract by a conductivity bridge fitted with a head phone (Wilcox 1950). Soluble carbonates and bicarbonates were estimated by methods given in U.S.D.A. Handbook (1954). Exchangeable cations were determined in neutral *N*-ammonium acetate extracts (U.S.D.A. 1954).

The leaching operations have been performed using aqueous solutions of $CaCl_2$ and NaCl. Five concentrations of solutions have been used so as to contain Ca^{2+}/Na^+ and Na^+/Ca^{2+} varying from 1 to 5, i.e. Ca^{2+} or Na^+ has been increased from 1 to 5 m.e./litre and the corresponding values of Na^+ or Ca^{2+} have been kept at 1 m.e./litre.

TABLE I

Some of the chemical properties of the soils used

Chemical characteristics	Saline type	Nonsaline-alkali			Saline-alkali		
	GP1	PP1	MP1	CP1	HP1	KP1	SP1
*p*H	8·200	10·300	10·400	10·000	10·400	10·000	9·700
Alkaline earth carbonates ($CaCO_3$, %)	1·700	8·800	17·400	12·100	15·100	14·500	13·500
EC $\times 10^3$ at 25 °C	10·500	2·700	3·210	–	5·010	14·100	9·400
Soluble cations, %							
Ca^{2+}	0·082	0·026	0·040	0·036	0·034	0·016	0·025
Mg^{2+}	0·029	0·010	0·012	0·014	0·010	0·021	0·014
Na^{+}	0·094	0·068	0·061	0·092	0·072	0·194	0·158
K^{+}	0·012	0·004	0·010	0·003	0·006	0·018	0·002
Soluble anions, %							
CO_3^{2-}	tr.	0·260	0·078	0·160	0·310	0·087	0·204
HCO_3^{-}	0·043	0·280	0·071	0·185	0·700	0·296	0·219
Cl^{-}	0·210	0·050	0·028	0·014	0·026	0·001	0·026
SO_4^{2-}	0·250	0·030	0·005	0·032	0·020	0·024	0·061
C.E.C. (m.e./100 g) ..	10·500	12·500	12·700	11·400	16·100	12·500	8·100

20·0 g of air-dried soil samples were taken in duplicate from the surface layers of each profile in conical flasks and shaken for one minute with 100 ml of mixed solution containing 1 m.e. Ca^{2+} and 1 m.e. Na^{+} per litre. The contents were immediately filtered through Buchner funnels under suction. The leachates were collected in separate volumetric flasks. After first leaching, the soils from the funnels were carefully transferred to the same conical flasks with 100 ml of the same solution, shaken for the same period and filtered again. These leachates were collected in a second set of volumetric flasks. In this manner, the soils were repeatedly leached for six times. In the leachates were determined *p*H, EC, CO_3^{2-} and HCO_3^{-}. The mean values have been used for representing the results which are reported in the form of separate graphs (Figs. 1 to 3).

Similarly 20·0 g of the soils in duplicate were repeatedly leached for six times with another mixed salt solution containing 2 m.e. Ca^{2+} and 1 m.e. Na^{+} per litre. The leachates were collected in separate flasks and analysed for the above constituents. Leachings of soils with mixed solutions containing 2, 4, 5 m.e. Ca^{2+} and 1 m.e. Na^{+} per litre were also performed. The results

(average values) obtained with Phulpur profile are shown in Fig. 1*a*. The soils of the first layer of Meja, Chial, Handia, Katoghan, Soraon and Ghurpur were similarly leached. In each series, two replications were made and the results are presented in the forms of graphs (Figs. 1*b* to 3).

Leachings with varying ratios of Na/Ca from 1 to 5 were also carried out similarly and the results have been given separately (Figs. 4*a* to 6).

Results and Discussion

(a) Leaching with Salt Solution Containing Excess Ca^{2+}

Phulpur Profile (PP_1)

The changes in *p*H, EC, CO_3^{2-} and HCO_3^- for Phulpur profile are represented in Fig. 1.

It is quite clear from the figures that the drop in *p*H is directly proportional to Ca^{2+} present in the leaching solution. A decrease in *p*H from 10·3 to 9·7 is observed upon leaching the soil with solution of $Ca^{2+}/Na^+ = 1$ but, when Ca^{2+}/Na^+ becomes 2, the drop in *p*H is still sharp, so much so that the sixth leachate records a *p*H of 9·2. As the concentration of Ca^{2+} is further increased from 3 m.e. to 5 m.e. per litre, a pronounced drop in *p*H is noted.

Some remarkable changes in EC values of this profile are perceptible. For example, EC of first leachate is on an increase as the ratio of Ca^{2+}/Na^+ is increased, but EC decreases in the second and fourth leaching at $Ca^{2+}/Na^+ = 1$. After second leaching, EC falls abruptly in presence of higher concentrations of Ca^{2+} up to fifth leachate but it again increases in sixth leachate. A regular decrease in EC is noted in presence of 5 m.e. Ca^{2+}, though in the second leaching it slightly increases. It clearly indicates that, with high proportions of Ca^{2+}, either adsorption or precipitation is taking place. In presence of 1 m.e. or 2 m.e. Ca^{2+}, such changes are not observed.

CO_3^{2-} decreases regularly from first to sixth leachate with all concentrations of Ca^{2+} but decrease is rapid in presence of higher concentrations of Ca^{2+}. Carbonate ions are not observed after fourth and third leaching with 3, 4 and 5 m.e. Ca^{2+}, respectively.

HCO_3^- also decreases from first to sixth leachate with all ratios of calcium.

Meja Profile (MP)

In Meja alkali soil profile (Fig. 1*a*) there is a gradual decrease in *p*H when Ca^{2+} in the leaching solutions is low (1–2 m.e./litre). However, with higher concentration of Ca^{2+}, a sharp fall in *p*H is noted. The *p*H falls up to 8·2 finally.

In this profile, no CO_3^{2-} is observed after fourth and third leaching with 1, 2 and 3 m.e. Ca^{2+} respectively and, in the presence of 4 and 5 m.e. Ca^{2+}, the soluble carbonates disappear after second leaching. The EC values decrease

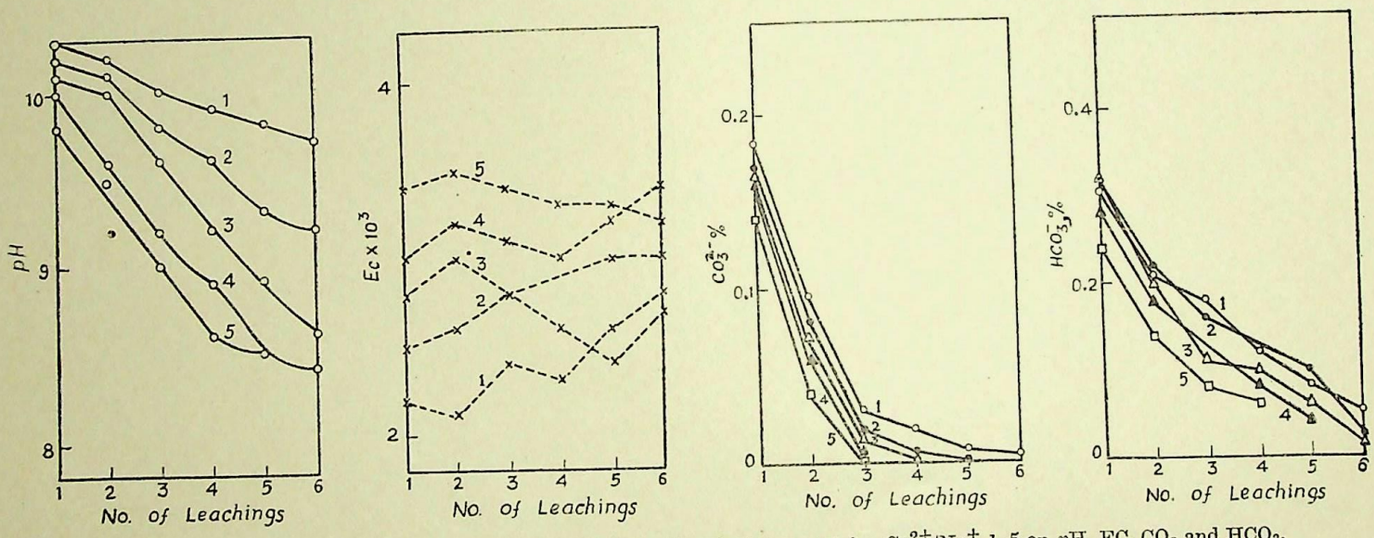

FIG. 1*a*. Leaching effects of a nonsaline-alkali soil (PP_1) with solution containing Ca^{2+}/Na^{+} 1–5 on *p*H, EC, CO_3 and HCO_3.

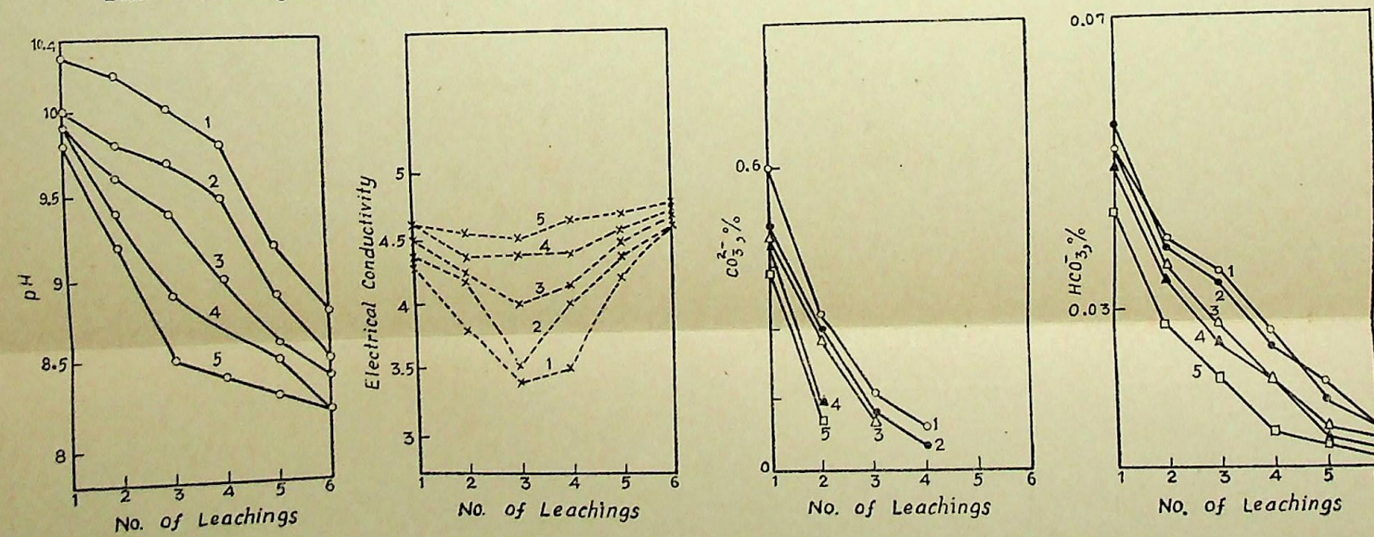

FIG. 1*b*. Leaching effects of a nonsaline-alkali soil (MP_1) with solution containing Ca^{2+}/Na^{+} 1–5 on *p*H, EC, CO_3 and HCO_3.

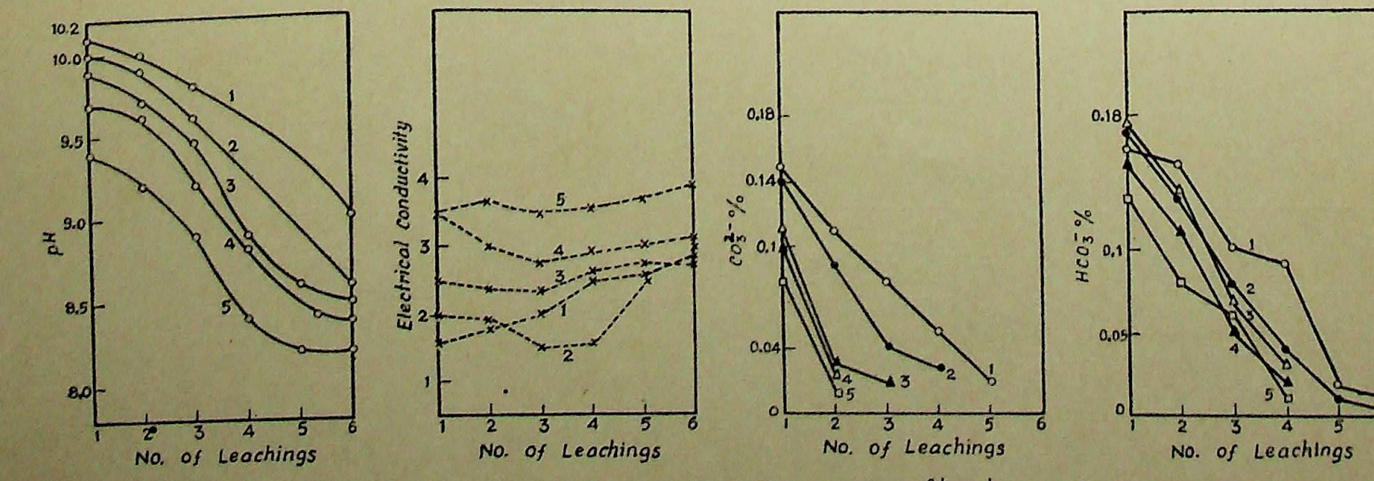

FIG. 1*c*. Leaching effects of a nonsaline-alkali soil (CP_1) with solution containing Ca^{2+}/Na^{+} 1–5 on *p*H, EC, CO_3 and HCO_3.

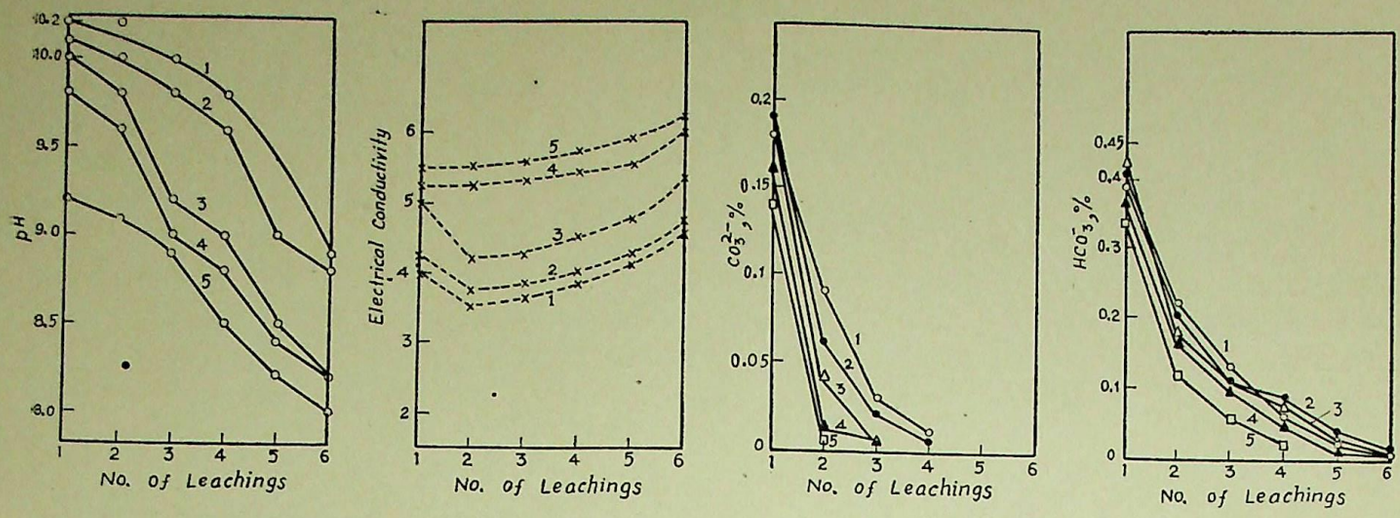

FIG. 2a. Leaching effects of a saline-alkali soil (HP_1) with solution containing Ca^{2+}/Na^+ 1–5 on *p*H, EC, CO_3 and HCO_3.

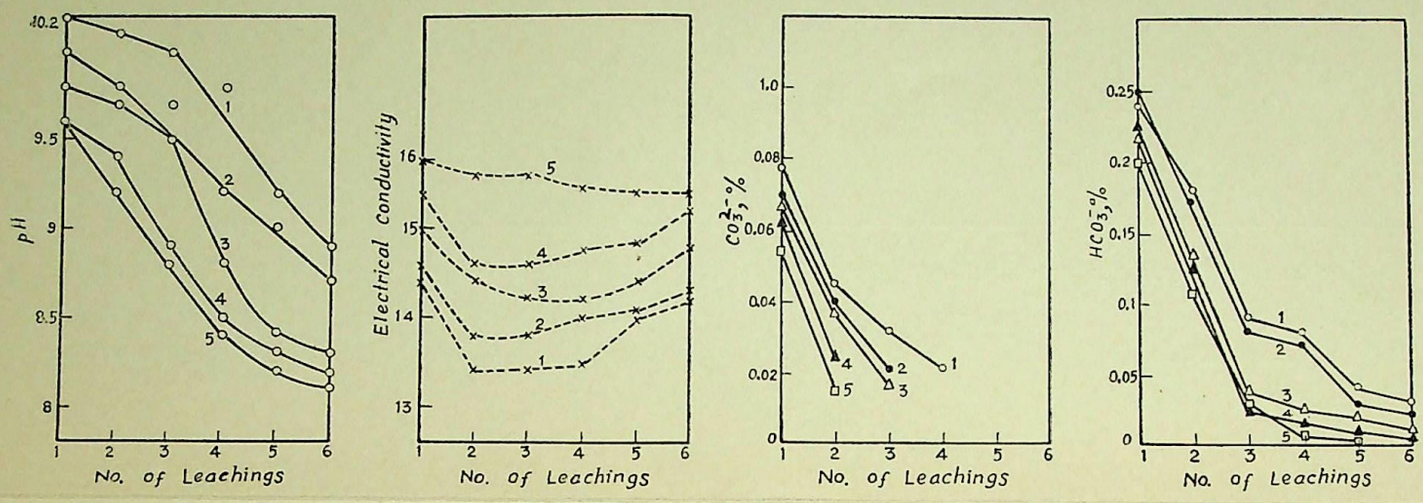

FIG. 2b. Leaching effects of a saline-alkali soil (KP_1) with solution containing Ca^{2+}/Na^+ 1–5 on *p*H, EC, CO_3 and HCO_3.

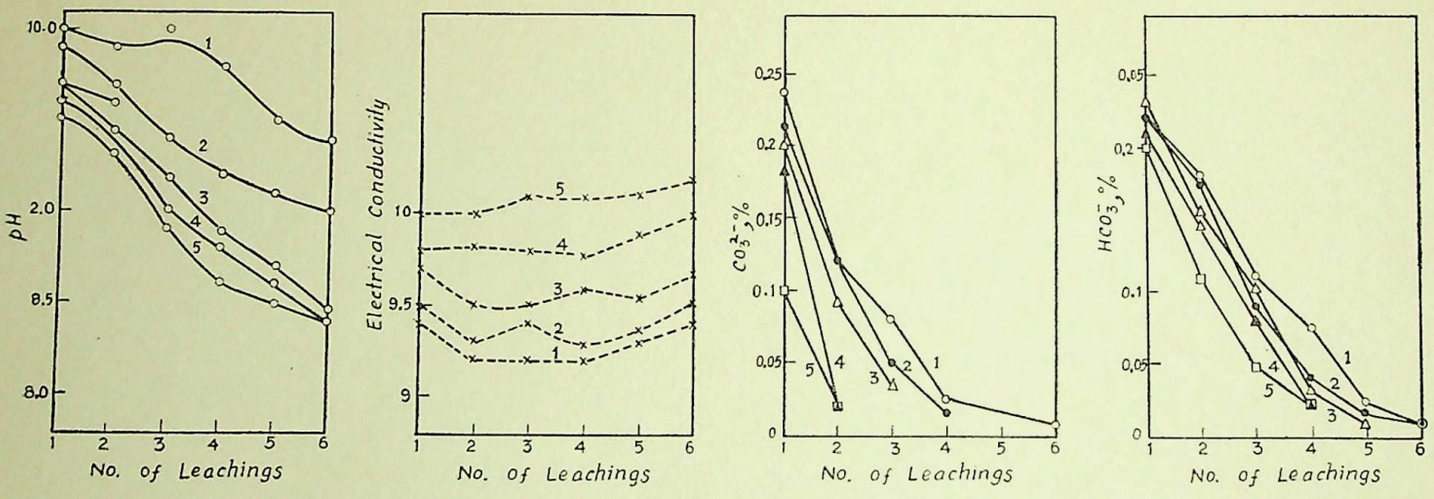

FIG. 2c. Leaching effects of a saline-alkali soil (SP_1) with solution containing Ca^{2+}/Na^+ 1–5 on *p*H, EC, CO_3 and HCO_3.

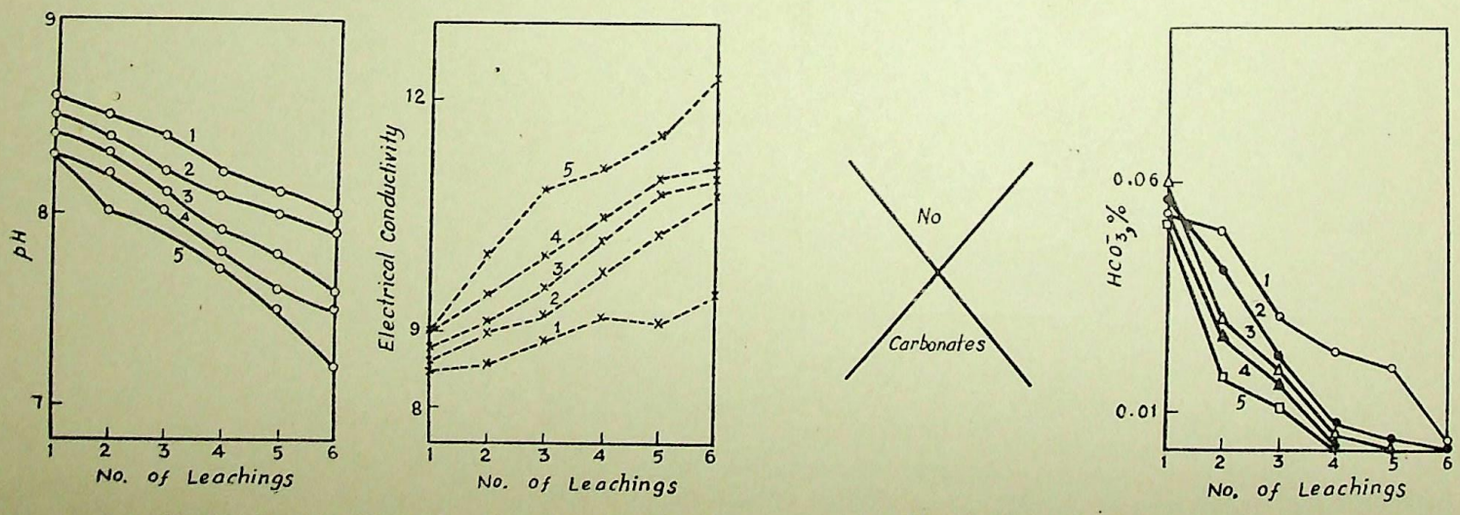

FIG. 3. Leaching effects of a saline soil (GP_1) with solution containing Ca^{2+}/Na^+ 1–5 on *p*H, EC, CO_3 and HCO_3.

up to the third leachate and then increase regularly up to sixth leachate in presence of 1 m.e. and 2 m.e. Ca^{2+} but with 4 and 5 m.e. Ca^{2+} there is not much decrease in EC. A decrease in EC with successive leachings of this profile again points to the phenomenon of adsorption or precipitation of Ca^{2+} as $CaCO_3$ because sufficient soluble CO_3^{2-} is available in the system.

Chial Profile (CP)

In Chial profile which is also alkali profile, the drop in *p*H is gradual, the ultimate *p*H of sixth leachate with 5 m.e. Ca^{2+} being 8·2. EC values of successive leachates denote a gradual increase. However, EC decreases up to the third leaching in presence of 2 m.e. Ca^{2+} and then increases. In this profile also, no CO_3^{2-} is observed after fifth, fourth, third and second leaching in presence of 1, 2, 3, 4 and 5 m.e. Ca^{2+}. However, with 1 and 2 m.e. Ca^{2+}, HCO_3^- is observed up to sixth leachate.

Handia Profile (HP)

Handia profile (Fig. 2*a*), which is saline-alkali profile, indicates somewhat a different trend with respect to *p*H and EC values. The drop in *p*H of the first leachate with increasing Ca^{2+} is noteworthy. The *p*H drops from 9·2 to 8·2 by leaching with 5 m.e. Ca^{2+}. EC increases gradually at all concentrations of Ca^{2+} with a break in second leachate at lower concentrations.

There is a sudden decrease in CO_3^{2-} up to the third leaching after which it disappears. HCO_3^- is observed up to sixth leachate except with 5 m.e. Ca^{2+} where it is absent after fourth leaching. Katoghan and Soraon profiles (Figs. 2*b*, 2*c*) exhibit similar changes in *p*H, EC, CO_3^{2-} and HCO_3^-.

Ghurpur Profile (GP)

In Ghurpur profile (Fig. 3), which is saline type, the changes with respect to *p*H, EC, CO_3^{2-} and HCO_3^- are different. The changes in *p*H are only slight and vary in a small range. EC regularly increases with increasing Ca^{2+}/Na^+ ratio. Soluble carbonates are entirely absent and HCO_3^- ions usually decrease with an increase in Ca^{2+} in the leaching water.

Changes in the Exchange-complex

The analysis of the soils left after repeated leaching with solution having $Ca^{2+}/Na^+ = 1$–5 is reported in Table II. It is observed that exchangeable Ca^{2+} in Phulpur profile has increased from 2·85 to 6·8 m.e. per 100 g of soil, after leaching with 5 m.e. Ca^{2+} plus 1 m.e. Na^+ while exchangeable Na^+ decreased from 9·2 to 1·75 m.e. per 100 g soil. In Meja profile, exchangeable Ca^{2+} increases from 5·8 to 6·2 and Na^+ decreases from 6·2 to 2·1. In Handia

TABLE II

Chemical changes in upper layers of soil profiles as influenced by leaching with mixed salt solution of $CaCl_2$ and $NaCl$

Soil profiles	Exchangeable calcium (m.e./100 g) at Ca^{2+}/Na^{++} ratios					Exchangeable sodium (m.e./100 g) at Ca^{2+}/Na^{+} ratios					Range of increase of Ex. Ca/Ex Na* of soils as Ca^{2+}/Na^{+} changes from 1 to 5	
	1	2	3	4	5	1	2	3	4	5	Range	Times increase
PP_1	2·85	3·2	4·5	5·2	6·8	9·2	8·5	6·2	4·6	1·7	0·30–4	12·80
MP_1	1·80	1·5	3·0	4·6	5·8	6·2	5·2	5·0	3·8	2·1	0·30–2·8	9·52
CP_1	2·50	3·1	4·2	5·8	6·5	6·2	5·0	3·9	2·6	1·3	0·40–5	12·50
HP_1	6·50	7·4	8·5	9·0	10·4	10·2	8·4	5·2	3·7	1·6	0·66–6·5	9·75
KP_1	4·50	5·6	5·8	6·8	7·5	9·2	8·5	6·5	4·8	3·8	0·50–2	4·00
SP_1	3·40	4·6	5·2	6·5	8·2	5·8	4·2	3·5	2·8	1·6	0·59–5·1	8·67
GP_1	5·80	5·3	5·4	5·5	6·0	1·2	1·3	1·2	1·2	0·8	4·80–7·5	1·30

* Increase in Ex. Ca/decrease in Ex. Na when the same soil is leached six times with salt solutions containing Ca^{2+}/Na^{+} varying from 1 to 5.

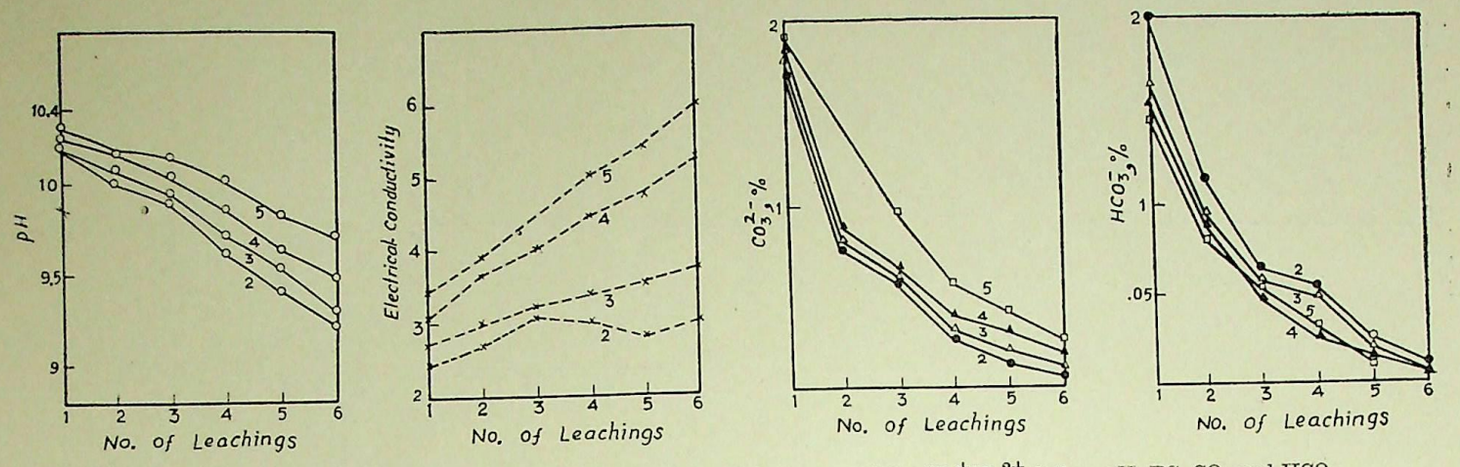

FIG. 4*a*. Leaching effects of a nonsaline-alkali soil (PP_1) with solution containing Na^+/Ca^{2+} 2–5 on *p*H, EC, CO_3 and HCO_3.

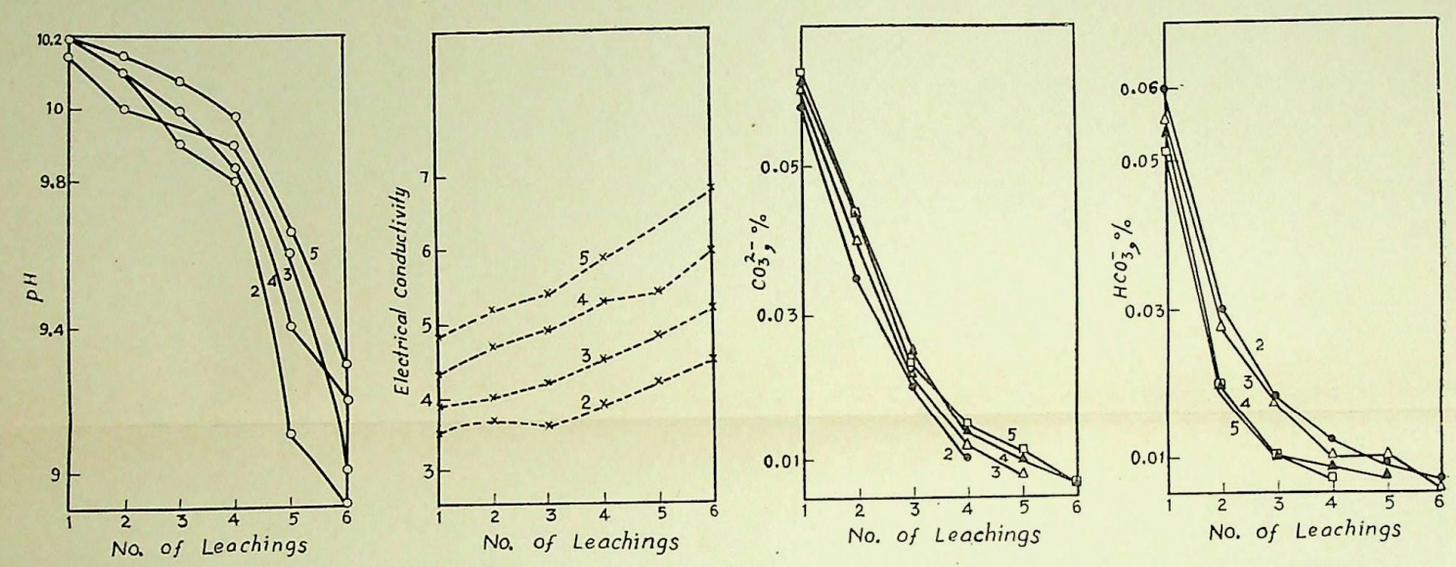

FIG. 4*b*. Leaching effects of a nonsaline-alkali soil (MP_1) with solution containing Na^+/Ca^{2+} 2–5 on *p*H, EC, CO_3 and HCO_3.

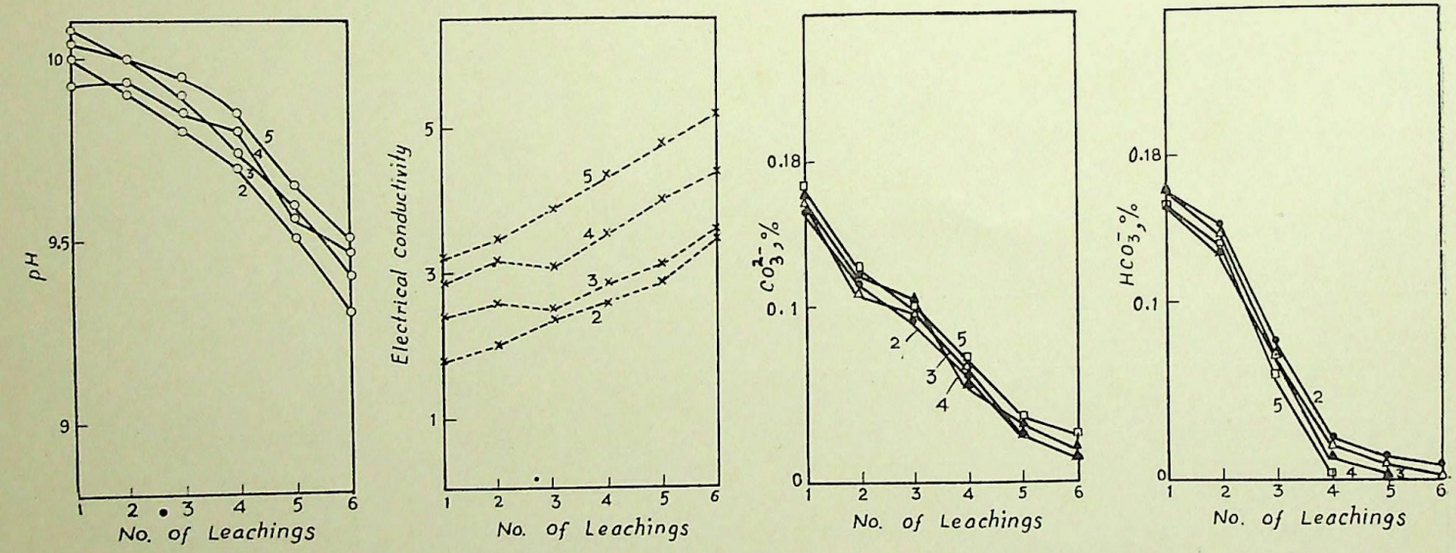

FIG. 4*c*. Leaching effects of a nonsaline-alkali soil (CP_1) with solution containing Na^+/Ca^{2+} 2–5 on *p*H, EC, CO_3 and HCO_3.

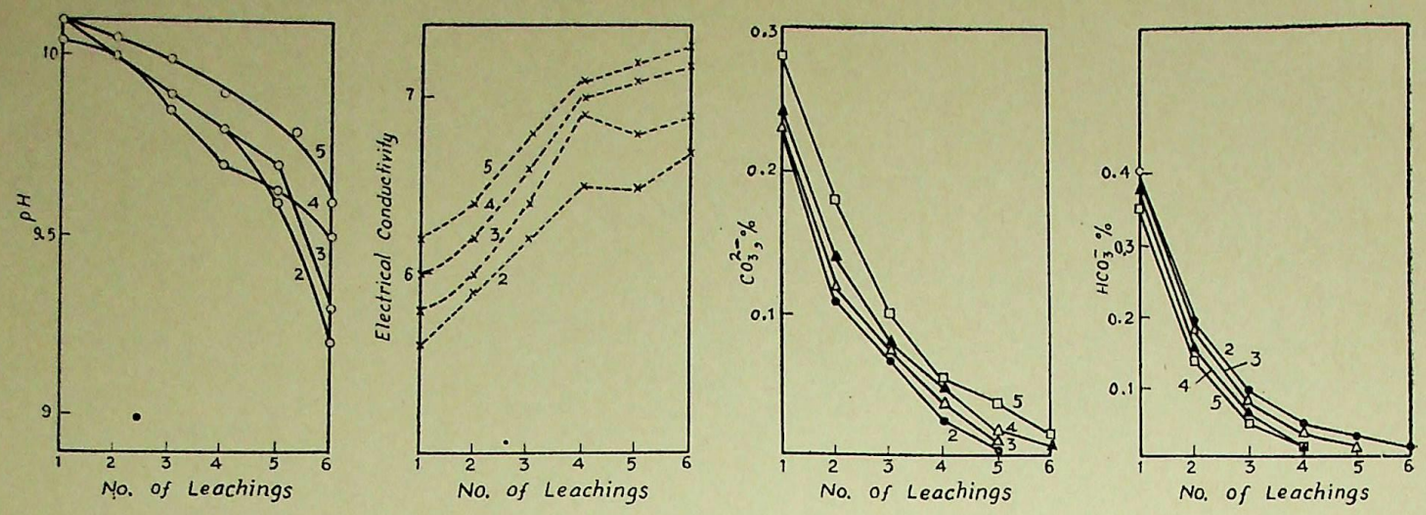

FIG. 5*a*. Leaching effects of a saline-alkali soil (HP_1) with solution containing Na^+/Ca^{2+} 2–5 on *p*H, EC, CO_3 and HCO_3.

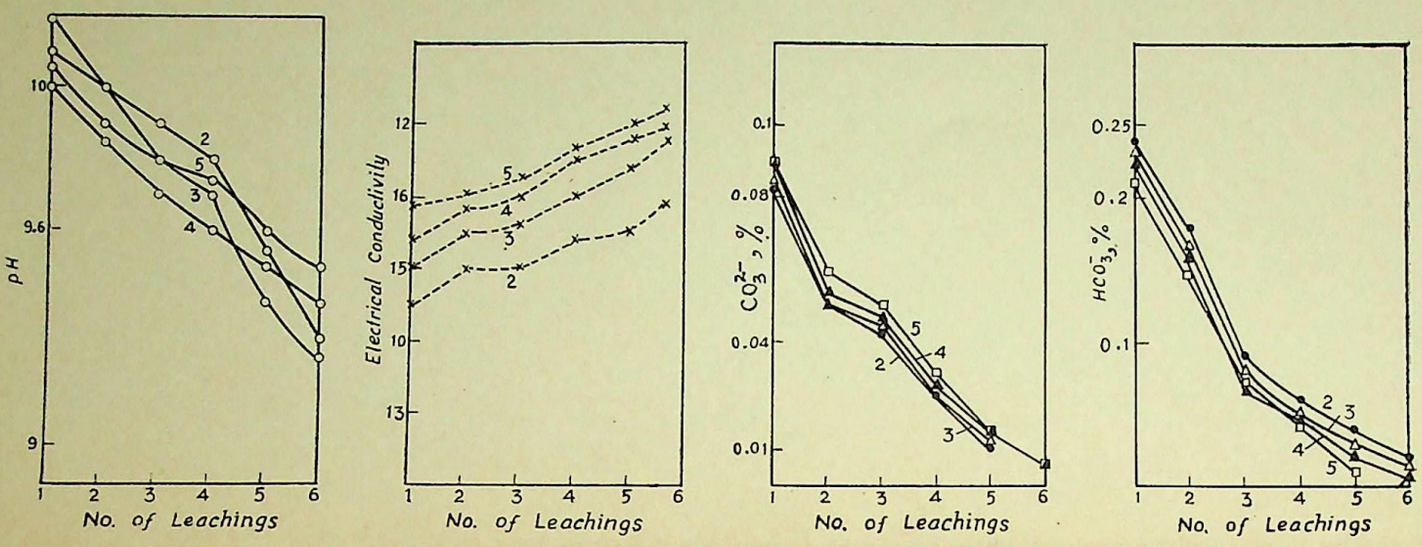

FIG. 5*b*. Leaching effects of a saline-alkali soil (KP_1) with solution containing Na^+/Ca^{2+} 2–5 on *p*H, EC, CO_3 and HCO_3.

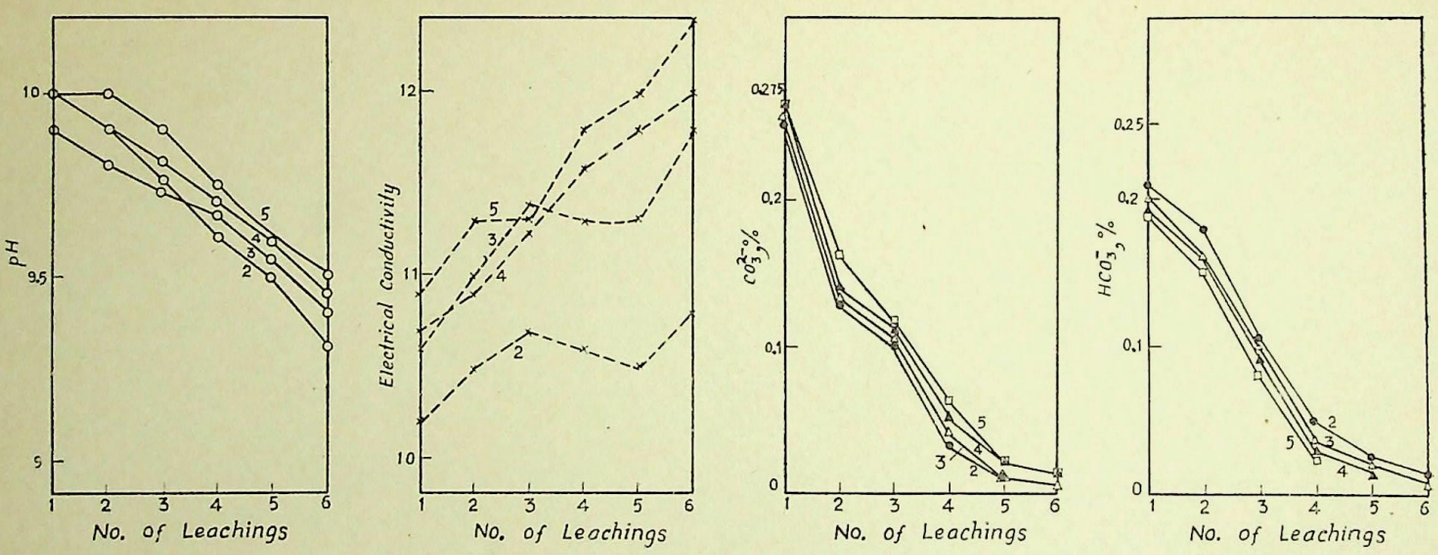

FIG. 5*c*. Leaching effects of a saline-alkali soil (SP_1) with solution containing Na^+/Ca^{2+} 2–5 on *p*H, EC, CO_3 and HCO_3.

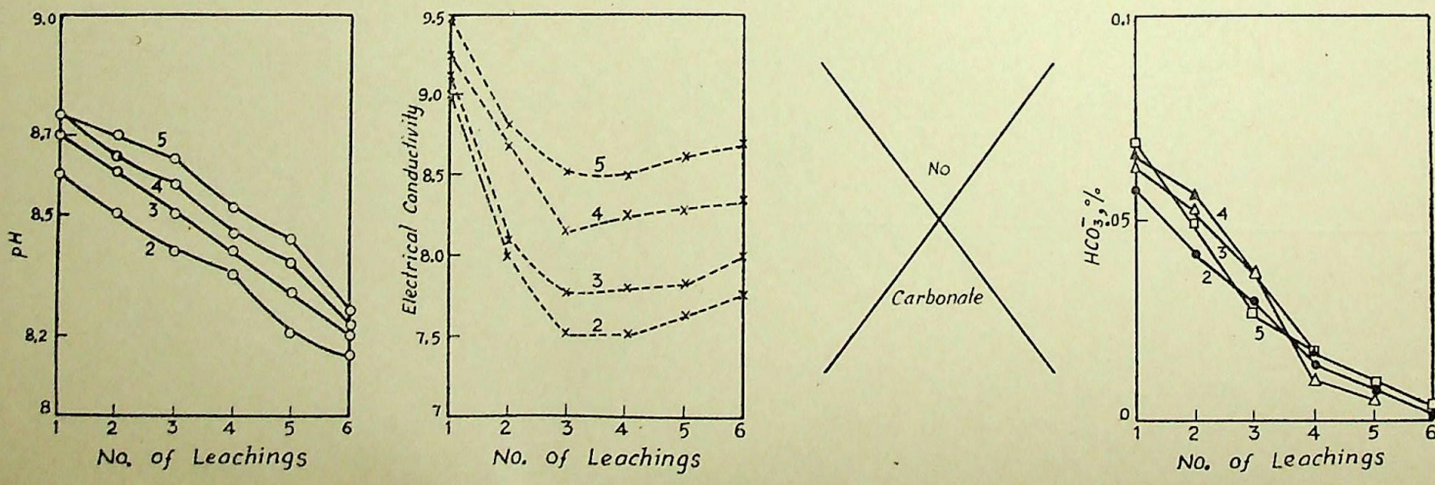

FIG. 6. Leaching effects of a saline soil (GP_1) with solution containing Na^+/Ca^{2+} 2–5 on *p*H, EC, CO_3 and HCO_3.

profile, the changes in exchangeable Ca^{2+} and Na^{+} are from 6·5 to 10·4 and 10·2 to 1·6, respectively. In Ghurpur profile, the changes are from 5·8 to 6·0 and 1·2 to 0·8, respectively. There is a regular increase in exchangeable Ca^{2+} and simultaneous decrease in exchangeable Na^{+} of all the leached soils. The quanta of increase in Ex. Ca^{2+}/Na^{+} ratio as a result of change in the ratio of Ca^{2+}/Na^{+} from 1 to 5 in leaching solutions are also tabulated (Tables II and III).

(b) Leaching with Salt Solution Containing Excess Na^{+}

The results of the changes in *p*H, EC, soluble CO_3^{2-} and HCO_3^{-} have been represented in the form of graphs (Figs. 4*a* to 6) for Phulpur, Meja, Chial, Handia, Katoghan, Soraon and Ghurpur soils, respectively.

Phulpur, Meja and Chial Profiles

From Fig. 4*a* it is observed that there is a regular drop in *p*H, as the Phulpur soil is leached successively but, on the contrary, *p*H of the leachates shows an increase. As the Na^{+}/Ca^{2+} ratio is increased from 2 to 5, a regular increase in the *p*H values is observed. The highest *p*H is noticed at 5 m.e. Na^{+}, the *p*H of the first leachate being as high as 10·3. This *p*H value decreases very slowly and finally stops at 9·7.

The EC values increase with increasing concentration of Na^{+} as the leaching is continued. As the Na^{+}/Ca^{2+} of leaching water is 2, this value is 2·4 and, when the concentration is increased to 5, this value increases to 3·4 mmhos/cm in the first leaching. When the soil is repeatedly leached with a higher concentration of Na^{+}, there is pronounced increase in the EC values, the exception being the leaching with $Na^{+}/Ca^{2+} = 2$, where it decreases after third leaching and then increases.

With each Na^{+}/Ca^{2+} ratio, repeated leachings mark a decrease in soluble CO_3^{2-} content, but it is not completely absent even after six leachings. It is curious that a high Na^{+}/Ca^{2+} ratio in the leaching solution is directly related with the appearance of soluble carbonates in the leachates. There is a regular increase in the soluble CO_3^{2-} with the increasing Na^{+} content. Quite contrary results are, however, noticed for soluble HCO_3^{-} appearing in the leachates, i.e. in presence of 2 m.e. Na^{+}, a concentration of 0·2% HCO_3^{-} is noticed in the first leachate but it decreases to 0·144% at 5 m.e. Na^{+}. It is interesting to note that with lower concentration of Na^{+} the leachates show high CO_3^{2-} and HCO_3^{-}. At Na^{+}/Ca^{2+} ratio of 5, the first leachate shows 0·144% and the fifth leachate 0·008% HCO_3^{-} but, in the sixth leachate, no HCO_3^{-} is observed. In the case of Meja and Chial profiles (Figs. 4*b*, *c*), leaching effects are similar to Phulpur profile. It is essentially due to similar nature of these profiles.

TABLE III

Chemical changes in different soil profiles as influenced by leaching with mixed salt solution of $CaCl_2$ and $NaCl$

Soil profiles	Exchangeable calcium (m.e./100 g) at Na^+/Ca^{2+} ratios					Exchangeable sodium (m.e./100 g) at Na^+/Ca^{2+} ratios					Range of increase of Ex. Ca/Ex. Na* ratios of soil as Ca^{2+}/Na^+ changes from 2 to 5	
	1	2	3	4	5	1	2	3	4	5	Range	Times increase over the second
PP_1	2·85	2·9	3·1	3·3	2·9	9·2	9·3	8·8	8·4	8·7	0·3–0·30	Slight
MP_1	1·80	2·3	2·5	2·7	2·4	6·2	5·8	5·3	5·1	5·3	0·4–0·45	,,
CP_1	2·50	2·7	3·1	4·0	3·5	6·2	5·4	4·5	3·8	4·2	0·5–0·58	,,
HP_1	6·50	6·8	7·2	8·0	7·5	10·2	9·8	8·5	8·0	8·4	0·7–0·90	,,
KP_1	4·50	4·8	5·2	5·5	5·2	9·2	9·0	8·6	8·3	8·5	0·5–0·60	,,
SP_1	3·40	3·9	4·2	4·5	4·0	5·8	5·2	4·8	3·9	4·2	0·7–1·00	,,
GP_1	5·80	5·7	5·9	6·0	5·7	1·2	1·4	1·2	1·0	1·4	4·0–4·00	,,

* Increase in Ex. Ca/decrease in Ex. Na shows a slight increase as the same soil is leached six times with salt solutions containing Na^+/Ca^{2+} varying from 2 to 5.

Handia, Katoghan and Soraon Profiles

When leaching is done with Handia, Katoghan and Soraon saline-alkali profiles (Figs. 5*a*, 5*b*, 5*c*) the trend in *p*H change is somewhat different. In Handia soil (Fig. 5*a*), the changes in *p*H of the successive leachates are not very marked with increasing concentrations of Na^+ in leaching water. Also, although *p*H increases with increased concentration of Na^+ (from 2 to 5 m.e.), the successive leachates do not show any marked change. This type of trend is not noticed with the soils of Phulpur, Meja and Chial profiles.

There is a regular increase* in EC of the successive leachates of Handia and Katoghan soils. In Soraon soil, however, the EC values show anomalous behaviour at Na^+/Ca^{2+} of 2 and 3. The EC values have generally decreased after third leaching at these concentrations of Na^+/Ca^{2+}. After fifth leachates, the conductivity has, however, increased. With $Na^+/Ca^{2+} = 4$ and 5, the tendency is towards an increase up to sixth leaching in Soraon soil.

Soluble carbonates disappear after fifth leaching, when these soils are washed with $Na^+/Ca^{2+} = 2$–3, but at higher concentrations of Na^+, CO_3^{2-} can be observed in sixth leachate. This shows that there is an increase of CO_3^{2-} with increased concentration of Na^+ in the leaching solution.

HCO_3^- regularly decreases with the increased concentrations of Na^+, so much so that after fifth leaching no HCO_3^- is observed at 3 m.e. Na^+ in Handia soil but in Soraon soil HCO_3^- is absent after fifth leaching at 4 m.e. Na^+.

Effect of Leaching a Saline Soil

Fig. 6 gives the leaching trend of saline soil. Here, at all ratios of Na^+/Ca^{2+}, there is no marked change in *p*H values hence, on increasing the concentration of Na^+ from 2 to 5 m.e. per litre, *p*H has gone up only from 8·6 to 8·8 (first leachate). At all concentrations of Na^+/Ca^{2+}, *p*H in the successive leachates has considerably decreased (the lowest value being 8·15).

EC shows peculiar behaviour in this type of soil. It has decreased up to the third leaching, after which it goes on increasing. It clearly points to an adsorption phenomenon which is confirmed by the exchangeable cations of the soil left after leaching. No carbonate ions are detected.

There is a gradual increase of HCO_3^- on increasing Na^+ concentration in this type of soil. A concentration of 0·058% HCO_3^- is noticed in the first leachate at 2 m.e. Na^+ which increases to 0·07% at 5 m.e. However, the amount of bicarbonates in the successive leachates gradually falls off at all concentrations of Na^+/Ca^{2+}.

* The increase in conductivity does not include the conductivity of the original soils.

Changes in the Exchange-complex

The soils left after six leachings were analysed for their exchangeable Ca^{2+} and Na^{+}. From Table III, it is clear that there is no decrease in the exchangeable Ca^{2+} of the soils leached with 2, 3 and 4 ratios of Na^{+}/Ca^{2+} in solutions. It is only at the ratio of 5 that exchangeable Ca^{2+} has slightly decreased. In other words, the exchangeable Ca^{2+} has increased and correspondingly exchangeable Na^{+} has decreased up to Na^{+}/Ca^{2+} ratio 4 and it is only at a ratio of 5 that the former shows a decrease.

It is clear from the results obtained that leaching of saline-alkali and alkali soils with water, containing increasing concentrations of Ca^{2+}, is quite effective in displacing exchangeable Na^{+} from the exchange-complex to a great extent. It shows, therefore, that if an irrigation water contains soluble calcium salts and is applied repeatedly to the soils followed by careful drainage practices, the soils can be successfully reclaimed. In both types of soils, i.e. saline-alkali and alkali, the process of leaching consists in replacing exchangeable Na^{+} by Ca^{2+} and then washing out the products of the exchange in the form of water-soluble salts, coupled with a decrease in *p*H which is quicker than with water alone. The displacement of Na^{+} by Ca^{++} from the exchange-complex of the soil can be illustrated as follows:

$$(1)\quad \boxed{\text{Soil}}\begin{matrix}\text{Na}\\ \text{Na}\end{matrix} + Ca^{2+} + 2Cl^{-} = \boxed{\text{Soil}}Ca + \underset{\text{(leachate)}}{2NaCl}$$

$$\text{(leaching water)}$$

$$(2)\quad CO_3^{2-} + Ca^{2+} \rightleftharpoons CaCO_3 .$$

Findings and Recommendations

The greater the amount of Ca^{2+} in leaching water, the greater is the success. The chemical amelioration of alkali soil may, thus, be brought about by the application of any calcium salt which is soluble in water to give sufficient Ca^{2+} in solution for the replacement of exchangeable Na^{+}. Gypsum, however, has a low solubility and in its comparison $CaCl_2$ is preferable because NaCl is formed as a result of the exchange reactions which is easier to wash out from the soil.

Leaching of saline-alkali and alkali soils under investigation is not effective with low concentrations of Ca^{2+}, i.e. when they were leached with solutions containing 1 m.e. and 2 m.e. Ca^{2+} the alkalinity did not decrease even after sixth leaching and the soil left over gave an alkaline reaction. Saline soil, when leached with different concentration of Ca^{2+}, usually behaved as if it is being leached with water alone. However, some interesting features of the experiments are noteworthy. At low Ca^{2+} concentrations in the leaching solutions, there is a decrease in exchangeable Ca^{2+} rather than an increase and the exchangeable Na^{+} remains practically constant. It is only at 5 m.e.

of Ca^{2+} that the exchangeable Ca^{2+} in the treated soil increased with a concomitant decrease in exchangeable sodium. Kelley and Thomas (1928), while conducting reclamation experiments of Fresno type black alkali soil, observed that leaching without chemical amendments failed to bring about desired chemical changes in the exchange-complex of the soil, which appears to support the present findings.

In saline-alkali and alkali soils there is a regular increase in *p*H value of the leachates as Na^+/Ca^{2+} concentration in leaching water is increased. It is, however, interesting to note that *p*H values of the successive leachates go on decreasing. This can be explained to be due to a continuous removal and subsequent decrease in the concentration of soluble CO_3^{2-} in the leachate coupled with the hydrolysis of some sodium from the exchange-complex because the hydrolysis of sodium from the exchange-complex and absorption of CO_2 may lead to the appearance of CO_3^{2-} according to the equation:

$$\text{Na-soil} + H_2O \rightarrow NaOH + \text{H-soil}$$
$$2NaOH + CO_2 \rightarrow Na_2CO_3 + H_2O.$$

However, due to the presence of soluble Na^+ in leaching water, the possibility of the hydrolysis of sodium from the exchange-complex is ruled out and also because the *p*H of the successive leachates have not increased, the continued presence of CO_3^{2-} in leachates has to be ascribed to some other cause. The presence of CO_3^{2-} up to the sixth leachate may, therefore, be due to the solubility of carbonates (from alkaline earth carbonates present in soils) in salt solution. It has been observed by Kelley (1951) that carbonates are more soluble in neutral salt solution than in distilled water and since the soils under investigation are rich in alkaline earth carbonates, especially $CaCO_3$, the presence of CO_3^{2-} as a result of leaching noted in the leachates is logical. The higher the Na^+ in the leaching water, the higher is the CO_3^{2-} concentration in the leachates.

Leachings of salt-affected soils respond differently depending upon the presence of exchangeable sodium and EC values. It has been found that leaching of saline-alkali (PP_1, MP_1, CP_1), nonsaline-alkali (HP_1, KP_1, SP_1) and saline soils (GP_1) could bring about three types of chemical changes. When the above types of soils are leached either with increasing ratio of Ca^{2+}/Na^+ or Na^+/Ca^{2+}, there is a marked change in the *p*H and EC values. It has been found that by leaching saline-alkali soils, *p*H decrease is rather sharp in contrast to the *p*H decrease in the case of nonsaline-alkali soils. In both types, CO_3^{2-} also decreases which forms the fundamental criterion in reclaiming alkali soils. In Ghurpur soil (saline type), the changes are rather different. The *p*H, however, tends to increase slightly with increasing ratio of Na^+/Ca^{2+}. This rules out the applicability of leaching the saline soils with waters containing soluble sodium.

The soils left after leaching give increased content of exchangeable Ca^{2+} and decreased exchangeable Na^{+}. This shows the beneficial effects of reclaiming device with water containing $Na^{+}/Ca^{2+} = 4$, but, when the content of soluble Na^{+} becomes higher than this value, the soils cannot be reclaimed.

References

Bower, C. A., and Reeve, R. C. (1960). Use of high salt water as flocculant and source of divalent cation for reclaiming sodic soil. *Soil Sci.*, **90** (2).

Christiansen, J. E. (1947). Some permeability characteristics of saline and alkali soils. *Agric. Engng, St. Joseph, Mich.*, **28**, 147–50.

Fireman, M. (1944). Permeability measurements on disturbed soil samples. *Soil Sci.*, **58**, 337–53.

Fireman, M., and Bodman, G. H. (1940). Effect of saline irrigation water on permeability. *Proc. Soil Sci. Soc. Am.*, **4**, 71–77.

Jackson, M. L. (1962). Soil Chemical Analysis. Asia Publishing House, Bombay, 46–47.

Kelley, W. P. (1951). Alkali Soils, their Formation, Properties and Reclamation. Reinhold Publishing Corporation, New York, 23.

Kelley, W. P., and Thomas, E. E. (1928). Reclamation of the Fresno type black alkali soil. *Bull. Calif. Agric. Expt. Stn.*, **455**, 1–37.

Quirk, J. P., and Schofield, R. K. (1955). The effect of electrolyte conc. on soil permeability. *J. Soil Sci.*, **6**, 163–78.

U.S. Salinity Laboratory (1954). Diagnosis and Improvement of Saline and Alkali Soils. U.S.D.A. Handbook, 60.

Wilcox, L. V. (1950). Electrical conductivity. *J. Am. Waterworks Assoc.*, **42**, 775–76.

THE DIPOLE MOMENTS OF SOME 2-PYRIDONES *

by Sekharipuram V. Anantakrishnan, F.N.I., *and* P. John Jacob,
Department of Chemistry, Madras Christian College, Madras 59

(*Received 27 February 1969*)

The dipole moments of *N*-methyl pyridone, 3 : 5-dibromo *N*-methyl pyridone and 5-bromopyridone have been measured in benzene and dioxan solutions at 35 °C. The values have been compared with those calculated allowing for intra-molecular electrostatic induction. While the *N*-methyl compounds indicate a partial ionic character of the bonds, bromo derivative indicates a tautomeric system. An estimate of the relative proportion of the forms has been made.

Introduction

The 2-pyridones are of interest on account of the possible tautomerism between keto and enol forms. X-ray studies (Penfold 1953) indicate such a behaviour in the unsubstituted compound. However, a methanolic solution of *N*-methyl pyridone shows a spectrum quite different from that of 2-ethoxy pyridine. Both the unsubstituted compound and the *N*-methyl compound show an absorption band in the carbonyl region (Hoegerle and Erlenmeyer 1956). At the same time, 2-pyridone is weakly basic without carbonyl properties, unaffected by alkali, and has a typical aromatic U.V. absorption. The simple structure I is inadequate and one has to consider a possible zwitterionic structure II. The *N*-methyl derivatives similarly may be represented by both structures III and IV. Elvidge and Jackman (1961) consider that the compound has 35 per cent aromatic character.

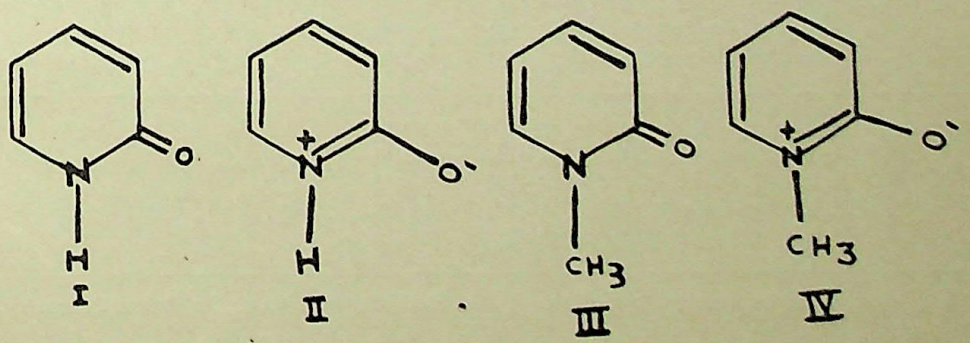

* Based on the Thesis submitted by P. J. J., approved for the Ph.D. Degree of the University of Madras in August 1963.

Experimental

The heterodyne beat method was used for the dielectric constant measurements and the circuit used by Few *et al.* (1952).

The cell used was of glass silvered to a definite height after degassing of the surface and dried at 110 °C and cooled in a vacuum desiccator before use. The cell was standardized with benzene and the dielectric constant of a solution got by the method of Everard *et al.* (1950). Dipole moments were calculated by Guggenheim's method (1951).

The solvents, benzene and dioxan, were purified by standard methods and had the following characteristics at the temperature of measurement, 35 °C.

	Dielectric constant	Refractive index	Density
Benzene ..	2·2535	1·4921	0·86278
Dioxan ..	2·1778	1·4155	1·01690

The relevant experimental data are given in Tables I, II and III.

Table I

Measurements with N-methyl pyridone

Solvent	Weight fraction W	Dielectric constant ϵ	Refractive index n	n^2	$\frac{d\epsilon}{dw}$ $w \to 0$	$\frac{dn^2}{dw}$ $w \to 0$	P
Benzene	0·0000000	2·2535	1·4934	2·2304			
	0·0053024	2·3598	1·4939	2·2317			
	0·0146420	2·4855	1·4948	2·2344	15·06	13·30	308·2
	0·0199680	2·5757	1·4951	2·2353			
	0·0361120	2·8641	1·4961	2·2383			
Dioxan	0·0000000	2·1778	1·4166	2·0068			
	0·0054301	2·2797	1·4178	2·0101			
	0·0143520	2·4502	1·4182	2·0113	18·88	0·35	341·02
	0·0199030	2·5633	1·4186	2·0124			
	0·0358840	2·8427	1·4192	2·0138			

The pyridone samples were kindly provided by Dr. B. S. Thyagarajan of the Madras University.

Discussion of Results

To obtain the calculated moments, the method of Smallwood and Herzfeld (1930) modified by Frank (1935) has been used for evaluating the induced

TABLE II

Measurements with 3:5-dibromo N-methyl pyridone

Solvent	Weight fraction W	Dielectric constant ϵ	Refractive index n	n^2	$\frac{d\epsilon}{dw}$ $w \to 0$	$\frac{dn^2}{dw}$ $w \to 0$	P
Benzene	0·0000000	2·2535	1·4935	2·2306			
	0·0057946	2·2882	1·4939	2·2317			
	0·0118080	2·3213	1·4944	2·2332	6·03	0·166	300·86
	0·0167660	2·3528	1·4950	2·2350			
	0·0236470	2·3930	1·4953	2·2359			
Dioxan	0·0000000	2·1778	1·4166	2·0068			
	0·0059586	2·2182	1·4172	2·0084			
	0·0109080	2·2525	1·4182	2·0113	6·75	0·356	287·21
	0·0157640	2·2913	1·4188	2·0130			
	0·0202540	2·3241	1·4194	2·0147			

TABLE III

Measurements with 5-bromo pyridone in dioxan

Weight fraction W	Dielectric constant ϵ	Refractive index n	n^2	$\frac{d\epsilon}{dw}$ $w \to 0$	$\frac{dn^2}{dw}$ $w \to 0$	P
0·0000000	2·1778	1·4166	2·0068			
0·0056417	2·2009	1·4174	2·0088			
0·0107620	2·2194	1·4183	2·0116	4·33	0·515	110·90
0·0146200	2·2318	1·4187	2·0127			
0·0184570	2·2441	1·4192	2·0141			

moments. The model for the purpose has been taken from Penfold's (1953) crystallographic work. In the methyl pyrrolidone, the moments involved are those due to two C—N bonds, the C=O bond and CH_3—N bond. While in the bromo compounds C—B_2 and possibly C—OH bonds have also to be taken into account, using scale models with the distances indicated in Fig. 1.

The calculated induced moments resolved in the perpendicular directions are presented in Table IV. The experimental and calculated values are given in Table V. Polarizability of the nitrogen atom is calculated from the atom refraction of tertiary nitrogen using the formula $\alpha = \frac{3R}{4\pi N_A}$, where R is molar refraction and N_A, Avogadro number. Other atom polarizabilities were similarly obtained as in our work with the coumarins.

The experimental values are in agreement with those reported earlier by Albert and Philips (1956) for *N*-methyl pyridone. The vector sum of

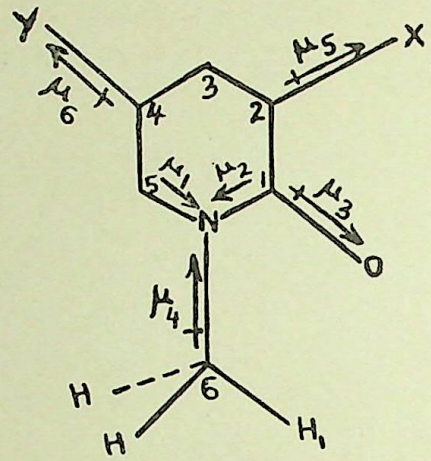

FIG. 1

Distances in A °		Angles in °	
N—C_1	1·401	N	125·1
C_1—C_2	1·444	C_1	112·9
C_2—C_3	1·334	C_2	122·3
C_3—C_4	1·421	C_3	122·2
C_4—C_5	1·371	C_4	116·0
C_5—N	1·375	C_5	121·8
N—C_6	1·480		
C_1—O	1·236		

TABLE IV

Resultant induced moments

Compound	Primary moment	*Induced moments*			
		μ_{ix} unreduced	μ_{ix} reduced	μ_{iy} unreduced	μ_{iy} reduced
	C—N	+0·3286	+0·2008	−0·5429	−0·3319
N-methyl pyridone	C—N	+0·1844	+0·1127	−0·2892	−0·1768
	C=N	+1·9735	+1·2070	+0·6784	+0·4147
	N—CH_3	+0·2179	+0·1332	+0·1184	+0·0741
3 : 5-dibromo					
N-methyl pyridone	C—N	+0·3800	+0·2323	−0·5226	−0·3195
	C—N	+0·2377	+0·1467	−0·2971	−0·1816
	C=O	+2·0483	+1·5400	+0·4933	+0·3015
	N—CH_3	+0·2509	+0·1532	+0·0447	+0·0273
	5 : C—B_2	+1·6842	+1·0290	−0·0896	−0·0547
	3 : C—B	+1·4281	+0·8728	−0·8829	−0·5396
	C—N	+0·1906	+0·1165	−0·2948	−0·1802
5-bromo pyridone	C—N	+0·1516	+0·0927	−0·1840	−0·1125
	C=O	+2·3286	+1·4230	+0·3452	+0·2110
	N—CH_3	+0·7447	+0·4552	+0·4555	+0·2784
	5 : C—B	+1·5717	+0·9610	−0·0979	−0·0598

the moments leads to a very low value. The earlier workers attribute the high value to the mesoionic character of the bond. Our results with hydroxy and methyl coumarin derivatives (Anantakrishnan and Jacob 1969) and with substituted *p*-xylenes (Anantakrishnan and Rao 1964) indicated a possible

TABLE V

Dipole moment values in Debye units

Compound	Experimental value		Calculated value
	Benzene	Dioxan	
N-methyl pyridone	3·95	4·15	3·00
3 : 5-dibromo *N*-methyl pyridone	3·90	3·81	3·10
5-bromo pyridone	—	2·37	0·60 (keto) 2·56 (enol)

interaction between the methyl hydrogen and group like C=O and $-NO_2$ and we have to consider a similar situation here. Also, one cannot rule out intramolecular hydrogen bonding as well. Elvidge and Jackman (1961) have estimated using NMR measurements of chemical shifts that the compound has 35 per cent aromatic character but there is no reason for departure from planarity of the molecule. For the pyridone these authors consider also the extreme non-aromatic structures V and VI. Taking the ionic form

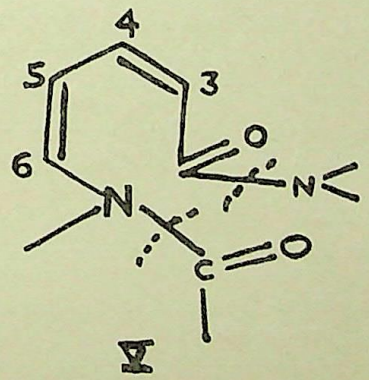

V

Fixed bond model structure A

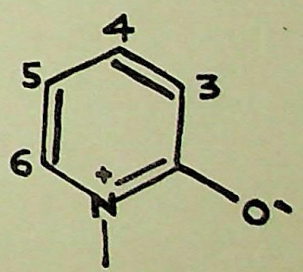

VI

Non-resonating azacyclohexatriene not a hybrid

of the compound, a moment of 11·04*D* making an angle of 45° with the direction of the covalent structure could be calculated. Using the covalent moment of 3·0*D* and the experimental value, the partial ionic character of the bond can be obtained using the equation

$$3{\cdot}95^2 = [3{\cdot}0(1-x)+11{\cdot}04\ x\ \cos\ 45]^2+[11{\cdot}04\ x\ \sin\ 45]^2.$$

The solution of this leads to a value of 16 per cent ionic contribution. The difference in estimates can arise from the uncertainties of the calculation and departure from planarity of the molecule. It is also well to recall the discussion on NMR studies where the limitations of using only dipole moments in the estimates are referred to.

3 : 5-dibromo *N*-methyl pyridone is different in several ways. X-ray studies (Sarma, personal communication) have shown that the molecule is completely non-planar and bond angles also differ from the parent compound and this is also borne out by scale models. The U.V. absorption spectrum shows a shift to longer wavelengths (Bradlow 1951). The difference between the calculated and observed values may suggest a large mesomeric moment but the steric effects adversely affect this contribution. The inadequacy of structural information precludes a precise calculation of the induced moments in the plane of the ring. There is also the consequent uncertainty in the angle between the direction of dipole and the line joining any position of the ring to the dipole centre, which affects the calculation. Small differences in 'r' can seriously alter the final figure, since it appears as a cubic function in the equation.

3-bromo pyridone presents a still different picture. Unlike the other two compounds, there is here the distinct possibility of keto-enol tautomerism. The moment clearly indicates a dominant enolic form. Association through intramolecular hydrogen bonding cannot be completely excluded. From the values calculated for the keto and enol forms and assuming that this association is not significant, the observed value corresponds to 15 per cent keto form at 35 °C in dioxan solution. The compound is thus essentially a hydroxy pyridine. This may be compared with the much larger estimate for the keto form from Penfold's crystallographic data. Further solvent solute interaction can preferentially stabilize the hydroxy form in dioxan.

References

Albert, A., and Philips, J. N. (1956). Ionization constants of heterocyclic substances. *J. Chem. Soc.*, 1294–1304.

Anantakrishnan, S. V., and Jacob, P. John (1969). Dipole moments of some coumarin derivatives—Parts I and II. *Indian J. Chem.*, under publication.

Anantakrishnan, S. V., and Rao, D. Setu (1964). Dipole moments of *p*-zylene derivatives. *Proc. Indian Acad. Sci.*, 60 A, 201–10.

Bradlow, L. (1951). Oxidation of some β-substituted pyridine alkiodides. *J. org. Chem.*, 16, 73–83.

Elvidge, J. A., and Jackman, L. M. (1961). Studies of aromaticity by nuclear magnetic resonance spectroscopy—Part I. *J. Chem. Soc.*, 859–66.

Everard, K. B., Hill, R. P. W., and Sutton, L. E. (1950). Evaluation of electric dipole moments. *Trans. Faraday Soc.*, 46, 417–23.

Few, A. V., Smith, J. W., and Witten, L. B. (1952). Accurate measurement of the dielectric constant of solutions. *Trans. Faraday Soc.*, 48, 211–15.

Frank, F. C. (1935). Dipole induction effect in dipole moment measurements. *Proc. R. Soc.*, 152 A, 171–96.

Guggenheim, E. A. (1951). Computation of electric dipole moments. *Trans. Faraday Soc.*, 47, 573–76.

Hoegerle, K., and Erlenmeyer, H. (1956). Uber die Reaktion Von α Pyridone Mit Chloramin. *Helv. chim. Acta.*, 39, 1203–7.

Penfold, A. R. (1953). Electron distribution in crystalline α pyridone. *Acta crystallogr.*, 6, 591–600.

Sarma, V. R. (Personal Communication).

Smallwood, H. M., and Herzfeld, K. F. (1930). Dipole moments of disubstituted benzenes. *J. Am. Chem. Soc.*, 52, 1919–27.

POTENTIALS FROM MODIFIED MATHIEU EQUATION

by L. K. Sharma, *Department of Applied Physics, Govt. Engineering College, Rewa (M.P.)*

(Communicated by P. L. Bhatnagar, F.N.I.)

(*Received 8 April 1970*)

A few solvable potentials for the Schrödinger equation have been evaluatad through modified Mathieu equation following the method of Bhattacharjie and Sudarshan (1962). The same potentials have also been obtained using the technique formulated by Bose (1963), thereby establishing the fact that the two methods agree with each other.

Solutions of the Schrödinger equation under one of the potentials constructed, viz.

$$V(r) = -V_0 \cosh 2\alpha r,$$

have been derived in terms of the product of H-function introduced by Fox and confluent hypergeometric function. Finally, the expression for the s-matrix has been obtained.

1. Introduction

Bhattacharjie and Sudarshan (1962) formulated a general method for deriving solvable potentials for the s-wave Schrödinger equation. Here they applied suitable functional transformations to a second-order differential equation. Finally, the expressions for which the transformed equation may behave as Schrödinger equation are deduced by choosing two conditions, viz. (a) setting the first derivative equal to zero and (b) setting the coefficient of the function $\phi(r)$ equal to $\{k^2-v(r)\}$ of the Schrödinger equation. It is then the variable term appearing in the latter condition that gives the potential to be evaluated.

Bose (1963), starting with the normal form of a second-order differential equation, transformed it to a form $\phi''+I_s(r)\phi = 0$, where

$$I_s(r) = z'^2 I(z)+\tfrac{1}{2}\{z, r\}, \{z, r\}$$

being the Schwarzian derivative. Thus for the condition under which this equation may behave as one variable Schrödinger equation, $I_s(r)$ should be equal to $\{k^2-v(r)\}$. Therefore, the variable term included in $I_s(r)$ supplies the potential to be evaluated.

Aly and Spector (1965) utilizing the modified Mathieu equation and following the technique of Bose constructed an inverse fourth power singular potential.

Sharma and Varma (1970) using the method of Bhattacharjie and Sudarshan evaluated a few solvable potentials from Whittaker and Jacobi differential equations.

The object of this paper is to construct further solvable potentials for the Schrödinger equation using the method of Bhattacharjie and Sudarshan through modified Mathieu equation. This has been done in section 2.

Finding that one of the potentials evaluated in section 2 is again an 'inverse fourth power potential', it can be said that the two general methods used for constructing solvable potentials for the Schrödinger equation completely agree in the sense that they give exactly similar results.

In section 3, it is further proved that the results obtained by these techniques are exactly the same.

In section 4, the solution of one of the potentials generated has been derived in terms of the product of H-function introduced by Fox (1961) and confluent hypergeometric function and then finally the expression for the s-matrix has been obtained.

2. Bhattacharjie and Sudarshan Technique

The modified Mathieu differential equation is given as

$$\psi''(x)-(a-2q\cosh 2x)\psi(x)=0. \quad .. \quad .. \quad .. \quad (2.1)$$

Applying the following transformations

$$z=e^x \quad \text{and} \quad \psi(z)=z^{-\frac{1}{2}}y(z),$$

eqn. (2.1) reduces to

$$y''(z)+\left[q/z^4+(\tfrac{1}{4}-a)\frac{1}{z^2}+q\right]y(z)=0. \quad .. \quad .. \quad (2.2)$$

By making further substitutions

$$z=f(r), \quad y(z)=g(r)\phi(r), \quad h(r)=\frac{d}{dr}\{\log_e g(r)\} \quad .. \quad .. \quad (2.3)$$

eqn. (2.2) is transformed to the form

$$\phi''(r)+A(r)\phi'(r)+B(r)\phi(r)=0 \quad .. \quad .. \quad .. \quad (2.4)$$

where

$$A(r)=\left[\frac{2g'(r)}{g(r)}-\frac{f''(r)}{f'(r)}\right] \quad .. \quad .. \quad .. \quad .. \quad .. \quad .. \quad .. \quad (2.5)$$

and

$$B(r)=\left[\frac{g''(r)}{g(r)}-\frac{g'(r)}{g(r)}\cdot\frac{f''(r)}{f'(r)}+\frac{q\{f'(r)\}^2}{\{f(r)\}^4}+(\tfrac{1}{4}-a)\left\{\frac{f'(r)}{f(r)}\right\}^2+q\{f'(r)\}^2\right]. \quad (2.6)$$

Now for eqn. (2.4) to be of the form of the following radial Schrödinger equation

$$\phi''(r)+\left[k^2-\frac{l(l+1)}{r^2}-V(r)\right]\phi(r)=0 \quad .. \quad .. \quad (2.7)$$

$$A(r)=0 \quad .. \quad .. \quad .. \quad .. \quad .. \quad .. \quad (2.8)$$

$$B(r)=k^2-\frac{l(l+1)}{r^2}-V(r) \quad .. \quad .. \quad .. \quad .. \quad (2.9)$$

and $V(r)$ should be independent of k.

Thus eqns. (2.5) and (2.8) yield

$$f'(r) = Cg^2(r) \quad .. \quad .. \quad .. \quad .. \quad (2.10)$$

where C is a constant.

Similarly, eqns. (2.6) and (2.9) yield

$$h'(r)-h^2(r)+\frac{q\{f'(r)\}^2}{\{f(r)\}^4}+(\tfrac{1}{4}-a)\left\{\frac{f'(r)}{f(r)}\right\}^2+q\{f'(r)\}^2 \equiv k^2-\frac{l(l+1)}{r^2}-V(r). \quad (2.11)$$

Choosing $Z = f(r) = \alpha r$, we obtain

$$k^2 = \alpha^2 q, \quad V(r) = -q/\alpha^2 r^4 \quad \text{and} \quad l(l+1) = (a-\tfrac{1}{4}) \quad .. \quad .. \quad (2.12)$$

a result which is exactly similar to the one obtained by Aly and Spector (1965).

Further potentials have been constructed for s-wave Schrödinger equation ($l = 0$) by giving other values to $f(r)$.

Thus for

$$z = f(r) = e^{\alpha r} \quad .. \quad .. \quad .. \quad .. \quad .. \quad (2.13)$$

the potential has the form

$$V(r) = -V_0 \cosh 2\alpha r \quad .. \quad .. \quad .. \quad .. \quad (2.14)$$

where

$$V_0 = (2q\alpha^2) \quad \text{and} \quad k^2 = -a\alpha^2. \quad .. \quad .. \quad .. \quad (2.15)$$

Similarly, for the choice

$$z = f(r) = \tan(\alpha r+\beta) \quad .. \quad .. \quad .. \quad .. \quad (2.16)$$

$$V(r) = -q\alpha^2\{\operatorname{cosec}^2(\alpha r+\beta)+\sec^2(\alpha r+\beta)\}^2 \quad .. \quad .. \quad (2.17)$$

where

$$(\tfrac{1}{4}-a) = 2q \quad \text{and} \quad k^2 = \alpha^2. \quad .. \quad .. \quad .. \quad (2.18)$$

3. Bose Technique

In this section applying transformations similar to those as used in section 2 and following the method of Bose (1963), the potentials evaluated in eqns. (2.14) and (2.17) are rederived.

Choosing again $z(r) = e^{\alpha r}$

$$I_s(r) = \alpha^2 e^{2\alpha r}\{q/e^{4\alpha r}+(\tfrac{1}{4}-a)1/e^{2\alpha r}+q\}-\frac{\alpha^2}{4} \quad .. \quad .. \quad (3.1)$$

and thus the potential $V(r) = -V_0 \cosh 2\alpha r$ has been reconstructed.

Similarly, for the choice

$$z(r) = \tan(\alpha r+\beta)$$

$$I_s(r) = \alpha^4 \sec^4(\alpha r+\beta)[q/\tan^4(\alpha r+\beta)+(\tfrac{1}{4}-a)/\tan^2(\alpha r+\beta)+q]+\alpha^2 \quad .. \quad (3.2)$$

and we obtain once again

$$V(r) = -q\alpha^2\{\operatorname{cosec}^2(\alpha r+\beta)+\sec^2(\alpha r+\beta)\}^2.$$

The above results clearly show that the two general methods formulated for deriving solvable potentials for the Schrödinger equation give identical results.

4. Solution

As the exact solution of the inverse fourth power singular potential has been already discussed by many authors (Wannier and Vogt 1954; Spector 1964; Aly and Müller 1966; Aly *et al.* 1969), thus an attempt is made here to write the solution of the Schrödinger equation under the potential

$$V(r) = -V_0 \cosh 2\alpha r$$

[$V(r)$ repulsive for $V_0 < 0$, attractive for $V_0 > 0$].

The two solutions (McLachlan 1947) of eqn. (2.1) may be written as a product of Bessel functions

$$\psi_1(x) = K_{2p+\nu} \sum_{n=-\infty}^{\infty} (-1)^n A_{2n}^{2p+\nu} J_n(v_1) J_{n+\nu}(v_2) \quad .. \quad .. \quad (4.1)$$

and

$$\psi_2(x) = K_{2p+\nu} \sum_{n=-\infty}^{\infty} (-1)^n A_{2n}^{2p+\nu} J_{n+\nu}(v_1) J_n(v_2) \quad .. \quad .. \quad (4.2)$$

where $v_1 = \sqrt{q}e^{-x}$ and $v_2 = \sqrt{q}e^{x}$.

Thus, two solutions $\phi_1(r)$ and $\phi_2(r)$ of the Schrödinger equation for the potential under consideration can be written as

$$\phi_1(r) = \sqrt{c/\alpha} K_{2p+\nu} \sum_{n=-\infty}^{\infty} (-1)^n A_{2n}^{2p+\nu} J_n(\sqrt{q}e^{-\alpha r}) J_{n+\nu}(\sqrt{q}e^{\alpha r}) \quad (4.3)$$

and

$$\phi_2(r) = \sqrt{c/\alpha} K_{2p+\nu} \sum_{n=-\infty}^{\infty} (-1)^n A_{2n}^{2p+\nu} J_{n+\nu}(\sqrt{q}e^{-\alpha r}) J_n(\sqrt{q}e^{\alpha r}). \quad (4.4)$$

Reducing the product of Bessel functions as a product of hypergeometric functions ${}_0F_1$ (Luke 1962), we get for $\phi_1(r)$

$$\phi_1(r) = \sqrt{c/\alpha} K_{2p+\nu} (\tfrac{1}{2}\sqrt{q})^{\nu} e^{\alpha r \nu} \sum_{n=-\infty}^{\infty} \frac{(-1)^n A_{2n}^{2p+\nu} (\frac{1}{4}q)^n}{\Gamma(n+1)\Gamma(n+\nu+1)} {}_0F_1(\overline{n+1};\ -\tfrac{1}{4}qe^{-2\alpha r})$$

$$\times {}_0F_1(\overline{n+\nu+1};\ -\tfrac{1}{4}qe^{2\alpha r}). \quad .. \quad .. \quad .. \quad .. \quad .. \quad .. \quad (4.5)$$

From eqn. (2.15) $\alpha = \dfrac{ik}{\sqrt{a}}$ and if ν is set such that $\nu = \sqrt{a}$, then

$$\phi_1(r) = \sqrt{c/\alpha} K_{2p+\sqrt{a}} (\tfrac{1}{2}\sqrt{q})^{\sqrt{a}} e^{ikr} \sum_{n=-\infty}^{\infty} \frac{(-1)^n A_{2n}^{2p+\sqrt{a}} (\frac{1}{4}q)^n}{\Gamma(n+1)\Gamma(n+\sqrt{a}+1)}$$

$$\times {}_0F_1(\overline{n+1};\ -\tfrac{1}{4}qe^{-2\alpha r}) {}_0F_1(\overline{n+\sqrt{a}+1};\ -\tfrac{1}{4}qe^{2\alpha r}). \quad .. \quad (4.6)$$

Thus, the general solution $\phi(r)$ may be written as

$$\phi(r) = Ae^{ikr} \sum_{n=-\infty}^{\infty} \frac{(-1)^n A_{2n}^{2p+\sqrt{a}} (\frac{1}{4}q)^n}{\Gamma(n+1)\Gamma(n+\sqrt{a}+1)} {}_0F_1(\overline{n+1};\ -\tfrac{1}{4}qe^{-2\alpha r}) {}_0F_1(\overline{n+\sqrt{a}+1};\ -\tfrac{1}{4}qe^{-2\alpha r})$$

$$+Be^{-ikr} \sum_{n=-\infty}^{\infty} \frac{(-1)^n A_{2n}^{2p+\sqrt{a}} (\frac{1}{4}q)^n}{\Gamma(n+1)\Gamma(n+\sqrt{a}+1)} {}_0F_1(\overline{n+1};\ -\tfrac{1}{4}qe^{2\alpha r}) {}_0F_1(\overline{n+\sqrt{a}+1};\ -\tfrac{1}{4}qe^{-2\alpha r}) \quad .. \quad (4.7)$$

For evaluating the product of the functions ${}_0F_1$ in the form of ${}_0F_1[\overline{\beta_1};\ cx^2] \times {}_0F_1[\overline{b_1};\ cx^{-2}]$, we make use of the result obtained by Singh (*in press*). The expression for the required product has been derived in terms of H-function and the Hermite polynomial (*see* Appendix).

Utilizing eqn. (A5) of the Appendix, we get for the general solution

$$\phi(r) = Ae^{ikr} \sum_{n=-\infty}^{\infty} \frac{(-1)^n A_{2n}^{2p+\sqrt{a}} (\frac{1}{4}q)^n}{\Gamma(n+1)} \sum_{\mu,\,\delta=0}^{\infty} \frac{e^{(e-2\alpha r)/2} (-\frac{1}{4}q)^{\delta} 2^{\mu-\frac{1}{2}}}{(n+1;\ \delta)(\delta)!\ (\mu)!\ 2^{2\delta}}$$

$$\times H_{1,\,3}^{2,\,0}\left[q \left| \begin{matrix} \left(1+\delta-\frac{\mu}{2},\ 1\right) \\ (1+2\delta,\ 2),\ (1,\ 1),\ (-n-\sqrt{a},\ 1) \end{matrix} \right. \right] H_{\mu}(e^{-\alpha r})$$

$$+Be^{-ikr} \sum_{n=-\infty}^{\infty} \frac{(-1)^n A_{2n}^{2p+\sqrt{a}} (\frac{1}{4}q)^n}{\Gamma(n+\sqrt{a}+1)} \sum_{\mu,\,\delta=0}^{\infty} \frac{e^{(e-2\alpha r)/2} (-\frac{1}{4}q)^{\delta} 2^{\mu-\frac{1}{2}}}{(n+\sqrt{a}+1;\ \delta)(\delta)!\ (\mu)!\ 2^{2\delta}}$$

$$\times H_{1,\,3}^{2,\,0}\left[q \left| \begin{matrix} \left(1+\delta-\frac{\mu}{2},\ 1\right) \\ (1+2\delta,\ 2),\ (1,\ 1),\ (-n,\ 1) \end{matrix} \right. \right] H_{\mu}(e^{-\alpha r}) \quad .. \quad .. \quad .. \quad (4.8)$$

where $H_{1,\,3}^{2,\,0}\left[q \left| \begin{matrix} (\ldots) \\ (\ldots),\ (\ldots),\ (\ldots) \end{matrix} \right. \right]$ is the H-function and $H_{\mu}(e^{-\alpha r})$ is the Hermite polynomial.

Now denoting

$$\left.\begin{matrix} \dfrac{(-1)^n A_{2n}^{2p+\sqrt{a}} (\frac{1}{4}q)^n}{\Gamma(n+1)} & \text{by } P_n \\ \dfrac{(-1)^n A_{2n}^{2p+\sqrt{a}} (\frac{1}{4}q)^n}{\Gamma(n+\sqrt{a}+1)} & \text{by } Q_n \end{matrix}\right\} \quad .. \quad .. \quad .. \quad (4.9)$$

and writing $H_{\mu}(e^{-\alpha r})$ in terms of confluent hypergeometric function (Gradshteyn and Ryzhik 1965), the expression for the general solution may be finally

written as

$$\phi(r) = Ae^{ikr} \sum_{n=-\infty}^{\infty} P_n \sum_{\mu,\,\delta=0}^{\infty} \frac{e^{(e-2\alpha r)/2}(-\frac{1}{4}q)^{\delta} 2^{\mu-\frac{1}{2}}}{(n+1;\ \delta)(\delta)!\ (\mu)!\ 2^{2\delta}}$$

$$\times H_{1,3}^{2,0}\left[q \left| \begin{matrix} \left(1+\delta-\frac{\mu}{2},\ 1\right) \\ (1+2\delta,\ 2),\ (1,\ 1),\ (-n-\sqrt{a},\ 1) \end{matrix} \right.\right] \frac{(-1)^{\frac{\mu}{2}}(\mu)!}{\left(\frac{\mu}{2}\right)!}\, {}_1F_1\left(-\frac{\mu}{2},\ \frac{1}{2};\ e^{-2\alpha r}\right)$$

$$+Be^{-ikr} \sum_{n=-\infty}^{\infty} Q_n \sum_{\mu,\,\delta=0}^{\infty} \frac{e^{(e-2\alpha r)/2}(-\frac{1}{4}q)^{\delta} 2^{\mu-\frac{1}{2}}}{(n+1+\sqrt{a};\ \delta)(\delta)!\ (\mu)!\ 2^{2\delta}}$$

$$\times H_{1,3}^{2,0}\left[q \left| \begin{matrix} \left(1+\delta-\frac{\mu}{2},\ 1\right) \\ (1+2\delta,\ 2),\ (1,\ 1),\ (-n,\ 1) \end{matrix} \right.\right] \frac{(-1)^{\frac{\mu}{2}}(\mu)!}{\left(\frac{\mu}{2}\right)!}\, {}_1F_1\left(-\frac{\mu}{2},\ \frac{1}{2};\ e^{-2\alpha r}\right). \quad (4.10)$$

Asymptotically, i.e. $r \to \infty$

$$\phi(r) \underset{r\to\infty}{\sim} Ae^{ikr}\left\{\sum_{n=-\infty}^{\infty} P_n \sum_{\mu,\,\delta=0}^{\infty} \frac{(-\frac{1}{4}q)^{\delta} 2^{\mu-\frac{1}{2}}}{(n+1;\ \delta)(\delta)!\ (\mu)!\ 2^{2\delta}}\right.$$

$$\left.\times H_{1,3}^{2,0}\left[q \left| \begin{matrix} \left(1+\delta-\frac{\mu}{2},\ 1\right) \\ (1+2\delta,\ 2),\ (1,\ 1),\ (-n-\sqrt{a},\ 1) \end{matrix} \right.\right] \frac{(-1)^{\frac{\mu}{2}}(\mu)!}{\left(\frac{\mu}{2}\right)!}\right\}$$

$$+Be^{-ikr}\left\{\sum_{n=-\infty}^{\infty} Q_n \sum_{\mu,\,\delta=0}^{\infty} \frac{(-\frac{1}{4}q)^{\delta} 2^{\mu-\frac{1}{2}}}{(n+\sqrt{a}+1;\ \delta)(\delta)!\ (\mu)!\ 2^{2\delta}}\right.$$

$$\left.\times H_{1,3}^{2,0}\left[q \left| \begin{matrix} \left(1+\delta-\frac{\mu}{2},\ 1\right) \\ (1+2\delta,\ 2),\ (1,\ 1),\ (-n,\ 1) \end{matrix} \right.\right] \frac{(-1)^{\frac{\mu}{2}}(\mu)!}{\left(\frac{\mu}{2}\right)!}\right\}. \quad .. \quad (4.11)$$

Equation (4.11), together with the requirement $\phi(r) = 0$ at $r = 0$, yields s-matrix

$$\sum_{n=-\infty}^{\infty} P_n \sum_{\mu,\,\delta=0}^{\infty} \frac{(-\frac{1}{4}q)^{\delta} 2^{\mu-\frac{1}{2}} (-1)^{\frac{\mu}{2}}}{(n+1;\ \delta)(\delta)!\ 2^{2\delta}\left(\frac{\mu}{2}\right)!} H^{2,0}_{1,3}\left[q \left| \begin{matrix} \left(1+\delta-\frac{\mu}{2},\ 1\right) \\ (1+2\delta,\ 2),\ (1,\ 1),\ (-n-\sqrt{a},\ 1) \end{matrix} \right.\right]$$

$$S(k) = \frac{\times {}_1F_1\left(-\frac{\mu}{2}, \frac{1}{2};\ 1\right)}{\sum_{n=-\infty}^{\infty} Q_n \sum_{\mu,\,\delta=0}^{\infty} \frac{(-\frac{1}{4}q)^{\delta} 2^{\mu-\frac{1}{2}} (-1)^{\frac{\mu}{2}}}{(n+\sqrt{a}+1;\ \delta)(\delta)!\ 2^{2\delta}\left(\frac{\mu}{2}\right)!} H^{2,0}_{1,3}\left[q \left| \begin{matrix} \left(1+\delta-\frac{\mu}{2},\ 1\right) \\ (1+2\delta,\ 2),\ (1,\ 1),\ (-n,\ 1) \end{matrix} \right.\right]}$$

$$\times {}_1F_1\left(-\frac{\mu}{2}, \frac{1}{2};\ 1\right). \quad .. \quad .. \quad .. \quad .. \quad .. \quad .. \quad .. \quad .. \quad (4.12)$$

Acknowledgements

The author is grateful to Prof. R. C. Varma for his guidance and constant help throughout the preparation of this paper. Thanks are also due to Shri F. Singh for several useful discussions.

Appendix

Utilizing eqn. (4.1) derived by Singh (*in press*)

$$x_u^{2\rho} {}_vF_v\left(\begin{matrix} \alpha_1, \ldots, \alpha_u; \\ \beta_1, \ldots, \beta_v \end{matrix} cx^{2d}\right) H^{n,\,l}_{p,\,q}\left[zx^{-2m} \left| \begin{matrix} \{(a_p,\ e_p)\} \\ \{(b_q,\ f_q)\} \end{matrix} \right.\right]$$

$$= \sum_{\mu,\,\delta=0}^{\infty} \frac{\prod_{j=1}^{u} (\alpha_j,\ \delta) e^{x^2/2} c^{\delta} 2^{\mu-2\rho-\frac{1}{2}}}{\prod_{j=1}^{v} (\beta_j,\ \delta) 2^{2\delta d} (\delta)!\ (\mu)!} H^{n+1,\,l}_{p+1,\,q+1}\left[z \cdot 2^{2m} \left| \begin{matrix} \{(a_p,\ e_p)\},\ \left(1+\rho+\delta d-\frac{\mu}{2},\ m\right) \\ (1+2\rho+2\delta d,\ 2m),\ \{(bq,\ fq)\} \end{matrix} \right.\right]$$

$$\times H_{\mu}(x) \quad .. \quad .. \quad .. \quad .. \quad .. \quad .. \quad .. \quad .. \quad .. \quad (A1)$$

where $H^{n,\,l}_{p,\,q}\left[\ldots \left| \begin{matrix} \{(\ldots)\} \\ \{(\ldots)\} \end{matrix} \right.\right]$ is the H-function introduced by Fox (1961) and $H_{\mu}(x)$ is the Hermite polynomial.

In eqn. (A1), m is a positive number, d being a positive integer and $\rho = 0, 1, 2, 3, \ldots$

We know that if

$$e_j = f_h = 1 \quad (j = 1,\ 2,\ 3, \ldots\ p;\ h = 1,\ 2,\ 3, \ldots,\ q)$$

$$H^{n,\,l}_{p,\,q}\left[zx^{-2m} \left| \begin{matrix} \{(a_p,\ 1)\} \\ \{(b_q,\ 1)\} \end{matrix} \right.\right] = G^{n,\,l}_{p,\,q}\left(zx^{-2m} \left| \begin{matrix} a_1, \ldots, a_p \\ b_1, \ldots, b_q \end{matrix} \right.\right) \quad .. \quad .. \quad (A2)$$

where $G^{n,\,l}_{p,\,q}\left(\ldots \left| \begin{matrix} \cdots \\ \cdots \end{matrix} \right.\right)$ is the Meijer's G-function.

Thus, choosing $\rho = 0$ and setting $u = 0$, $v = 1$, $d = m = 1$, eqn. (A1) reduces to

$$ {}_0F_1(\overline{\beta_1};\ cx^2)\, G^{n,\,l}_{p,\,q}\left[zx^{-2}\,\middle|\,\begin{matrix}a_1, \ldots;\ a_p\\ b_1, \ldots;\ b_q\end{matrix}\right] = \sum_{\mu,\,\delta=0}^{\infty} \frac{e^{x^2/2} c^{\delta} 2^{\mu-\frac{1}{2}}}{(\beta_1;\ \delta) 2^{2\delta} (\delta)\,!\,(\mu)\,!} $$

$$ \times H^{n+1,\,l}_{p+1,\,q+1}\left[4z\,\middle|\,\begin{matrix}(a_1, 1), \ldots, (a_p, 1)\left(1+\delta-\frac{\mu}{2}, 1\right)\\ (1+2\delta, 2), (b_1, 1), \ldots, (b_q, 1)\end{matrix}\right] H_{\mu}(x). \quad \ldots \text{(A3)} $$

Further, putting $n = 1$, $1 = p$ and replacing q by $q+1$, a_j by $(1-a_j)$, $(j = 1, 2, \ldots, p)$, similarly, setting $b_1 = 0$ and replacing b_j by $1-b_{j-1}$ $(j = 2, 3, \ldots, q+1)$, we obtain after utilizing the reduction formula for G-function into ${}_pF_q$ function (Bateman project 1953)

$$ {}_0F_1(\overline{\beta_1};\ cx^2)\, \frac{\prod_{j=1}^{p} \Gamma(a_j)}{\prod_{j=1}^{q} \Gamma(b_j)}\, {}_pF_q\left[\begin{matrix}a_1, \ldots, a_p\\ b_1, \ldots, b_q\end{matrix};\ -zx^{-2}\right] = \sum_{\mu,\,\delta=0}^{\infty} \frac{e^{x^2/2} c^{\delta} 2^{\mu-\frac{1}{2}}}{(\beta_1;\ \delta) 2^{2\delta} (\delta)\,!\,(\mu)\,!} $$

$$ \times H^{2,\,p}_{p+1,\,q+2}\left[4z\,\middle|\,\begin{matrix}(1-a_1, 1) \ldots (1-a_p, 1), \left(1+\delta-\frac{\mu}{2}, 1\right)\\ (1+2\delta, 2), (1, 1), (1-b_1, 1) \ldots (1-b_q, 1)\end{matrix}\right] H_{\mu}(x). \quad \ldots \text{(A4)} $$

Finally, putting $p = 0$, $q = 1$, we get the required product of hypergeometric functions as

$$ {}_0F_1(\overline{\beta_1};\ cx^2)\, {}_0F_1(\overline{b_1};\ -zx^{-2}) = \Gamma(b_1) \sum_{\mu,\,\delta=0}^{\infty} \frac{e^{x^2/2} c^{\delta} 2^{\mu-\frac{1}{2}}}{(\beta_1;\ \delta) 2^{2\delta} (\delta)\,!\,(\mu)\,!} $$

$$ \times H^{2,\,0}_{1,\,3}\left[4z\,\middle|\,\begin{matrix}\left(1+\delta-\frac{\mu}{2}, 1\right)\\ (1+2\delta, 2), (1, 1), (1-b_1, 1)\end{matrix}\right] H_{\mu}(x). \quad \ldots \text{(A5)} $$

References

Aly, H. H., and Müller, H. J. W. (1966). Scattering by the singular potential r^{-4}. *J. Math. Phys.*, 7, 1–9.

Aly, H. H., Müller, H. J. W., and Vahedi-Faridi, N. (1969). Some remarks on scattering by singular potentials. *Nuovo Cim. lett.*, 2, 485.

Aly, H. H., and Spector, R. M. (1965). Some solvable potentials for the Schrödinger equation. *Nuovo Cim.*, 38, 149–52.

Bateman project (1953). Higher Transcendental Functions. Vol. I. McGraw-Hill Book Co., Inc., New York, p. 215.

Bhattacharjie, A., and Sudarshan, E. C. G. (1962). A class of solvable potentials. *Nuovo Cim.*, 25, 864–79.

Bose, A. K. (1963). Solvable potentials. *Phys. Lett.*, 7, 245–46.

Fox, C. (1961). The G- and H-functions as symmetrical Fourier kernels. *Trans. Am. math. Soc.*, 98, 395–429.

Gradshteyn, I. S., and Ryzhik, I. M. (1965). Table of integrals, series and products. Academic Press, p. 1033 [eqn. 8.953(1)].

Luke, Y. L. (1962). Integrals of Bessel Functions. McGraw-Hill Book Co., Inc., New York, p. 22 [eqn. 1.4.1(1).

McLachlan, N. W. (1947). Theory and Applications of Mathieu Functions. Oxford University Press, p. 244.

Sharma, L. K., and Varma, R. C. (1970). Derivation of a few solvable potentials for the Schrödinger equation. *Indian J. pure appl. Phys.*, 8, 66–69.

Singh, F. (*in press*). Application of E operator to evaluate an infinite integral and heat conduction. *La Ricerca, Italy.*

Spector, R. M. (1964). Exact solution of the Schrödinger equation for inverse fourth power potential. *J. math. Phys.*, 5, 1185–89.

Wannier, G. H., and Vogt, E. (1954). Scattering of ions by polarization forces. *Phys. Rev.*, 95, 1190–98.

SOLVABLE POTENTIALS FROM ASSOCIATED LEGENDRE EQUATION

by L. K. Sharma, *Department of Applied Physics,*
Government Engineering College, Rewa

(Communicated by A. N. Mitra, F.N.I.)

(*Received 22 April 1970*)

Two solvable potentials for the *s*-wave Schrödinger equation have been evaluated by using associated Legendre differential equation following the method of Bhattacharjie and Sudarshan (1962). The same potentials are also obtained using the technique developed by Bose (1963), thus establishing the fact that the two methods formulated for constructing solvable potentials agree with each other. Solutions for the potentials and their corresponding expressions for *s*-matrices have also been obtained.

Bargmann (1949) developed the method of constructing phase equivalent potentials for which Schrödinger equation may be solved in terms of elementary functions, thereby rendering the computation of corresponding phase shifts possible. Bhattacharjie and Sudarshan (1962), applying suitable functional transformations to a second order differential equation, established a general technique for evaluating solvable potentials for the Schrödinger equation. Bose (1963), starting with the normal form of the second order differential equation and using the Schwarzian derivative, formulated another method for constructing the potentials. They have obtained solvable potentials from hypergeometric, confluent hypergeometric and Bessel equations. Aly and Spector (1965) following the technique of Bose (1963) derived an inverse fourth power singular potential through modified Mathieu equation. Sharma and Varma (1970) using the method of Bhattacharjie and Sudarshan (1962) evaluated further solvable potentials from Whittaker and Jacobi differential equations.

The object of this paper is to construct two solvable potentials for *s*-wave Schrödinger equation by transforming associated Legendre differential equation following the method of Bhattacharjie and Sudarshan (1962).

By applying Bose's (1963) technique to associated Legendre equation, the potentials so derived are similar to those which have been obtained by the method of Bhattacharjie and Sudarshan (1962). It is, therefore, established that the two general methods used for evaluating solvable potentials completely agree with each other.

Finally the solutions and corresponding expressions for *s*-matrices have been obtained for both the potentials.

Bhattacharjie and Sudarshan's Method

The associated Legendre differential equation (Erdélyi 1953) is given as

$$(1-Z^2)W''(Z)-2ZW'(Z)+\left[n(n+1)-\frac{m^2}{(1-Z^2)}\right]W(Z)=0 \quad .. \quad (1)$$

where Z, n and m are unrestricted.

Equation (1) can also be written in the form

$$\frac{d}{dZ}[(1-Z^2)W'(Z)]+\left[n(n+1)-\frac{m^2}{(1-Z^2)}\right]W(Z)=0. \quad .. \quad (2)$$

Using the transformation

$$\rho=\tfrac{1}{2}\log\frac{1+Z}{1-Z}, \quad .. \quad .. \quad .. \quad .. \quad (3)$$

eqn. (2) becomes

$$W''(\rho)+\left[\frac{4n(n+1)e^{2\rho}}{(e^{2\rho}+1)^2}-m^2\right]W(\rho)=0 \quad .. \quad .. \quad (4)$$

which is the form required to evaluate the solvable potentials.

Making the following substitutions in eqn. (4)

$$\rho=f(r), \quad W(\rho)=g(r)\phi(r), \quad h(r)=\frac{d}{dr}\{\log_e g(r)\}, \quad .. \quad .. \quad (5)$$

we get

$$\phi''(r)+A(r)\phi'(r)+B(r)\phi(r)=0 \quad .. \quad .. \quad .. \quad (6)$$

where

$$A(r)=\frac{2g'(r)}{g(r)}-\frac{f''(r)}{f'(r)} \quad .. \quad .. \quad .. \quad .. \quad (7)$$

$$B(r)=\frac{g''(r)}{g(r)}-\frac{g'(r)}{g(r)}\cdot\frac{f''(r)}{f'(r)}+\frac{4n(n+1)e^{2f(r)}\{f'(r)\}^2}{\{e^{2f(r)}+1\}^2}-m^2\{f'(r)\}^2. \quad .. \quad (8)$$

For eqn. (6) to be the following s-wave radial Schrödinger equation

$$\phi''(r)+[k^2-V(r)]\phi(r)=0 \quad .. \quad .. \quad .. \quad (9)$$

[with units $E=k^2$],
the values of $A(r)$ and $B(r)$ should be such that

$$A(r)=0, \quad B(r)=k^2-V(r) \quad .. \quad .. \quad .. \quad (10)$$

and $V(r)$ should be independent of k.

Thus eqns. (7) and (10) yield the relation

$$f'(r)=Cg^2(r) \quad .. \quad .. \quad .. \quad .. \quad (11)$$

where C is the integration constant.

Similarly eqns. (8) and (10) produce

$$h'(r)-h^2(r)+\frac{4n(n+1)e^{2f(r)}\{f'(r)\}^2}{\{e^{2f(r)}+1\}^2}-m^2\{f'(r)\}^2\equiv k^2-V(r). \quad .. \quad (12)$$

Now under the choice

$$\rho = f(r) = \alpha r \quad .. \quad .. \quad .. \quad .. \quad (13)$$

eqn. (12) becomes

$$\frac{4\alpha^2 n(n+1)e^{2\alpha r}}{\{e^{2\alpha r}+1\}^2} - m^2\alpha^2 \equiv k^2 - V(r). \quad .. \quad .. \quad .. \quad (14)$$

Equation (14) yields the potential of the form

$$V(r) = -\frac{n(n+1)\alpha^2}{\cosh^2 \alpha r} \quad .. \quad .. \quad .. \quad .. \quad (15)$$

and

$$-m^2\alpha^2 = k^2. \quad .. \quad .. \quad .. \quad .. \quad (16)$$

For $n = 1$ this potential takes the simple form

$$V(r) = -\frac{2\alpha^2}{\cosh^2 \alpha r}. \quad .. \quad .. \quad .. \quad .. \quad (17)$$

The following relation was deduced by Bargmann (1949) for linear type of potentials

$$V(r) = 2\left\{\left(\frac{w'}{w}\right)^2 - \frac{w''}{w}\right\}. \quad .. \quad .. \quad .. \quad (18)$$

On substituting $w(r) = \cosh \alpha r$ in eqn. (18) one gets

$$V(r) = -\frac{2\alpha^2}{\cosh^2 \alpha r}. \quad .. \quad .. \quad .. \quad .. \quad (19)$$

Hence the potential derived in eqn. (19) through associated Legendre equation may be known as one of Bargmann's potentials of the linear type. Bhattacharjie and Sudarshan (1962) also derived a similar potential by transforming the hypergeometric equation.

For $n = 1$ and $\rho = f(r) = -\frac{\alpha r}{2}$, $V(r)$ takes the form of an Eckart (1930) type of potential.

As a next example, consider the transformation eqns. (11) and (12) with the choice

$$\rho = f(r) = \tfrac{1}{2} \log \frac{1+e^{-\alpha r/2}}{1-e^{-\alpha r/2}} \quad .. \quad .. \quad .. \quad (20)$$

the following relations are obtained

$$g(r) = -\sqrt{\alpha/2c}\, e^{-\alpha r/4}(1-e^{-\alpha r})^{-\frac{1}{2}} \quad .. \quad .. \quad .. \quad (21)$$

and

$$\frac{\alpha^2}{2}\frac{e^{-\alpha r}}{(1-e^{-\alpha r})^2} - \frac{\alpha^2}{4}\frac{e^{-2\alpha r}}{(1-e^{-\alpha r})^2} - \frac{\alpha^2}{4}\frac{e^{-\alpha r}}{(1-e^{-\alpha r})} + \frac{n(n+1)\alpha^2}{4}\frac{e^{-\alpha r}}{(1-e^{-\alpha r})}$$

$$- \frac{m^2\alpha^2 e^{-\alpha r}}{4(1-e^{-\alpha r})^2} - \alpha^2/16 \equiv k^2 - V(r). \quad .. \quad .. \quad .. \quad (22)$$

By rearrangement of the terms and setting

$$A = \frac{\alpha^2}{4}\{n(n+1)-m^2+1\} \text{ and } B = -\frac{\alpha^2}{4}n(n+1)\} \quad .. \quad (23)$$

the potential of the following form is obtained

$$V(r) = -\left\{\frac{Ae^{-\alpha r}+Be^{-2\alpha r}}{(1-e^{-\alpha r})^2}\right\} \quad .. \quad .. \quad .. \quad (24)$$

and

$$k^2 = -\alpha^2/16. \quad .. \quad .. \quad .. \quad .. \quad (25)$$

The potential derived in eqn. (24) may be recognized as Manning-Rosen-Newing potential energy function proposed for diatomic molecules (Manning and Rosen 1933; Newing 1935, 1940).

Bose's Method

The normal form of an ordinary differential equation can be written as

$$v''(\rho)+I(\rho)v(\rho) = 0. \quad .. \quad .. \quad .. \quad .. \quad (26)$$

Setting $\rho = \rho(r)$, one gets

$$(\rho')^2 I(\rho)+\tfrac{1}{2}\{\rho, r\} = I_s(r) \quad .. \quad .. \quad .. \quad (27)$$

where $\{\rho, r\}$ is the Schwarzian derivative.

Now $I_s(r)$ of the s-wave radial Schrödinger equation is given by

$$I_s(r) = k^2-V(r). \quad .. \quad .. \quad .. \quad .. \quad (28)$$

Thus combining equations (27) and (28)

$$(\rho')^2 I(\rho)+\tfrac{1}{2}\{\rho, r\} = k^2-V(r). \quad .. \quad .. \quad .. \quad (29)$$

The $I(\rho)$ of the associated Legendre equation is given as

$$I(\rho) = \left[\frac{n(n+1)}{\cosh^2\rho}-m^2\right]. \quad .. \quad .. \quad .. \quad (30)$$

Hence putting again $\rho = \alpha r$ in eqn. (27), one gets

$$I_s(r) = \alpha^2\left[\frac{n(n+1)}{\cosh^2\alpha r}-m^2\right]. \quad .. \quad .. \quad .. \quad (31)$$

Thus the potential of the form given by eqn. (15) can be obtained by this method also.

Again for the choice

$$\rho = \tfrac{1}{2}\log\frac{1+e^{-\alpha r/2}}{1-e^{-\alpha r/2}}$$

$$I_s(r) = \frac{n(n+1)\alpha^2 e^{-\alpha r}}{4(1-e^{-\alpha r})} - \frac{m^2\alpha^2 e^{-\alpha r}}{4(1-e^{-\alpha r})^2}+\frac{\alpha^2}{16}\left\{\frac{6e^{-\alpha r}-e^{-2\alpha r}-1}{(1-e^{-\alpha r})^2}\right\}. \quad .. \quad (32)$$

Equation (32) on simplification yields once again the potential of the form

$$V(r) = -\left[\frac{Ae^{-\alpha r}+Be^{-2\alpha r}}{(1-e^{-\alpha r})^2}\right],$$

where A and B are constants defined in eqn. (23).

Thus it is apparent that for the same choice in the value of ρ, similar potentials have been evaluated by the above two methods formulated for deriving solvable potentials.

Solutions

(A) *For the Potential*

$$V(r) = -\frac{n(n+1)\alpha^2}{\cosh^2 \alpha r}.$$

The solution of eqn. (1) is written in terms of $Q_n^m(z)$, the Legendre function of the second kind.

Thus expressing $Q_n^m(z)$ as a sum (Erdélyi 1953) of two hypergeometric functions

$$W(Z) = Q_n^m(Z) = Ae^{im\pi}{}_2F_1(a_1, b_1;\ c_1;\ \xi)+Be^{im\pi}{}_2F_1(a_2, b_2;\ c_2;\ \xi) \qquad (33)$$

and choosing suitable values for A, a_1, b_1, c_1, ξ, B, a_2, b_2 and c_2 from the table of expansions given in Erdélyi (1953), the solution may be finally written as

$$W(Z) = e^{im\pi}.2^{m-1}\Gamma(m)(Z^2-1)^{-m/2}{}_2F_1\left(\frac{1}{2}+\frac{n}{2}-\frac{m}{2},\ \frac{-n}{2}-\frac{m}{2};\ 1-m;\ 1-Z^2\right)$$

$$+e^{im\pi}2^{-m-1}\frac{\Gamma(1+n+m)\Gamma(-m)}{\Gamma(1+n-m)}(Z^2-1)^{m/2}{}_2F_1\left(\frac{1}{2}+\frac{n}{2}+\frac{m}{2},\ \frac{-n}{2}+\frac{m}{2};\right.$$

$$\left.1+m;\ 1-Z^2\right). \qquad .. \quad .. \quad .. \quad .. \quad .. \quad .. \quad .. \quad (34)$$

The above equation with the transformations $z = \tanh \rho$ from eqn. (3), $\rho = \alpha r$ from eqn. (13), and with the value of $m = ik/\alpha$ from eqn. (16) will be as follows:

$$\phi(r) = \sqrt{c/4\alpha}e^{-k\pi/\alpha}\Gamma(ik/\alpha)(-1)^{-ik/\alpha}(1+e^{-2\alpha r})^{ik/\alpha}e^{ikr}{}_2F_1\left(\frac{1}{2}+\frac{n}{2}-\frac{ik}{2\alpha},\ \frac{-n}{2}-\frac{ik}{2\alpha};\right.$$

$$\left.1-\frac{ik}{\alpha};\ \mathrm{sech}^2\,\alpha r\right)+\sqrt{c/4\alpha}e^{-k\pi/\alpha}\frac{\Gamma(1+n+ik/\alpha)\Gamma(-ik/\alpha)}{\Gamma(1+n-ik/\alpha)}(-1)^{ik/\alpha}$$

$$\times(1+e^{-2\alpha r})^{-ik/\alpha}e^{-ikr}{}_2F_1\left(\frac{1}{2}+\frac{n}{2}+\frac{ik}{2\alpha},\ \frac{-n}{2}+\frac{ik}{2\alpha};\ 1+\frac{ik}{\alpha};\ \mathrm{sech}^2\,\alpha r\right). \qquad (35)$$

Asymptotically $\phi(r)$ can be written as

$$\phi(r) \underset{r\to\infty}{\sim} \left\{\sqrt{c/4\alpha}e^{-k\pi/\alpha}\Gamma(ik/\alpha)(-1)^{ik/\alpha}\right\}e^{ikr}+\left\{\sqrt{c/4\alpha}e^{-k\pi/\alpha}\frac{\Gamma(1+n+ik/\alpha)}{\Gamma(1+n-ik/\alpha)}\right.$$

$$\left.\times\Gamma(-ik/\alpha)(-1)^{ik/\alpha}\right\}e^{-ikr}. \qquad .. \quad .. \quad .. \quad .. \quad .. \quad (36)$$

Hence the s-matrix in the explicit form is given as

$$s(k) = \frac{\Gamma(1+n+ik/\alpha)\Gamma(-ik/\alpha)}{\Gamma(ik/\alpha)\Gamma(1+n-ik/\alpha)} \quad .. \quad .. \quad .. \quad (37)$$

This expression for the s-matrix can be further simplified to the form

$$s(k) = \prod_{n=1}^{n} \left(\frac{k-in\alpha}{k+in\alpha}\right). \quad .. \quad .. \quad .. \quad .. \quad (38)$$

Thus the repulsive potential under consideration has a s-matrix with 'redundant poles' at $k = -in\alpha$ in the lower half plane and a sequence of zeroes which are mirror images of these poles.

By inserting $n = 1$ in eqn. (38) the expression for the s-matrix takes the form

$$s(k) = \left(\frac{k-i\alpha}{k+i\alpha}\right) \quad .. \quad .. \quad .. \quad .. \quad (39)$$

a result in agreement with Bhattacharjie and Sudarshan (1962).

The unitarity (Wu and Ohmura 1962) of the s-matrix can also be established from eqn. (39).

(B) *For the Potential*

$$V(r) = -\left[\frac{Ae^{-\alpha r}+Be^{-2\alpha r}}{(1-e^{-\alpha r})^2}\right].$$

Utilizing the expression for $W(z)$ as given in eqn. (34) and writing the value of $g(r)$ from eqn. (21), the solution $\phi(r)$ can be written as

$$\begin{aligned}\phi(r) = &-e^{im\pi}\sqrt{2c/\alpha}e^{\alpha r/4}(1-e^{-\alpha r})^{\frac{1}{2}}2^{m-1}\Gamma(m)(-1)^{-m}(1-e^{-\alpha r})^{-m/2} \\ &\times {}_2F_1\left(\frac{1}{2}+\frac{n}{2}-\frac{m}{2},\ -\frac{n}{2}-\frac{m}{2};\ 1-m;\ 1-e^{-\alpha r}\right) - e^{im\pi}\sqrt{2c/\alpha} \\ &\times e^{\alpha r/4}(1-e^{-\alpha r})^{\frac{1}{2}}2^{-m-1}\frac{\Gamma(-m)\Gamma(1+n+m)(-1)^m}{\Gamma(1+n-m)}(1-e^{-\alpha r})^{m/2} \\ &\times {}_2F_1\left(\frac{1}{2}+\frac{n}{2}+\frac{m}{2},\ -\frac{n}{2}+\frac{m}{2};\ 1+m;\ 1-e^{-\alpha r}\right). \quad .. \quad .. \quad (40)\end{aligned}$$

Choosing $m = \frac{1}{2}$, $\phi(r)$ is given as

$$\begin{aligned}\phi(r) = &\ e^{i\pi/2}\sqrt{c/\alpha}e^{\alpha r/4}(1-e^{-\alpha r})^{1/4}\Gamma(1/2){}_2F_1\left(\frac{n}{2}+\frac{1}{4},\ -\frac{n}{2}-\frac{1}{4};\ \frac{1}{2};\ 1-e^{-\alpha r}\right) \\ &+e^{i\pi/2}\sqrt{c/4\alpha}e^{\alpha r/4}(1-e^{-\alpha r})^{3/4}\frac{\Gamma(-1/2)\Gamma(n+3/2)}{\Gamma(n+1/2)}{}_2F_1\left(\frac{n}{2}+\frac{3}{4},\ -\frac{n}{2}\right. \\ &\left.+\frac{1}{4};\ \frac{3}{2};\ 1-e^{-\alpha r}\right). \quad .. \quad .. \quad .. \quad .. \quad .. \quad .. \quad .. \quad (41)\end{aligned}$$

From eqn. (25) $\alpha = \pm 4ik$ and thus, for determining the s-matrix explicitly, the values of α are chosen such that $\alpha = +4\,ik$ in the first term and $\alpha = -4ik$ in the second term of the solution.

From (Erdélyi 1953)

$$ {}_2F_1\left(\frac{1}{4}+\frac{n}{2},\ -\frac{n}{2}-\frac{1}{4};\ \frac{1}{2};\ 1\right) = \cos\left(\tfrac{1}{2}+n\right)\frac{\pi}{2} $$

and

$$ {}_2F_1\left(\frac{3}{4}+\frac{n}{2},\ -\frac{n}{2}+\frac{1}{4};\ \frac{3}{2};\ 1\right) = \sin\left(\tfrac{1}{2}+n\right)\frac{\pi}{2}\Big/(n+\tfrac{1}{2}). $$

Therefore, asymptotically $\phi(r)$ can be written as

$$ \phi(r) \underset{r\to\infty}{\sim} e^{i\pi/2}\sqrt{c/\alpha}e^{ikr}\Gamma(1/2)\cos\left(n+\tfrac{1}{2}\right)\frac{\pi}{2} $$

$$ +e^{i\pi/2}\sqrt{c/4\alpha}e^{-ikr}\Gamma(-1/2)\sin\left(n+1/2\right)\frac{\pi}{2}. \quad .. \quad (42) $$

Hence the s-matrix for the particular value of $m = \frac{1}{2}$ has the simple form

$$ s(k) = \tan\left(n+\tfrac{1}{2}\right)\frac{\pi}{2}. \quad .. \quad .. \quad .. \quad .. \quad (43) $$

Here the s-matrix evidently is independent of k.

Acknowledgement

The author is grateful to Professor R. C. Varma for stimulating discussions and constant encouragement.

References

Aly, H. H., and Spector, R. M. (1965). Some solvable potentials for the Schrödinger equation. *Nuovo Cim.*, **38**, 149.

Bargmann, V. (1949). On the connection between phase shifts and scattering potentials. *Rev. mod. Phys.*, **21**, 488.

Bhattacharjie, A., and Sudarshan, E. C. G. (1962). A class of solvable potentials. *Nuovo Cim.*, **25**, 864.

Bose, A. K. (1963). Solvable potentials. *Phys. Lett.*, **7**, 245.

Eckart, C. (1930). The penetration of a potential barrier by electrons. *Phys. Rev.*, **35**, 1303.

Erdélyi, A. (1953). Higher Transcendental Functions, Vol. I. McGraw-Hill Book Co., Inc., New York, pp. 120–35 and 101.

Manning, M. F., and Rosen, N. (1933). A potential function for the vibrations of diatomic molecules. *Phys. Rev.*, **44**, 953.

Newing, R. A. (1935). Note on the interrelation of the equilibrium nuclear distance with other molecular constants for diatomic molecules. *Phil. Mag.*, **19**, 759.

———— (1940). On the Interrelation of molecular constants for diatomic molecules—II. *Phil. Mag.*, **29**, 298.

Sharma, L. K., and Varma, R. C. (1970). Derivation of a few solvable potentials for the Schrödinger equation. *Indian J. pure appl. Phys.*, **8**, 66.

Wu, T., and Ohmura, T. (1962). Quantum Theory of Scattering. Prentice-Hall, Inc., New York, p. 14.

A STUDY OF THE MINERALIZATION OF RADIOACTIVE ELEMENTS IN SINGHBHUM SHEAR ZONE, BIHAR*

by S. C. Sarkar, *Department of Geological Sciences, Jadavpur University, Calcutta 32*

The paper deals with some salient aspects of the mineralization of radioactive and the associated elements along the Singhbhum shear zone. The shear zone in general and the down-dip warps in schistosity and the shear surfaces in particular are the loci of mineralization. Ore shoots generally trend towards NNE–NE, subparallel with the dominant lineations in the zone. Rich veins of radioactive minerals and copper sulphides do not generally coincide. Locally, however, there is concentrated mineralization of nickel and molybdenum along with uranium. The ore zone is at places characterized by the development of cherty quartz and oligoclase veins with abundant inclusions of dusty hematite. Radioactive minerals so far recorded and studied are uraninite, pitchblende, xenotime, allanite, autunite, meta-autunite, torbernite, schoepite, meta-schoepite. Details of these as well as other ore minerals associated with them are discussed. The nature of the ore mineralization, the source of the ore materials and the process of their deposition are discussed. A hypogene middle-high temperature hydrothermal origin, with the ore materials essentially derived from an unknown source, is suggested here.

Introduction

Singhbhum shear zone, which has for the last half century been considered as the largest copper-producing area in the country, has in recent years also come to be known as one of the rich zones of radioactive ores in the country. The area is located at the north-eastern end of the Indian Peninsula and the mineralization has taken place in the Precambrian rocks formed by metamorphism and metasomatism of basic volcanic and (ortho-) sedimentary rocks. As would seem natural, the entire Singhbhum shear zone is not uniformly mineralized and differential concentration of ore materials has given rise to ore deposits of varying size and richness. Some of the deposits have been located, starting from the south, at Khadandungri-Kanyaluka-Bhalki, Mainajharia-Bagjata, Pathargara-Surda, Jaduguda-Bhatin, Naroapahar, Keruadungri, Rajgaon-Tamadungri, Sankhadih-Galudih areas (Fig. 1).

Control of Mineralization

The ore bodies have been emplaced along a zone of dislocation of regional dimension, known as the Singhbhum shear zone. This has been the principal locus. In the shear zone the schistosity, shear planes and bedding (wherever

* Paper presented at the symposium on Geology and Mineralogy of Atomic Minerals Deposits and their development for use in the Nuclear Power Programme in India held in New Delhi on 14–16 October, 1968, under the auspices of INSA, Convener Prof. D. N. Wadia.

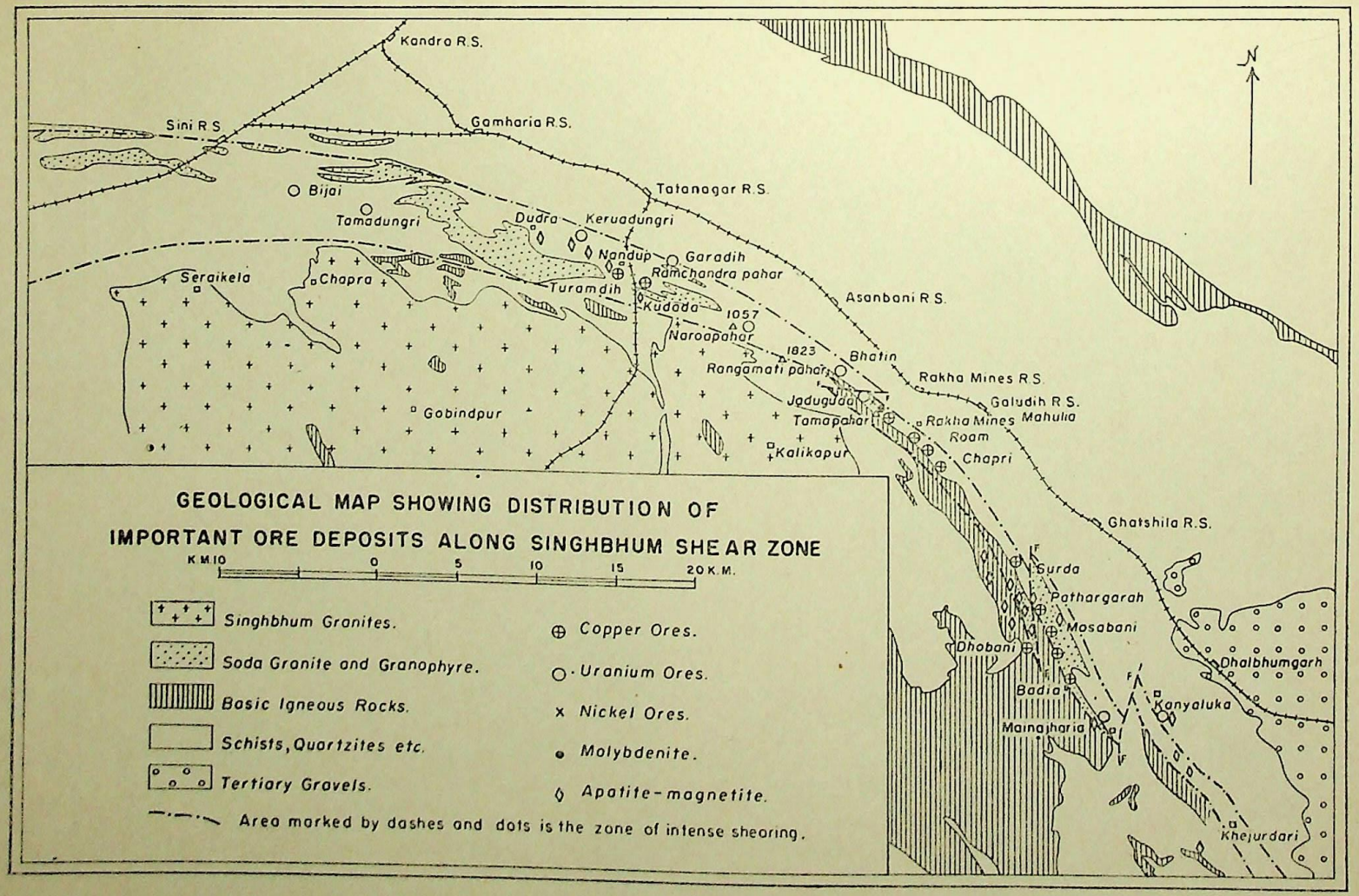

FIG. 1

VERTICAL LONGITUDINAL SECTION OF F.W. LODE, JADUGUDA MINES, SHOWING THE OCCURRENCE OF URANIUM, MOLYBDENUM & NICKEL
(BY COURTESY, D.A.E)

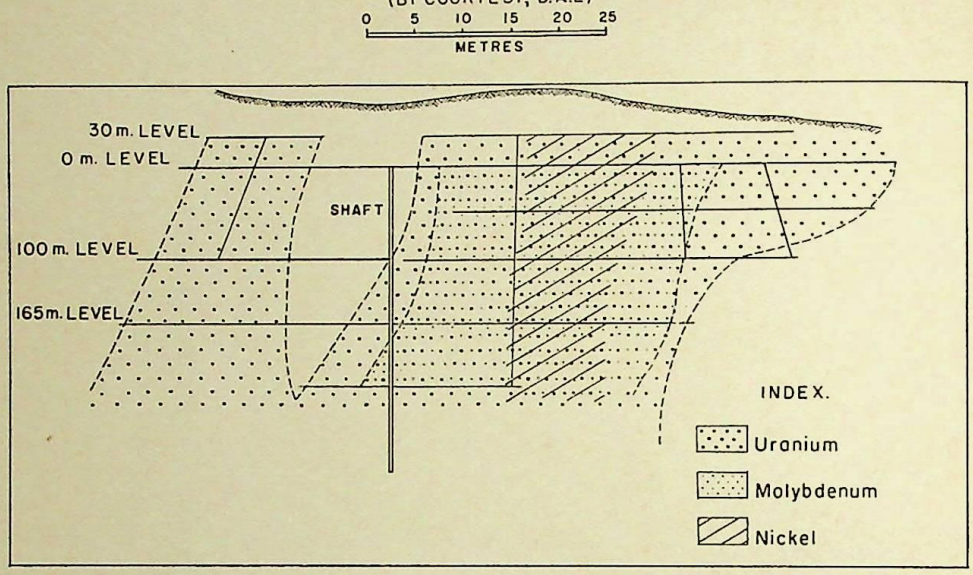

FIG. 2

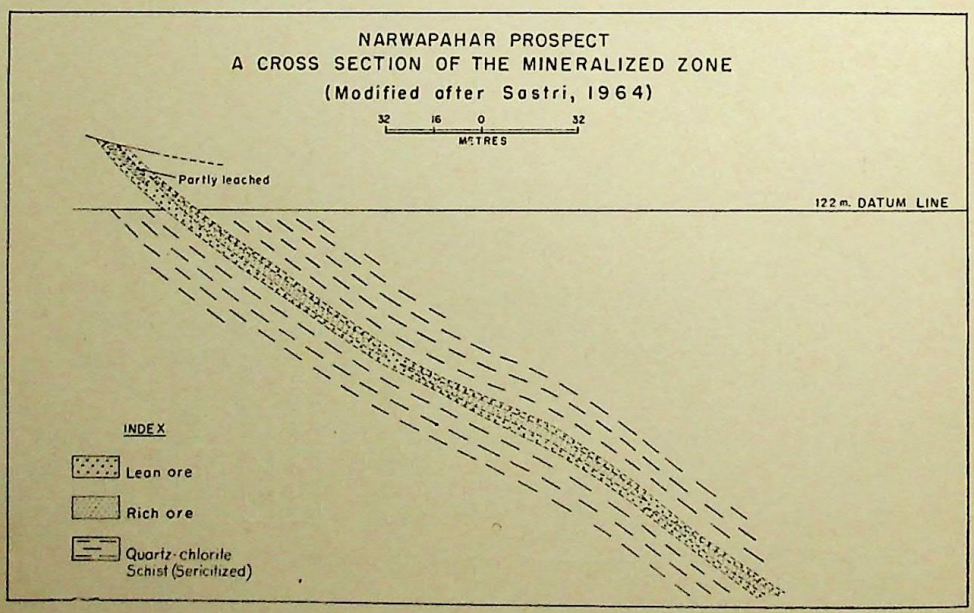

FIG. 3

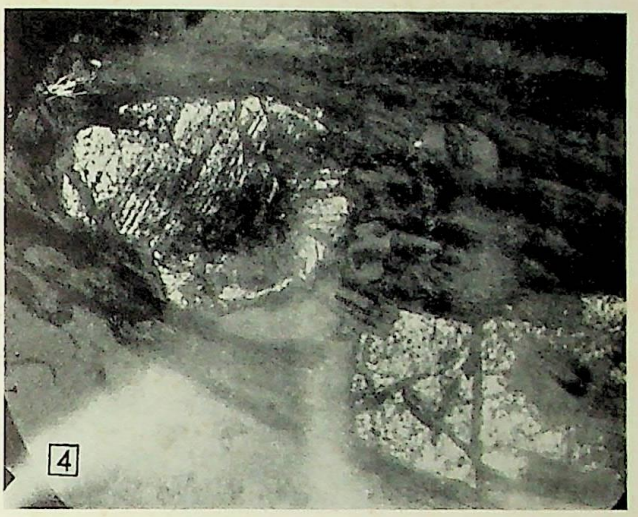

FIG. 4. Martite, Jaduguda, showing inherited (III) cleavages of magnetite. ×168.

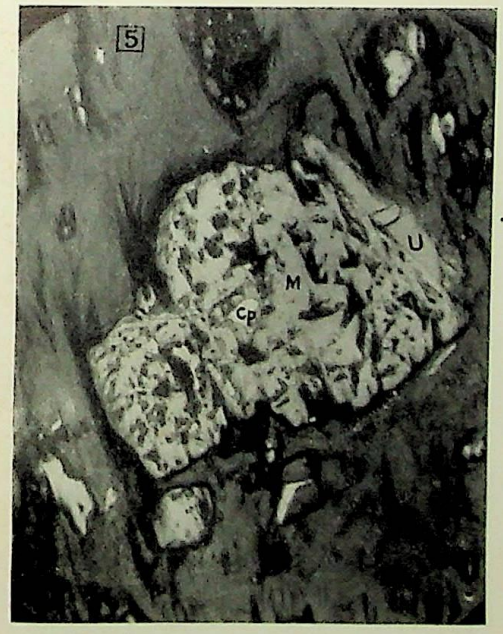

FIG. 5. Fractures in Jaduguda magnetite, filled in by chalcopyrite (*Cp*). Uraninite (*U*) abutting against magnetite (*M*) grain. ×72.

FIG. 6. Pitchblende forming a composite polygon with grains of quartz at the core. ×168.

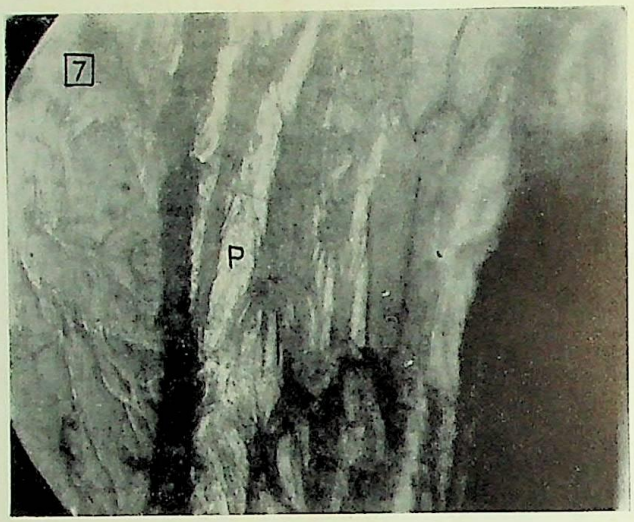

FIG. 7. Pitchblende (*P*) filling in schistosity planes in the host rock, Jaduguda. ×168.

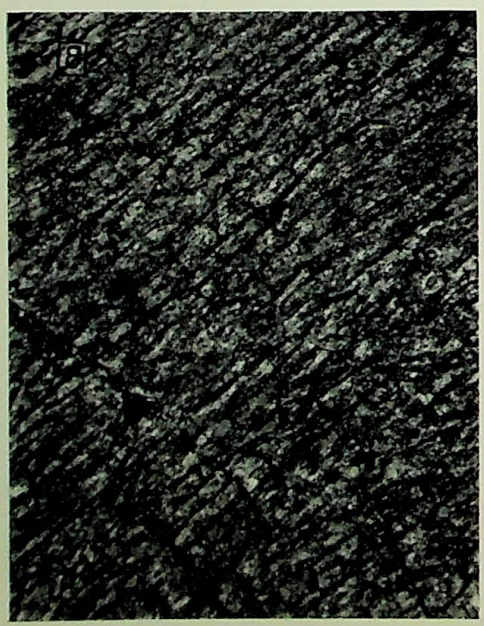

FIG. 8. Xenotime, Kanyaluka. Distinctive (110) cleavage visible. ×160.

FIG. 9. Allanite (*A*) overgrown by epidote, Mosaboni. ×80.

Fig. 10. Autoradiograph of uraninite disseminated in the ore, Jaduguda.

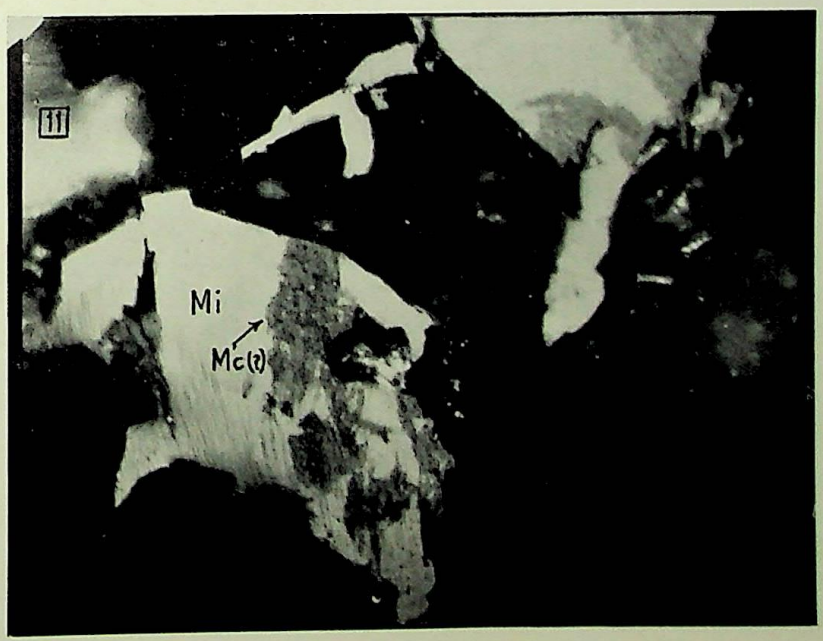

Fig. 11. Millerite (*Mi*) partially replaced by mackinawite (*Mc*), central Jaduguda. ×168.

traceable) are parallel to sub-parallel with one another and the ore bodies are broadly parallel with them. The warps in the schistosity and shear planes have been found to be generally better concentrators of ore mineralization. As these warps trend parallelly with the predominant linear structures (a-) in the area, the ore shoots formed also trend sub-parallel with these structures. Some post-mineralization transverse faults have offset the ore bodies, as in the Jaduguda-Bhatin area.

Apparently the biotite-chlorite-quartz schists ('granular rock') in the central part of the ore-zone (containing Jaduguda-Bhatin area) have been better as the host rocks compared to the biotite-schists or quartz-chlorite schists, playing hosts at most other places. But possibly the mechanical property of these rocks or the chance-location of the mineralization sites, rather than petrochemistry of the rocks, should deserve credit for this. Although mineralization of both copper and uranium has taken place along the Singhbhum shear zone, zones of intense copper and radioactive ore mineralization do not coincide. On the surface or in penetrated depth, the migmatites or the 'soda granites' do not show any visible relationship with the radioactive ore deposits.

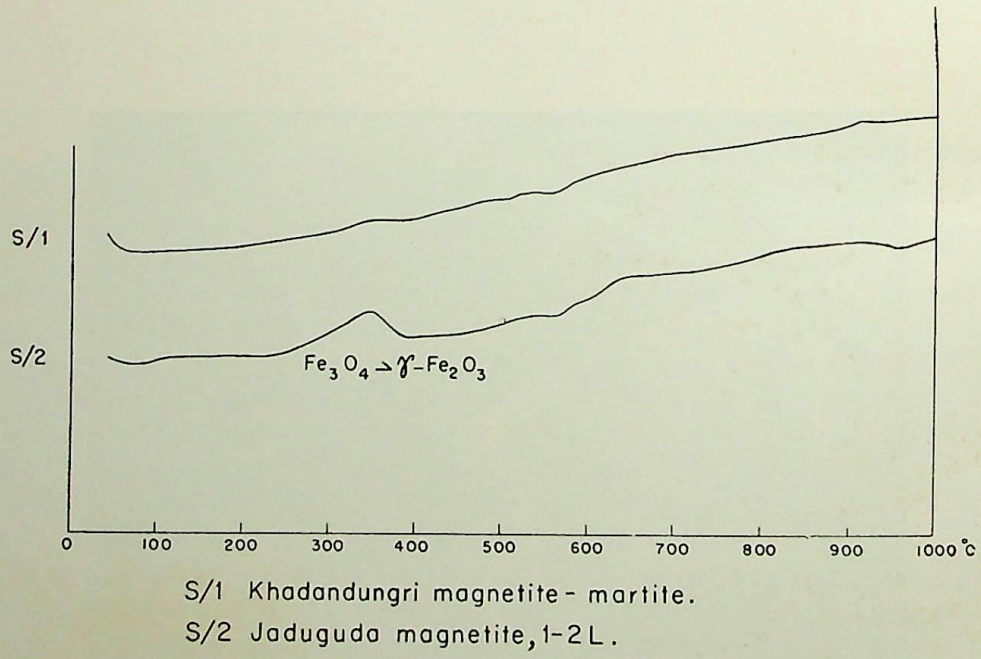

Fig. 12. Differential thermal analysis curves showing absence of metamictization in the iron oxides from Singhbhum.

Wall Rock and Ore Zone Alterations

There is no definite pattern of wall rock and ore zone alterations along the zone of radioactive ore deposition in Singhbhum although locally it is not

very inconspicuous. The entire zone of this mineralization is characterized by silicification and tourmalinization. But it is difficult to assert how much of these are associated with the mineralization of radioactive elements, since the zone, as is well known, also happens to be one of pronounced shearing as well as locus of copper mineralization. However, the association of hematitic cherty vein quartz with uranium ores in Jaduguda Mine is too conspicuous to be oversighted. Besides, veinlets and lenses of Na-feldspars (Na-oligoclase) reddened with hematite dusts are often noted in the radioactive deposits of Jaduguda-Bhatin, Rajda-Naroa and Rajgaon areas. At Rajgaon carbonatization is also noted in the zone of uranium mineralization. Small but varying amounts of sericitization and chloritization along the zone of uranium mineralization have been noted in many places.

Mineralogy of the Ores

Radioactive Minerals

Primary radioactive minerals identified and studied by the author are uraninite, allanite and xenotime. Bhattacharyya and others (1966) have reported the occurrence of monazite also.

Uraninite here is isometric. In view of the fact that thorium is practically absent in Singhbhum uraninite, in its formula of UO_{2+x} the value of x, therefore, should not exceed 0·2 (Alberman and Anderson in Berman 1957). Uraninite grains vary in size in the range of 0·05–0·02 mm. Grains in Naroapahar deposit and those in the further west are smaller in the range. Uraninite has so far not been found in the surficial or near-surface ores. Allanite has been found mostly in the border zone between the soda granites and the basic volcanics or their derivatives such as the chlorite schists, etc. Overgrowth of epidote around short prisms of allanite is a common observation (Fig. 9). Allanite is sometimes metamicted. Xenotime has been found mostly in the Bhalki-Kanyaluka area in biotite schists. Individual xenotime grain in an aggregate in the area often exceeds 1 cm. Apatite is a common associate of the mineral. Allanite is also sometimes present.

The secondary radioactive minerals consist of pitchblende, autunite, meta-autunite, torbernite, schoepite, meta-schoepite. Pitchblende is either shooty or forms rims around grains of gangue minerals such as quartz and magnetite and fills fractures in them or schistosity in the host rock (Figs. 6 and 7).

Autunite —Light yellow, flaky aggregates form along schistosity planes. Weakly reactive to luminescence.
$N_z \sim 1{\cdot}580$.

Meta-autunite —Forms rosy aggregates and is more reactive to luminescence.

Torbernite —Green flakes in aggregates, usually along schistosity. $N_z = 1{\cdot}60–1{\cdot}604$.

Schoepite-meta-schoepite —Replaces autunite and meta-autunite. Yellow prismatic grains, pleochroic.

N_x —Colourless, 1·694–1·705.

N_z —Yellow, 1·737–1·750.

Uranium is partly leached out from a zone below the surface often extending to a depth of 30–40 metres as in Jaduguda and Naroa (Fig. 3).

Radioactivity in other Minerals

Many of the gangue minerals in the ores show radioactivity in various intensities. These minerals include magnetite, martite, apatite, chlorite, tourmaline and even quartz. The phenomenon has been recorded by Bhattacharyya and others (1966). This has been restudied by the present author and the results of this study are shown in the following Table (I).

TABLE I

eU_3O_8-content in gangue mineral

Mineral	% eU_3O_8	
	Author	Bhattacharyya and others (1966)
Chlorite ..	0·027	–
Biotite ..	–	0·080
Tourmaline ..	0·23	0·880
Apatite ..	0·11	0·12
Quartz ..	0·017	0·036
Sulphides (pyrite and chalcopyrite) ..	Traces	Traces
Magnetite ..	0·027–0·16	0·23

Karkhanavala (1958) noted that the uranium content (expressed as U_3O_8) increased with the increasing hematite content. According to him uranium is located in hematite-structure. While others (Rao 1960; Bhattacharyya *et al.* 1966) think that oxidation of magnetite in Jaduguda leads to the formation of magnetite-maghemite and changes in the original lattice of the magnetite made accommodation of uranium possible. For the explanation of the occurrence of uranium in magnetite, Rao and Bhattacharyya *et al.* (op. cit.) support the opinion of Walker and Osterwald (1956) that uranium can occur in the magnetite lattice, while according to Karkhanavala uraninite

associated with magnetite is the source of radioactivity of the latter phase. The present author, however, will like to put his observation as such: uranium content in magnetite as well as oxidation of magnetite increase with approach towards the surface and the oxidation of magnetite may produce mostly maghemite, mostly martite or both (*see* Tables II, III and IV). Near the surface the oxidation product is predominantly martite (Fig. 4). Therefore, a conclusion like 'Jaduguda magnetites contain about 65 per cent γ-Fe_2O_3' by Rao (in Bhattacharyya *et al.*, op. cit.) will seem less warranted. Greater

TABLE II

Composition of magnetite

	1	2	3
FeO ..	26·06	29·76	30·42
Fe_2O_3 ..	68·06	65·86	67·37
Al_2O_3 ..	6·00	2·61	1·00
TiO_2 ..	0·13	0·28	Traces
MnO ..	0·08	0·006	0·19
CaO ..	0·09	0·18	–
MgO ..	0·46	0·60	0·05
V_2O_5 ..	–	–	0·08
H_2O^+ ..	0·32	0·42	–
H_2O^- ..	0·11	0·08	–

(analyst : B. P. Gupta)

Calculated Norms

Hercynite ($FeO.Al_2O_3$) ..	9·83	5·65	2·99
Ulvospinel ($2FeO.TiO_2$) ..	0·27	0·61	—
Magnesioferrite ($MgO.Fe_2O_3$) ..	1·78	3·28	0·25
Jacobsite ($MnO.Fe_2O_3$) ..	0·19	0·01	0·68
Magnetite ($FeO.Fe_2O_3$) ..	50·65	85·17	92·44
Maghemite (Fe_2O_3) ..	37·54	5·28	3·69

Note—Calcium has been left out of calculation as there is no calcium-bearing spinel known as yet. It is likely that the element here occurs in a minute but discrete phase as apatite. Vanadium has been allotted to magnetite.

1. Magnetite from Jaduguda (central) 1–2 level
2. ,, 3 level
3. ,, 5 level

TABLE III

Relationship of oxidation of magnetite and its eU_3O_8-content

Depth in the Jaduguda mine	State of oxidation of magnetite	eU_3O_8
1-2 level	Fe_2O_3 40% (mostly normative)	0·16
2 level (100 m)		0·079
3 level (165 m)	Fe_2O_3 5% (normative only)	0·027

values of eU_3O_8 in the oxidized magnetite may be explained better as due to adsorption of uranium in it. That at least a large part of uranium in the iron-oxides under discussion occurs as a discrete easily extractable phase/phases will be evident from the results of the leaching tests done by the author (Table IV). The leaching in these cases was done with dil. (1 : 1) HCl for a period of five minutes with $-60+80$ mesh material. This may be noted that leaching was found to be more perfect with the prolongation of the time of action or diminution of grain size in the probe.

TABLE IV

Leaching tests on 'radioactive' magnetites

Locality	Nature of the ore	% eU_3O_8	
		Before leaching	After leaching
Khadandungri*	'Magnetite'—martite (martite 80% approx.)	0·13	0·092
Pathargarah	'Magnetite' (with approx. 20% martite and 30–32% maghemite)	0·006	Traces
Jaduguda 1-2 L	Magnetite (with very little or no martite and 38–40% maghemite)	0·14	0·028
3 L	Magnetite	0·050	0·040

* Average grades of Khadandungri and Jaduguda ores are same.

Substitution of iron by uranium in the magnetite structure cannot also be supported from a crystallochemical point of view, particularly because of the large ionic radii of the latter, assuming that Goldschmidt's laws of substitution (1937) will more or less hold good in case of magnetite, which is predominantly ionic in bond-characters. Moreover, uranium, taken within a

mineral structure would affect it through the geological time and will lead to the metamictization of the phase. D.T.A. and X-ray analyses have not been found to show any such effects (Fig. 12) (cf. Karkhanavala, op. cit.).

Nickel and Molybdenum in Association with Uranium

Significant mineralization of nickel and molybdenum has been noted at places in association with uranium mineralization. It is intense in Jaduguda, closely followed by that in Bhatin. In Keruadungri ores only nickel is reported (Bhola 1966).

It may be recorded that in Jaduguda, the concentration of uranium and that of nickel are almost directly variable. Samples of chlorite, one each from central Jaduguda and eastern Jaduguda gave the NiO-content of 0·29 and 0·26 respectively. Ny of this chlorite is $1{\cdot}6290\pm0{\cdot}0002$; cell: $a = 5{\cdot}39\pm 0{\cdot}02$ Å, $b = 9{\cdot}28$–$9{\cdot}32\pm0{\cdot}02$ Å, $c = 14{\cdot}27$–$14{\cdot}28\pm0{\cdot}02$ Å, $\beta = 96°\ 57'$–$97°\ 7'\pm 30'$. A biotite sample from central Jaduguda on analysis was found to contain 0·34 p.c. NiO. It is interesting to note that the same chlorite and biotite occurring beyond the limits of Jaduguda along the ore zone do not contain nickel. Pyrite occurring at central Jaduguda in the zone of uranium mineralization has been found to contain up to 2·4 p.c. of nickel. Cell-edge of this pyrite is of the order of $5{\cdot}415\pm0{\cdot}005$ Å. This high content of nickel in pyrite may be explained in two ways: (*a*) pyrite formed at high temperatures did not re-equilibrate with the falling temperature, since pyrite forming at 200 °C and below cannot have more than 0·5 p.c. nickel dissolved in it (Clark and Kullerud 1963); (*b*) minute grains of millerite included in pyrite gave this high value. Millerite appears and becomes the most important nickel mineral below 100 metre-level. It occurs as granular aggregates with occasional prisms and also fills the fractures in the associated pyrite grains. Millerite is replaced along margins and fractures by a mineral whose optical properties are closest to those of mackinawite (Fig. 11). The phase is too minute to be confirmed by X-ray analysis. Nickel in Jaduguda also occurs as pentlandite and its alteration product violarite along with the copper sulphides which occur mainly in the foot-wall side of the uranium lodes. These minerals do not appreciably contribute to the nickel values in the Jaduguda uranium ores.

Molybdenum occurs as molybdenite. Preliminary studies indicate the presence of rhenium in molybdenite in trace quantities (< 5 ppm).

It is interesting to note here that the assemblage of elements in the radioactive ores of the zone, particularly those of Jaduguda-Bhatin area, do not conform to any of the sub-types of the 'five-element' assemblage suggested by Schneiderhöhn (1955), but constitute a type of its own, i.e. hematitic *uranium-nickel-molybdenum ore*. Millerite, which is the principal nickel mineral here, is usually rare in multi-element uranium deposits.

Ore Genesis

Genesis of radioactive ores and with them nickel and molybdenum minerals at places along the shear zone poses a very interesting problem. For the convenience of discussion the problem may be divided into three parts: nature of the mineralization, source of the ore materials and the process of ore deposition.

The mineralization under discussion is epigenetic-hydrothermal. This is borne out by the mineralogy of the primary radioactive minerals, and that of the associated minerals of nickel and molybdenum, development of hematite-bearing cherty quartz and Na-oligoclase and also a small but observable amount of chlorite and sericite along the ore zone. Ore bodies often branch out and coalesce. Presence of cubic uraninite, xenotime and molybdenite suggests a moderate high temperature type of hydrothermal mineralization (cf. Kerr 1956, Heinrich 1958, Kotliar 1961). If the nickel-content in pyrite as reported in an earlier section is due to solid solution of NiS_2 in FeS_2 then the above conclusion will be corroborated by pyrite also. The fact that the zone of ore deposition coincides with the zone of a regional disjunctive structure (Singhbhum shear zone), when considered alone, may not get its full weight since the shear planes are also sub-parallel with the stratification in the host rocks and this latter fact may lead one to suggest that the mineralization is syngenetic sedimentary. But the observations noted above plus the mode of occurrence of uranium-nickel-molybdenum mineralization at Jaduguda (Fig. 2) will definitely suggest the mineralization to be hydrothermal-epigenetic in character.

Regarding the source of the ore materials opinions vary. According to Bhola and others (1966), the solutions for radioactive ore mineralization came from the soda granites occurring at different places along the zone, the soda granites having presumably been thought to be magmatic in origin as believed by Dunn and Dey (1942). Banerji (1962) on the other hand thought the soda granitic rocks to be migmatitic in origin and according to him the uraniferous minerals were partly indigenous to the migmatitic materials and were partly extraneous, having been derived from the shear zone rocks during migmatization. The author is in agreement with Banerji on that the soda granites along the shear zone are essentially of migmatitic (metasomatic) origin. But most of the uranium deposits along the zone are not closely associated with the soda granitic rocks and besides the host rocks of most of the deposits are any of biotite schists, chlorite-quartz schists and sericite-quartz-chlorite schists. These rocks are mostly derivatives of mafic volcanic rocks and they are known for their poverty of radioactive elements. Under such circumstances neither the migmatizing fluids nor the host rocks may be considered to have remarkably contributed to the formation of the radioactive ores. Solutions came from below.

The problem is further complicated by the deposition of molybdenite and nickel-bearing minerals in the zone of radioactive ore deposition. Vein deposits of molybdenum are thought to be genetically connected with a granitic (silicic) source while nickel should be related to a mafic or ultramafic one. According to Barsukov and others (1967) the source of such elements as nickel, cobalt, etc., in a complex uranium deposit is the mafic rock in the immediate neighbourhood of such deposits. Elements like nickel and cobalt, etc., are leached out of such a rock by the rising hydrotherm. Such an explanation may hold good for particular deposits but will be insufficient to explain all cases. For in Singhbhum shear zone alone there are places where the host rocks are equally mafic (if not more) as those of Jaduguda and there no mineralization of nickel has taken place. In Jaduguda a peridotitic intrusive occurs in the neighbourhood which might give out nickel on hydrothermal leaching. But no ultramafic rock has so far been located in the Bhatin area where nickel has been mineralized in almost the same intensity as in Jaduguda. The following suggestion is advanced to explain the occurrence of uranium and nickel in some deposits. Nickel goes into the structure of early silicates and excess, if there is any, will remain in solution. Uranium because of its large ionic radii is accommodated in only a few rock-forming minerals and the bulk of it accumulates in late solutions. So if at the source there is some excess of nickel or nickel is introduced at a late stage, that nickel will be accumulated along with uranium in the hydrothermal solutions.

Many of the uranium deposits of the world, particularly those accompanied by multi-element mineralization, are characterized by the deposition of hematite and apparent absence of pyrrhotite in the gangue as well as in the host rocks. As examples may be cited the deposits of Erzbirze in Germany; Cornwall in England; Gold-fields, Great Bear Lake, Lake Athabaska, Colorado, Front Range deposits in North America and the Myponga deposit in Australia (Rumbold 1954, Conybeare and Campbell 1951, Campana *et al.* in Heinrich 1958). Reddish hematitic albitization is, however, also prominent in Cobalt, Ontario, around calcitic veins of native silver and complex arsenides of cobalt and nickel (Thomson 1957). Reddish feldspathization with calcite and minor amount of chlorite and sericite is also conspicuous in the copper deposit of the Chilean Coast Ranges (Mayer and Hemley 1967). The common association of hematite with uraninite lead some workers to suggest that hematite in these cases may be product of oxidation of ferrous iron during probable reduction of U^{6+} to U^{4+} according to the following equation:

$$3H_2O + 2Fe^{2+} + [U^{6+}O_2]^{2+} = Fe_2O_3 + UO_2 + 6H^+$$

(McKelvey *et al.* 1956).

But, as has been noted above, occurrence of hematite is not exclusive to uranium veins though more frequent, and even in Jaduguda where the deposition of the mineral has been maximum in the zone it is found to occur below a certain depth (100 m level) in the ore body and elsewhere in the zone veins of hematitic cherty quartz and oligoclase have been found to occupy only very small parts of uranium lodes. A portion of the hematite formed together with uraninite but the bulk of it apparently preceded. These observations may be taken to suggest that the occurrence of hematite in the uranium deposits may, in general, have no 'cause and effect' relationship. Rather, they represent an association of minerals which are products of the same chemical environment, i.e. high oxidation potential. Where alkali/H^+ ratios were sufficiently high Na-feldspars formed in addition (cf. Mayer and Hemley, op. cit.). It is more likely that the precipitation of uraninite here took place in accordance with the other suggestion of McKelvey and others (op. cit.) which recommends precipitation of uraninite due to decrease in temperature, pressure or both.

During metasomatic introduction of nickel to chlorite and biotite the metal came in some form, soluble in an aqueous medium (hydrolysed chloride ?). But later, as the sulphur species in the solution increased, it precipitated in the form of sulphides.

Acknowledgements

The author is grateful to the late Prof. D. N. Wadia, Geological Adviser to the Government of India, for his kind permission to work in some of the mines and prospects of the Department of Atomic Energy and thankful to the field-officers of the Department (including UCIL) for their sincere co-operation. He is also grateful to Dr. T. N. Shadlun of the Academy of Sciences, U.S.S.R., Dr. A. S. Bhatnagar of the Physics Laboratory, D.A.E., and the Geological Survey of India for help during the study.

References

Banerji, A. K. (1962). *Econ. Geol.*, **57**, 50–71.

Barsukov, V. L., Belyayev, Yu I., Sergeyeva, E. I., and Sokolova, N. T. (1967). *Izv. Akad. Nauk. SSSR*, Ser. Geol., 8, 66–84.

Berman, R. M. (1957). *Am. Miner.*, 42, 705–28.

Bhattacharyya, T. K., Shankaran, A. V., and Shivananda, S. R. (1966). Contributions to the Geology of Singhbhum. Jadavpur University, 59–74.

Bhola, K. L. (1966). Abst. Papers, Symp. Base Metals, 56.

Bhola, K. L., Rama Rao, Y. N., Suri Shastri, C., and Mehta, N. R. (1966). *Econ. Geol.*, **61**, 162–73.

Clark, L. A., and Kullerud, G. (1963). *Econ. Geol*, **58**, 853–85.

Conybeare, C. E. B., and Campbell, C. D. (1951). *Am. Miner.*, **36**, 70–79.

Dunn, J. A., and Dey, A. K. (1942). *Mem. geol. Surv. India*, **69** (2).

Goldschmidt, V. M. (1937). *J. chem. Soc.*, 655–73.

Heinrich, E. Wm. (1958). Mineralogy and Geology of the Radioactive Raw Materials. McGraw-Hill, New York.

Karkhanavala, M. D. (1958). *Geochim. cosmochim. Acta*, **15**, 229–36.

Kerr, P. F. (1956). *Int. Conf. Peaceful Uses Atomic Energy*, **6**, 5–59.

Kotliar, V. N. (1961). Geologia Mestorozhdenii Urana. Gosgeoltekhizdat, Moscow.

Mayer, C., and Hemley, J. J. (1967). Geochemistry of Hydrothermal Ore Deposits. (Barnes, H. L., Ed.). Holt, Rinehart and Winston Inc., 167–235.

McKelvey, V. E., Everhart, D. L., and Garrebs, R. M. (1956). *Int. Conf. Peaceful Uses Atomic Energy*, **6**, 551–61.

Rumbold, R. (1954). *Min. Mag.*, **91**, 16–27.

Sarkar, S. C. (1966). Contributions to the Geology of Singhbhum (Deb, S., Ed.). Jadavpur University, 91–101.

Schneiderhöhn, H. (1955). Erzlagerstatten Kurzvorlesungen Zur Einfurung und zur Wiederholung. Gustav Fischer Verlag, Jena.

Suri Sastry, C. (1964). Symp. Uranium Prospecting and Mining in India, 126–33.

Thomson, R. (1957). Struct. Geol. Canad. Ore Deposits (II), 377–87.

Walker, G. W., and Osterwald, F. W. (1956). *Econ. Geol.*, **51**, 213–22.

A MINERALOGICAL STUDY OF SOME LITHIUM-BEARING MICAS OF INDIA*

by N. K. Rao *and* G. V. U. Rao, *Metallurgy Division, Bhabha Atomic Research Centre, Trombay, Bombay*

Chemical, optical and X-ray studies of fourteen lithium-bearing micas occurring in some pegmatites of Rajasthan and Bihar have been carried out. The lithia content of these micas varies from 0·50 to 5·00 per cent. The variation in N_α is from 1·537 to 1·567, in N_γ from 1·555 to 1·595, in $2V$ from 31° to 52° and in specific gravity from 2·67 to 2·83. The optical properties are, however, not systematically related to lithia content though micas rich in lithia have lower refractive indices.

Study of X-ray powder patterns of these lepidolites shows that twelve of them with lithia content ranging from 0·5 to 3·6 per cent have normal muscovite ($2M_1$) structure and only two having lithia content of 4·85 and 5 per cent have ($2M_2$) monoclinic lepidolite structure. These latter two are from Monghyr District, Bihar, and Jeevan Mines, Ajmer District, Rajasthan, respectively.

The study shows that in India lithium-bearing muscovites are much more common compared to true lepidolites. It is difficult to distinguish lithium-bearing muscovites from lepidolites without X-ray examination.

Introduction

Lithium containing micas are known to occur in pegmatites in different parts of India. In the absence of detailed optical, chemical and X-ray studies, they have been loosely referred to as lepidolites. It is known that in addition to lepidolites, a number of muscovites also contain appreciable amounts of lithia (Stevens 1938; Levinson 1953). In order to determine whether micas referred to as lepidolites in India are true lepidolites, chemical, optical and X-ray study of fourteen such mica samples from pegmatites of Bihar and Rajasthan was carried out. Lepidolites from the same locality are separated on the basis of their colour. Seven of these are from Jeevan Mines, Ajmer District, Rajasthan, and three from Monghyr District, Bihar. Localities of the other four samples are not known; probably they are from other pegmatites of Bihar and Rajasthan.

Preparation of Samples and Method of Study

Most of the samples were nearly pure. They contained small amounts of quartz and felspar, which are brittle and can be crushed more easily. The samples were crushed in an iron mortar by giving a few gentle strokes and

* Paper presented at the Symposium on Geology and Mineralogy of Atomic Minerals Deposits and their development for use in the Nuclear Power Programme in India held in New Delhi on 14-16 October, 1968, under the auspices of INSA. Convener: Prof. D. N. Wadia.

sieved through 100 mesh Tyler sieve. The finer fraction contained more of the brittle minerals. The process was repeated till the coarse fraction was free from quartz and felspar. Where the samples contained more of quartz, felspar and other minerals *lepidolite* concentrates were obtained by flotation using Armac 16D reagent at a *p*H of 3·4 (Madhavan *et al.* 1966) and purified by the above method. All the samples used in this study were of ~ 99 per cent purity.

The refractive indices were determined by the immersion method. γ and β were determined on cleavage flakes, while for determining α the following method was used. A drop of the appropriate liquid was placed on a glass slide. Observing the drop under the microscope, few flakes of the sample were dropped into the liquid with the help of a wet needle. Some of the flakes would remain vertical for a short time, from which α could be determined. This method was quite convenient where the mica flakes were thick. Where the flakes were very thin, a mixture of quartz grains (−70+100 mesh) and the sample was used. When the mixture was dropped into the immersion liquid some of the flakes adjacent to quartz grains would be nearly vertical and could be manipulated with the help of a fine needle. The specific gravity was determined with a specific gravity bottle using toluene. The $2V$ was determined using a Leitz 5 axis universal stage. Thick flakes of mica showing uniform first order yellow or higher order interference colours were found to be most suitable for the $2V$ determination. Some of the flakes showed uneven anisotropism and the $2V$ varied from place to place in the same flake. The $2V$ given in this paper is the average of at least ten determinations.

Results

The colour, refractive indices, specific gravity, $2V$ and Li_2O content of fourteen *lepidolites* studied are given in Table I. Eight of these showing wide variation in physical properties and Li_2O content were selected for complete chemical analysis. The chemical analyses of these are given in Table II.

From the chemical analysis the composition of the mica can be calculated and the normal method is to calculate the cationic proportions on the basis of 24(O, OH, F) anions (Deer *et al.* 1962). However, when considerable amount of H_2O^+ is present other modifications of this method are adopted (Hendricks and Ross 1941; Ganguly 1951; Brown and Norrish 1952).

In calculating the composition here, Brown and Norrish's method is adopted, as these micas contain considerable amount of H_2O^+. However, slight modification in their method has been found necessary as, in the present samples, the presence of F has also to be taken into account. The equations given by them are modified as follows:

$$\frac{4}{n}+3y = h+f \qquad \ldots\ \ldots\ \ldots\ \ldots \quad (1)$$

and

$$\frac{24}{n}+y=\Sigma O+f \quad .. \quad .. \quad .. \quad .. \quad (2)$$

where ny is the proportion of H_3O^+ ion in the composition, h, f and ΣO are the total atomic proportion of hydrogen, fluorine and oxygen respectively

TABLE I

Locality, physical and optical properties and Li_2O content of lepidolites

Code No.	Colour	Refractive Index			Specific gravity	$2V$	Li_2O content
Lp-1	Yellow	1·564	1·592	1·595	2·78	44°	0·50
Lp-2	Yellowish green ..	1·558	1·587	1·590	2·83	37°	0·90
Lp-3	Dark grey	1·552	1·577	1·578	2·76	33°	2·30
Lp-4	Dark greyish violet ..	1·545	1·567	1·569	2·80		2·65
Lp-5	Medium violet ..	1·547	1·568	1·569	2·64	44°	2·65
Lp-6	Pinkish violet ..	1·548	1·573	1·575	2·74	44°	2·65
Lp-7	Light violet	1·537	1·554	1·555	2·73	31°	5·00
Lp-8	Light violet	1·541	1·568	1·569	2·83	41°	3·60
Lp-9	Pinkish violet ..	1·546	1·565	1·567	2·76	46·5°	3·00
Lp-10	Medium violet ..	1·545	1·569	1·571	2·78	42°	2·95
Lp-11	Dark greyish violet ..	1·548	1·573	1·574	2·78	46·5°	2·60
Lp-12	White with violet tinge ..	1·548	1·571	1·572	2·66	45·5°	3·50
Lp-13	Pinkish violet ..	1·537	1·554	1·555	2·75	51°	4·85
Lp-14	Light violet	1·547	1·571	1·573	2·78	42°	3·25

N.B.—Lp-1 to Lp-7 are from Jeevan Mines, Ajmer District, Rajasthan; Lp-12 to Lp-14 are from Monghyr District, Bihar; localities of Lp-8 to Lp-11 are unknown.

TABLE II

Chemical analyses of lepidolites

Code No.	Lp-1	Lp-5	Lp-7	Lp-9	Lp-11	Lp-12	Lp-13	Lp-14
SiO_2	46·72	48·38	52·08	49·32	50·12	52·42	50·02	48·35
Al_2O_3	35·25	30·35	23·25	29·60	28·10	27·60	25·10	30·25
Fe_2O_3	0·71	0·94	1·10	0·57	0·16	0·29	0·29	0·86
FeO	1·07	1·00	—	—	—	—	—	—
MnO	0·39	0·78	0·67	0·72	0·83	0·67	1·33	1·00
Li_2O	0·50	2·65	5·00	3·00	2·60	3·50	4·85	3·25
Na_2O	0·33	0·33	0·33	0·66	0·45	0·70	0·33	0·33
K_2O	9·45	8·45	9·00	9·10	11·57	9·00	10·50	9·90
F	—	2·92	6·45	3·69	3·07	3·26	4·80	3·49
H_2O^+	5·14	5·48	5·07	4·49	4·54	4·10	4·60	4·06
H_2O^-	—	—	—	—	0·23	—	0·10	0·10
Total	99·56	101·28	102·95	101·15	101·67	101·54	101·92	101·59
$F = 0$	—	1·26	2·72	1·55	1·28	1·37	2·04	1·47
	99·56	100·02	100·23	99·60	100·49	100·17	99·90	100·12

TABLE III

Position in the structure	Ions	Lp-1		Lp-5		Lp-9		Lp-11		Lp-12		Lp-14		Lp-7		Lp-13	
Z	Si	6·20	8·00	6·22	8·00	6·30	8·00	6·48	8·00	6·62	8·00	6·19	8·00	6·47	8·00	6·38	8·00
	Al	1·80		1·78		1·70		1·52		1·38		1·81		1·53		1·62	
Y	Al	3·71	4·21	2·82	4·47	2·75	4·43	2·76	4·22	2·73	4·61	2·76	4·62	1·87	4·54	2·15	4·81
	Fe^{+3}	0·07		0·09		0·06		0·02		0·03		0·08		0·10		0·03	
	Fe^{+2}	0·12		0·11		—		—		—		—		—		—	
	Mn	0·04		0·08		0·08		0·09		0·07		0·11		0·07		0·14	
	Li	0·27		1·37		1·54		1·35		1·78		1·67		2·50		2·49	
X	Na	0·09	1·87	0·08	2·10	0·16	2·08	0·11	2·42	0·17	1·87	0·08	1·99	0·08	2·34	0·08	2·40
	K	1·60		1·39		1·48		1·91		1·45		1·62		1·35		1·71	
	H_3O^+	0·18		0·63		0·44		0·40		0·25		0·29		0·91		0·61	
OH,	OH	4·00	4·00	2·81	4·00	2·51	4·00	2·74	4·00	2·70	4·00	2·59	4·00	1·47	4·00	1·93	4·00
F	F	—		1·19		1·49		1·26		1·30		1·41		2·53		2·07	

as obtained from the chemical analysis, and n is the factor by which the atomic proportion of cations obtained from chemical analysis is to be multiplied to obtain the proportion in the unit formula.

The compositions calculated on this basis is given in Table III.

Chemistry of Lithium-bearing Micas and Lepidolites

The general formula which describes the chemical composition of micas is $X_2Y_{4-6}Z_8O_{20}(OH, F)_4$ where X is mainly K, Na, or Ca, Y is mainly Al, Mg, Fe or Li, and Z is mainly Si or Al.

When the number of Y ions is four, the mica is called di-octahedral and when it is 6, tri-octahedral. Muscovite is a typical di-octahedral mica, with only two-thirds of possible six octahedral positions (Y-sites) filled. Lithian muscovites and most of the lepidolites are in between di- and tri-octahedral in composition, and only those micas which contain above 5·5 per cent Li_2O have all their Y-sites occupied and are tri-octahedral.

From the chemical analyses and calculated composition, it can be seen that Lp-1 has a typical muscovite composition, and that others have composition in between di- and tri-octahedral micas. Based on the lithia content (Deer *et al.* 1962) only Lp-7 and Lp-13 can be classified under lepidolites, while others are only lithium-bearing muscovites.

Classified on the basis of $K^+ + Na^+$ content and H_3O^+ ions (Taboadela and Ferrandis 1957) Lp-5 comes under the category of hydromuscovites, while Lp-9, Lp-12 and Lp-14 approach the composition of hydromuscovites. Lp-11 is a lithium muscovite.

Lp-7 and Lp-13 only are lepidolites but they differ from normal lepidolites (Stevens 1938) in having excess of H_2O^+. Of these Lp-7 is decidedly deficient in ions of X-sites and this coupled with considerable amount of H_3O^+ in that position warrants its inclusion under the category of hydromicas; and, by analogy with hydromuscovites, may be termed hydrolepidolite. Lp-13 has a composition in between that of lepidolite and hydrolepidolite. Both these micas have $2M_2$ lepidolite structure and it may be mentioned here that occurrence of $2M_2$ hydromuscovite has been reported (Threadgold 1959).

X-ray Study—X-ray powder patterns of these micas show that all of them except Lp-7 and Lp-13 have normal $2M_1$ muscovite structure. According to Levinson (1953) muscovites can contain up to 3·3 per cent Li_2O without any change in the structure, and that above this lithia content a transitional structure occurs which is slightly different from normal $2M_1$ of muscovite. To this polymorph he proposed the term lithian muscovite. However, no such polymorph was observed in the case of Lp-12 and Lp-8, which have a Li_2O content of 3·5 and 3·6 per cent respectively. It is possible that the occurrence of lithian muscovite polymorph does not depend only on the Li_2O content, but

also on whether the Li ion is present in isomorphic replacement of Al in octahedral sites, or occupies the vacant octahedral sites in that structure, as in muscovites only two-thirds of octahedral sites are occupied.

The *d*-spacings of Lp-1, Lp-5 and Lp-12 along with that of $2M_1$ muscovite (Yoder and Eugster 1955) is given in Table IV. These three micas contain Li_2O per cent of 0·5, 2·65 and 3·50 respectively.

TABLE IV

X-ray d-spacings of $2M_1$ muscovite and lithium-bearing muscovites

$2M_1$ Muscovite (Yoder and Eugster 1955)		Lp-1 (0·5% Li_2O)		Lp-5 (2·65% Li_2O)		Lp-12 (3·50% Li_2O)	
d(Å)	I	*d*(Å)	I	*d*(Å)	I	*d*(Å)	I
10·04	> 100	10·60	VS	10·56	S	10·61	S
		9·63	VS	9·63	S	9·65	S
5·02	55	5·12	MS	5·10	M	5·10	M
		4·88	MS	4·90	M	4·90	M
4·48	55	4·47	S	4·45	S	4·46	S
4·46	65						
4·39	14						
4·30	21	4·27	VW				
4·11	14	4·15	VVW				
3·97	12	4·03	VVW	3·98	VW		
3·89	37	3·88	MW	3·89	W	3·88	W
3·74	32	3·72	W	3·71	W	3·70	W
3·50	44	3·46	MW	3·47	MW	3·53	MW
3·35	> 100	3·30	S	3·29	S	3·29	S
3·21	47	3·17	M	3·17	M	3·18	M
3·00	47	2·96	M	2·97	M	2·96	M
2·87	35	2·83	M	2·88	M	2·84	MW
2·80	22	2·77	M	2·77	M	2·76	W
2·59	50	2·57	VS	2·56	VS	2·57	VS
2·58	45						
2·56	90						
2·51	20	2·46	M	2·48	M	2·46	M
2·46	19			2·44	MW		
2·38	24	2·38	MW	2·37	M	2·39	M
2·247	12	2·25	W	2·25	W	2·25	W
2·149	10	2·13	M	2·13	M	2·13	M
2·132	23						
2·010	75	1·988	S	1·982	S	1·982	S
1·975	14	1·964	W	—		—	
1·670	12	1·660	MW	1·659	MW	—	
1·653	17	1·641	MW	1·645	M	1·647	MW
1·499	40	1·502	S	1·501	S	1·500	S

N.B.—In addition there are many very weak lines which are omitted from the list.

Lp-7 and Lp-13 have *d*-spacings similar to that of $2M_2$ lepidolite (Smith and Yoder 1956), which was earlier described as 6-layer monoclinic by Levinson (1953).

One important difference exists between powder patterns of micas reported herein and standard $2M_1$ and $2M_2$ micas. The basal reflections (002) at 10 Å and (004) at 5 Å are doubled; each of them made up of two reflections of equal intensity at 10·5 Å and 9·5 Å and 5·1 Å and 4·9 Å respectively. The hydrated nature of these micas is perhaps responsible for this feature.

The *d*-spacings of Lp-7 and Lp-13 along with that of $2M_2$ lepidolite given by Levinson (1953) are given in Table V.

TABLE V

X-ray d-spacings of $2M_2$ lepidolites

Lp-7		Lp-13		$2M_2$ Lepidolite (Levinson 1953)	
d(Å)	I	*d*(Å)	I	*d*(Å)	I
10·49	S	10·52	S	9·89	MS
9·46	S	9·45			
5·11	M	5·12	M	4·99	M
4·85	M	4·89			
4·45	S	4·48	M	4·49	M
3·92	VVW				
3·80	VW			3·84	W
3·67	VW				
3·60	MW	3·61	MW	3·61	M
3·46	W	3·48	W	3·47	M
3·28	M	3·28	M	3·31	M
3·19	M	3·18	MW	3·19	M
3·09	W	3·08	W	3·07	M
2·96	W	2·98	W		
2·85	MW	2·86	M	2·88	M
2·73	W	2·76	W	2·755	M
		2·66	VW		
2·57	VS	2·58	VS	2·572	VS
2·45	M	2·46	M	2·416	M
2·37	M	2·38	M		
2·24	W	2·25	W	2·248	VVW
2·20	W	2·19	VW	2·190	VVW
2·13	M	2·13	M		
2·02	M	2·01	M	2·039	VW
1·974	S	1·976	S	1·985	S
1·947	VW				
1·811	VW				
1·717	W	1·718	W		
1·690	VW			1·684	
1·642	W	1·645	W	1·633	VVW
1·503	M	1·501	S	1·506	M

Physical Properties

The refractive indices do not seem to be having any direct relationship with the Li_2O content. However, lepidolites and muscovites with high Li_2O content have lower refractive indices than muscovites and low lithia-bearing muscovites. $2V$ also is not related to the Li_2O content. The colour seems to be related to the ratio of $Fe^{+}+Fe^{+3}$ to Mn^{+2} in the composition; when the former dominates the colour will be shades of yellow, green, grey or brown, while muscovites and lepidolites with MnO have shades of violet colour.

Conclusions

The chemical and X-ray study of fourteen samples of so-called *lepidolites* of India show that twelve of them are only lithia-bearing muscovites ranging in lithia content from 0·5 to 3·6 per cent. Only two of them having lithia content of 4·85 and 5·00 per cent are true lepidolites. Further, most of these lithia-bearing micas contain appreciable amount of constitutional water and are deficient in interlayer ions—i.e. alkalies. The physical properties do not show any appreciable variation with the lithia content of the micas.

Acknowledgements

The authors' thanks are due to Dr. K. K. Majumdar, Head, Ore Dressing Section, B.A.R.C., Bombay, and Dr. V. K. Moorthy, Head, Metallurgy Division, B.A.R.C., Bombay, for their sustained interest in this investigation. Thanks are also due to Dr. M. Sankar Das, Head, Analytical Division, B.A.R.C., Bombay, for chemical analysis and Mrs. Uma Nayak for help in X-ray study.

References

Brown, G., and Norrish, K. (1952). Hydrous micas. *Min. Mag.*, **29**, 929–932.

Deer, W. A., Howie, R. A., and Zussman, J. (1962). Rock forming minerals, **3**, Sheet Silicates, Longmans.

Ganguly, A. K. (1951). Hydration of exchangeable cations in silicate minerals. *Soil Sci.*, **71**, 239–244.

Hendricks, S. B., and Ross, C. S. (1941). Chemical composition and genesis of glauconite and caledonite. *Am. Miner.*, V. **26**, 683–708.

Levinson, A. A. (1953). Studies in the mica group: Relationship between polymorphism and composition in the muscovite lepidolite series. *Am. Miner.*, **38**, 88–107.

Madhavan, T. R., Viswanathan, K. V., and Majumdar, K. K. (1966). Beneficiation of lepidolite ores. *Trans. Indian Inst. Metals*, **19**, 224–226.

Smith, J. V., and Yoder, A. S. (1956). Experimental and the critical studies in the mica polymorphs. *Min. Mag.*, **31**, 209–235.

Stevens, R. E. (1938). New analyses of lepidolites and their interpretation. *Am. Miner.*, **23**, 607–628.

Taboadela, M. M., and Ferrandis, A. V. (1957). The mica minerals in 'The Differential Thermal Investigation of Clays' (Mackenzie: ed.), pp. 165–190.

Threadgold, I. M. (1959). A hydromuscovite with the $2M_2$ structure from Mount Lyell, Tasmania. *Am. Miner.*, **44**, 488–494.

Yoder, H. S., and Eugster, A. P. (1955). Synthetic and natural muscovites: *Geochim. cosmochim. Acta.* **8**, 225–280.

DETRITAL ZIRCON FROM RANCHI-PURULIA AREA*

by N. P. Subrahmanyam *and* G. V. U. Rao, *Ore Dressing Section, Metallurgy Division, Bhabha Atomic Research Centre, Trombay, Bombay 85*

Inland placer deposits have been discovered recently over an extensive area in the older alluvium capping the peneplaned surfaces of Archaean shield in Ranchi and Purulia districts. The biggest deposit is near Katahaldih. Microscopic and statistical studies of detrital zircons from the locality show that 43 per cent show zoning, 8 per cent show overgrowths, outgrowths, aggregates and 2 per cent show rare types of twinning.

The elongation ratio (l/b) of 52 per cent of the grains is 1 to 2, of 47 per cent of the grains is 2 to 4 and of 1 per cent of the grains is 4. The elongation frequency maximum is 2·0. These zircons are stubby compared to zircons derived from igneous granites, whose elongation frequency maximum is about 2·5.

A wide variety of overgrowths, outgrowths, aggregates and twins observed are described in detail.

The high proportion of stubby and metasomatically transformed zircons indicates that the porphyritic granites of Ranchi-Purulia area, from which these zircons are derived, are either autochthonous or parautochthonous but not igneous in origin.

Introduction

The inland placers of Ranchi-Purulia plateau cover some six hundred square kilometers and contain rich concentrations of heavy minerals. The heavy mineral content of these placer deposits varies from 2 to 10 per cent and some rich sands contain monazite (1 to 0·45 per cent), ilmenite (1·10 to 0·46 per cent), zircon (0·40 to 0·04 per cent), rutile (0·20 to 0·89 per cent), sillimanite (1·00 to 0·06 per cent) and magnetite (0·27 to 0·09 per cent). A sample was obtained from such a placer deposit near the village Katahaldih (Lat. 23° 26′ 45″ ; long. 86° 13′ 00″), Purulia district, West Bengal. Zircons have been separated from this sample and microscopic studies have revealed that these zircons contain a high proportion of zoned crystals, outgrowths, overgrowths, aggregates, interpenetration twins and a limited variety of other twins.

Geology of the Area

The bed rock in this region forms part of the Chota-Nagpur gneisses. Though in recent maps (G.S.I. 1962) it was shown as forming part of the Chota-Nagpur gneisses, in the older maps a porphyritic granite was marked separately in this area extending for many miles westwards from the town of Purulia into Ranchi district (Ball 1881).

---

* Paper presented at the Symposium on Geology and Mineralogy of Atomic Minerals Deposits and their development for use in the Nuclear Power Programme in India held in New Delhi on 14–16 October, 1968, under the auspices of INSA. Convener : Prof. D.N. Wadia.

Large placer deposits of heavy minerals have been located in this belt. Porphyritic granites and the associated quartzo-felspathic bands are the primary source of these deposits. The heavy minerals derived by the disintegration of parent rocks have accumulated in the alluvium in the immediate vicinity of the sources rocks. This alluvium is laid down in the now extinct shallow sluggish streams which have apparently carried away the light minerals (Shirke and Chatterji 1958).

METHOD OF STUDY

From the heavy mineral concentrate, zircon has been isolated by employing electrostatic separator, isodynamic separator and finally by heavy media separation. Zircon concentrate of 99 per cent purity thus obtained has been systematically sampled and microscopic studies have been made on 400 grains of zircon.

DESCRIPTION OF ZIRCONS

(i) *Colour*

The zircons are mostly colourless though a few of them are brownish and greyish.

(ii) *Habit*

The zircons contain a mixture of angular (4 per cent), semi-rounded (30 per cent) and rounded (66 per cent) grains. In the angular crystals, prismatic faces are normally *predominating* but in a few crystals pyramid or pinacoidal faces are predominating over the prismatic faces (Fig. 1).

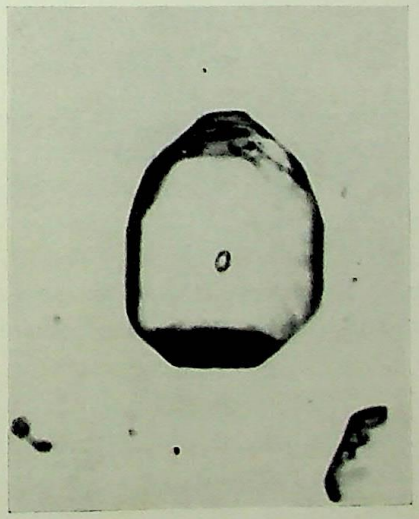

FIG. 1. Zircon with pinacoidal faces well developed (×230).

Statistical studies of these zircons show that they vary in length from 0·075 mm to 0·400 mm, their mean length being 0·163 mm. Their breadth varies from 0·050 mm to 0·163 mm, their mean breadth being 0·080 mm. Their elongation ratio (l/b) is varying from 1 to 4·2, 52 per cent of them being slightly elongated (l/b, 1–2), 42 per cent being moderately elongated (l/b, 2–4) and 1 per cent highly elongated (l/b, >4). These zircons have an elongation frequency maximum at 2·0 (Fig. 2).

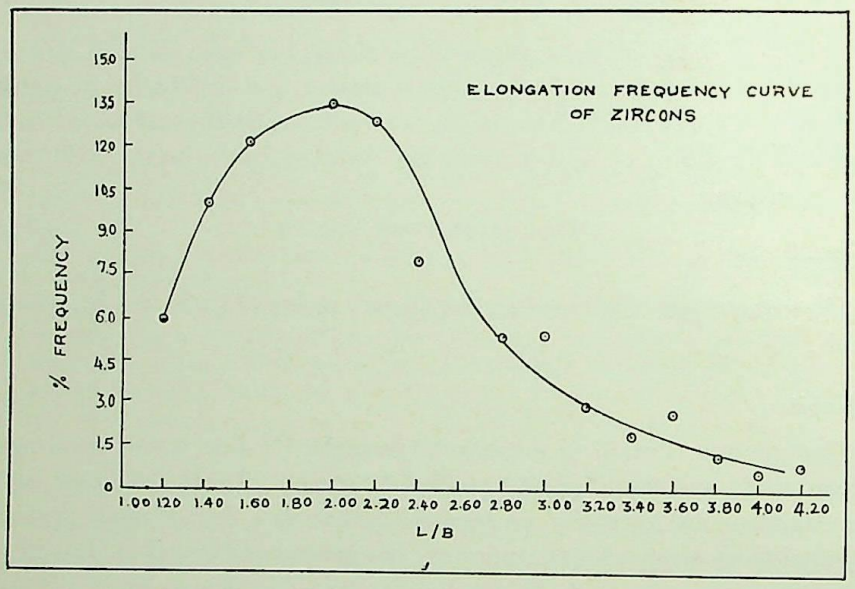

FIG. 2. Elongation frequency curve of Ranchi-Purulia zircons.

(iii) *Inclusions*

The following inclusions have been noted in the zircons (*a*) spherical and ovoid cavities, some of them gas-filled and others partially filled with liquid, (*b*) magnetite, (*c*) ilmenite, (*d*) some reddish-brown isotropic opaques, (*e*) monazite, (*f*) euhedral zircons and in some cases small-zoned zircons, (*g*) rutile, (*h*) tourmaline and (*i*) some dusty inclusions. Though preferred orientation is not found normally, in a few cases the inclusions are oriented parallel to the elongation of zircon and sometimes they are arranged zonally.

(iv) *Microfractures*

Longitudinal and diagonal cracks are observed in some of these zircons. In a few cases the cracks are radiating from the centre of the crystal with dusty inclusions. In such zircons the central portions seem to be metamict and isotropic whereas the outer zoned shells are anisotropic. The cracks are also radiating from monazite and some other opaque mineral centres.

(v) *Zoning*

Zoning is one of the most conspicuous features of these zircons. Zoning is observed in 43 per cent of these zircons which is a high proportion compared to other assemblages of zircons found in India (Rao and Rao 1968). It is observed that more bands of fine zoning are seen when the vertical crystallographic axis is placed parallel to the vibration direction of the lower nicol, showing that, though the N_O is the same for all the zones, N_E is slightly varying. From this it appears that there was variation in the composition of the mother liquor, as the zircon crystals grew, resulting in abrupt changes in the composition of the crystallizing zircon such that the N_O is the same in all zones but N_E showing a distinct range of values. Normally, all the zones of zircon are oriented in the same direction but a rare zircon has been found in which the successive zones are slightly differing in their orientation giving rise to a small core which is not extinct at any position.

(vi) *Outgrowths and Overgrowths*

A relatively high proportion of the zircons (nearly 8 per cent) is showing growth phenomena such as outgrowths, overgrowths, aggregates and fused crystals. Outgrowths are to be found mostly on prismatic or pyramidal planes of semi-rounded crystals and in some cases on perfectly rounded crystals. The outgrowths are mostly pyramidal, but some rounded outgrowths are

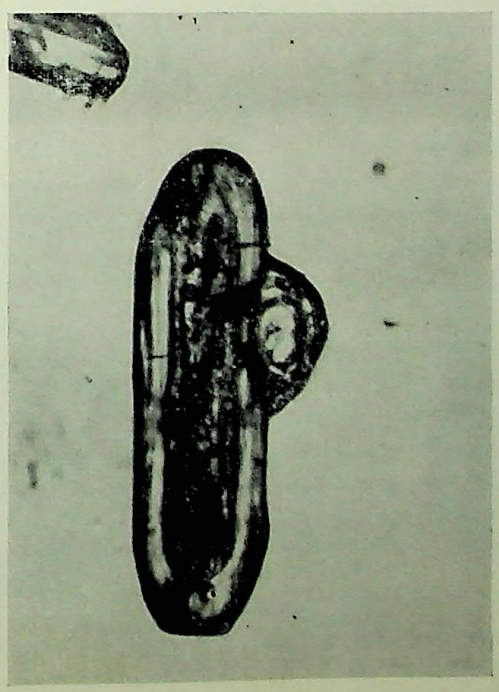

FIG. 3. Round outgrowth on euhedral crystal (×230).

also observed (Fig. 3). Almost all the outgrowths have the same orientation as the host mineral. A large number of overgrowths are also present in which the cores are mostly rounded grains. Aggregates of zircons are also found in this assemblage. Normally they are attached parallelly on 110 planes in two's and three's (Figs. 4, 5) but aggregation on 111 plane is also observed.

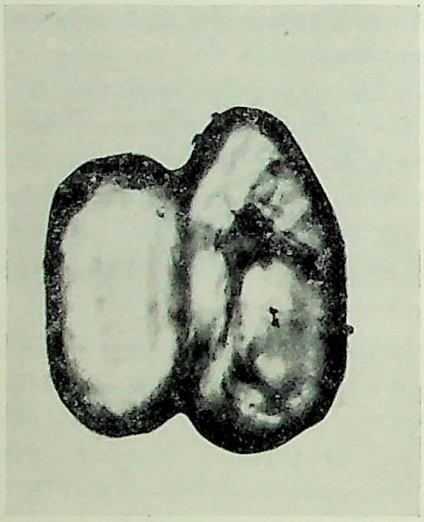

FIG. 4. Parallel aggregate of two zircons on prismatic faces (× 230).

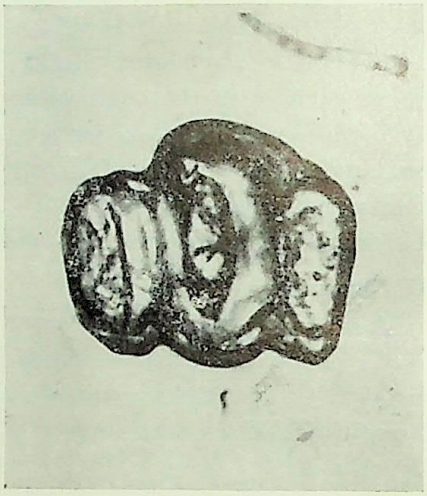

FIG. 5. Parallel aggregate of three zircons on prismatic faces (× 230).

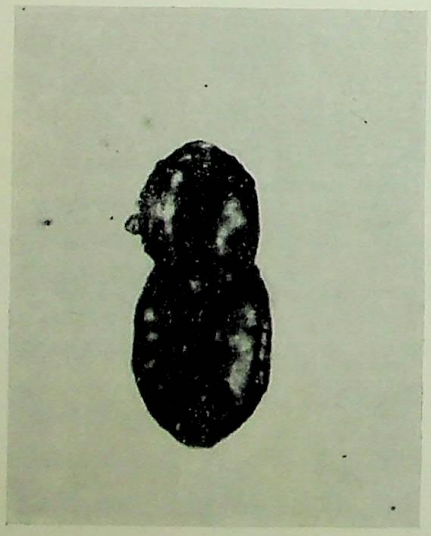

FIG. 6. Dumb-bell-shaped fused crystal of zircon (× 230).

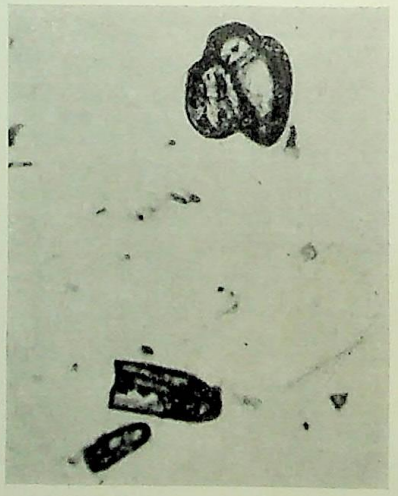

FIG. 7. A fused aggregate of zircon (× 110).

In addition to these types of growth phenomena, dumb-bell-shaped crystals (Fig. 6) and various types of fused aggregates of zircons with the same orientation are also observed (Fig. 7).

(vii) *Twinning*

A relatively moderate proportion of zircons, nearly 2 per cent of them, are showing a variety of twins. A rare case of interpenetration twin of zircon has been observed (Fig. 8), with the components of the twin getting extinct at the same position. In addition to the common geniculate twin with the composition plane (101), twins with (301) and (001) as composition planes are observed (Fig. 9). Twins with composition planes (001) and (301) are found to be comparatively more frequent than the geniculate twins.

Discussion

The sizes and elongations of a sample of self-nucleated, free-growing crystals depend upon their physico-chemical environment. Shortly after its emplacement, and before the crystallization of the main constituent minerals, physico-chemical conditions may be expected to be nearly uniform throughout a magmatic pluton. Because of the short range of crystallization of zircon, the environmental uniformity in all parts of the pluton during emplacement is likely to be reflected in the uniformity of sizes and elongation of zircons. Thus, the study of these parameters provide 'tracers' to the earliest magmatic conditions (Larsen and Poldervaart 1957). By virtue of their crystallization from a magma, elongation frequency curves of zircons from intrusive granites show a maximum at an elongation ratio greater than 2·0 (around 2·5). Zircons from sediments on the other hand are frequently rounded and elongation curves show the maximum at an elongation ratio less than 2·0 (around 1·5). Static granites, formed *in situ* by ultrametamorphism of such sediments, show an intermediate elongation frequency maximum and also show evidence of recrystallization of the rounded crystals to the well-formed magmatic zircons (Poldervaart 1950). In the formation of autochthonous granites, zircons exhibit growth phenomena such as outgrowths, aggregate crystals and overgrowths. A high proportion of zircons with such growth phenomenon is considered as a convincing laboratory evidence of Reads' granite series (Poldervaart and Ekelmann 1955).

The Katahaldih zircons show all the evidence of metasomatic transformation and recrystallization, zoning is observed in 43 per cent of zircons. Outgrowths, overgrowths, aggregates and fused crystals of various shapes have been observed in 8 per cent of zircons. Rare types of twins are observed in 2 per cent of these zircons. Normally in igneous granites a majority of zircons will be moderately elongated (1/*b*, 2–4), but in these zircons 52 per cent are slightly elongated (1/*b*, 1–2) and only 47 per cent are moderately

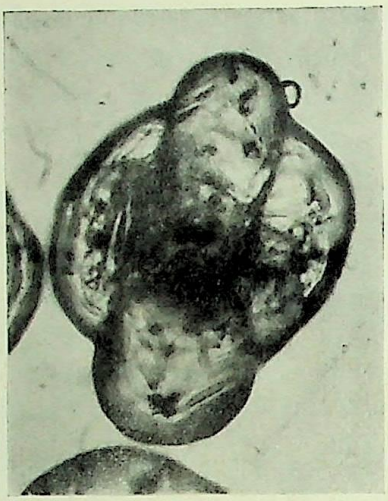

FIG. 8. Interpenetration twin of zircon (×500).

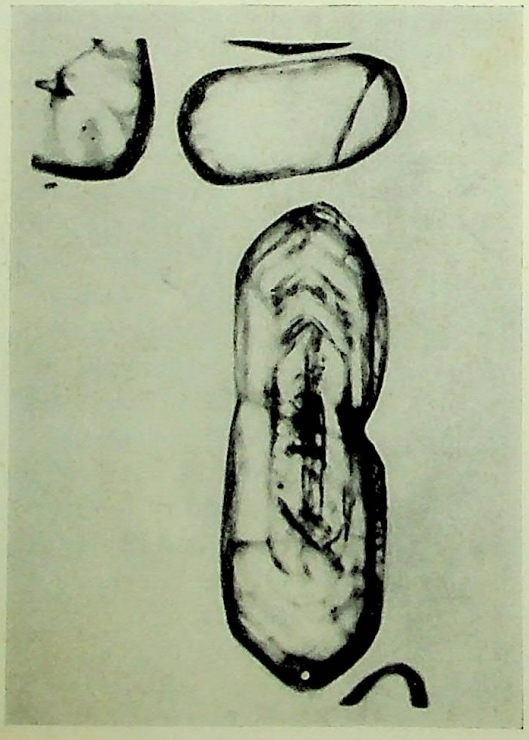

FIG. 9. Twinned zircon with pinacoidal composition plane (×230).

elongated. Their elongation frequency maximum is at 2·0. Such high porportion of metasomatically transformed zircons and their stubby habit is a convincing evidence to show that the porphyritic granites of Ranchi-Purulia area are granites formed *in situ* by the ultrametamorphism of earlier formed sediments.

Conclusions

From the high proportion of metasomatically transformed zircons and their stubby habit compared to zircons derived from normal igneous granites, it has been concluded from laboratory evidences that the porphyritic granites of Ranchi-Purulia area are probably static granites but not igneous in origin. They may be either autochthonous or parautochthonous granites.

Acknowledgements

The authors' sincere thanks are due to Dr. K. K. Majumdar, Head, Ore Dressing Section, and to Dr. V. K. Moorthy, Head, Metallurgy Division, Bhabha Atomic Research Centre, for their interest in the work.

References

Ball, V. (1881). *Memoirs geol. surv. India*, 18, 35–38.

G.S.I. (1962). Geological map of India (sixth edition).

Larsen, L. H., and Poldervaart, A. (1957). Measurement and distribution of zircons in some granitic rocks of magmatic origin. *Mineralog. Mag.*, 31, 544–564.

Poldervaart, A. (1950). Statistical studies of zircons as a criterion in granitization. *Nature*, 165, 574–575.

Poldervaart, A., and Ekelmann, F. D. (1955). Growth phenomena in zircon of autochthonous granites. *Bull. Geol. Soc. Am.*, 66, 947.

Rao, N. K., and Rao, G. V. U. (1968). Unpublished paper.

Shirke, V. G., and Chatterji, B. D. (1958). Monazite sands of Bihar and West Bengal. U.N. Conference on Peaceful Uses of Atomic Energy, 2, 713.

A NOTE ON THE OCCURRENCE OF RADIOACTIVE ALLANITE IN THE BIVANGAON-KANSA AREA, DISTRICT BOLANGIR, ORISSA*

by R. N. Bose,† B. R. Dash *and* L. M. Das, *Geological Survey of India, 4 Prag Narain Road, Lucknow (U.P.)*

While conducting systematic geophysical surveys for lead ores in the Saintala area during the season 1966–67, the occurrences of allanite at Bivangaon (20° 25′ 18″: 83° 21′ 03″) and Kansa (20° 22′ 56″: 83° 22′ 24″) were examined. This roused further interest and a preliminary survey with a portable Geiger counter was carried out. A short account of this survey and the results of chemical analysis of a few samples have been presented in this paper.

Occurrence of Allanite

The area under investigation lies in the Eastern Ghat Pre-Cambrian belt. The essential rock types are those of the khondalite series, which include garnetiferous graphite-sillimanite schists, quartzites and associated calc-granulites. Granitic rocks are also met with in the area (Jayaram 1959). The two occurrences, respectively, at Bivangaon and Kansa (Fig. 1), are separated from each other by a distance of about 5 km. in a N.W.-S.E. direction, the prevalent direction of strike of the rock formations in the area.

The occurrence near Bivangaon is located in a paddy field at a distance of about 570 m. from the village in a S35°W direction. Small patches of khondalitic rocks are observed at various distances. No quartz or pegmatite veins are seen in the immediate vicinity, though exposures of granitic rocks can be seen at a distance of half a kilometre to the west. The mineral occurs in big lumps associated with fluorite and calcite. It is dark brown in colour having a resinous/greasy lustre and a subconchoidal fracture. Crystalline and tabular forms are also seen. The occurrence appears to extend in a N55°W–S55°E direction.

Small boulders of allanite strewn sparsely on the ground are seen near Jampodor (20° 25′ 10″: 83° 20′ 55″) at a distance of about 300 m. from the occurrence at Bivangaon.

The occurrence at Kansa is located in a khondalitic country at a distance of about one kilometre to the north-west of the village and apparently extends in the N55°W–S55°E direction. Calcite appears to be the dominant mineral

* Paper presented at the Symposium on Geology and Mineralogy of Atomic Minerals Deposits and their development for use in the Nuclear Power Programme in India held in New Delhi on 14–16 October, 1968, under the auspices of INSA. Convener: Prof. D. N. Wadia.

† *Present address:* Geophysics Division, Geological Survey of India, 150 Maredpalli, Secunderabad 26.

that occurs as large rhombohedral crystals strewn all over the surface. Fluorite is scarce. Allanite also is not very frequent, reportedly the same was removed by some local enterpriser. In the hand specimen the mineral is seen in long and slender crystals of deep brown colour; medium to fine-grained varieties in lumps are also seen.

Fig-1

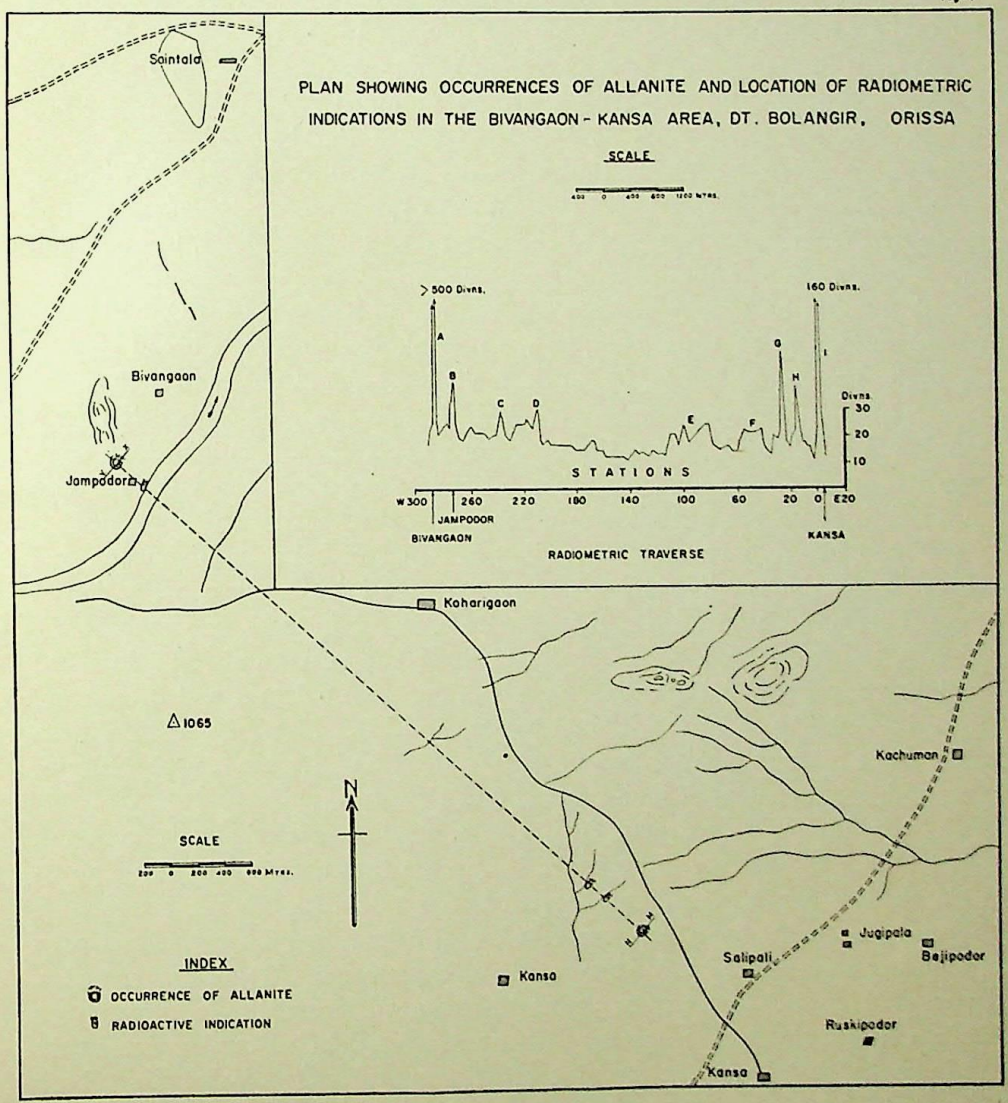

FIG 1

RADIOMETRIC SURVEY

The instrument used for the survey was a portable Geiger counter (type GM 100A) manufactured by the Trombay Electronic Instruments. About 60

counts of radiation per minute corresponding to 10 divisions of the 'High' sensitivity range of the instrument was the background value for the area.

The survey was carried out on a reconnoitory basis to study the response over the known occurrences and to decipher the sub-surface disposition of the bodies. In all 10 traverses laid at intervals of 10 m. with stations spaced at 10 m. were observed over the Bivangaon occurrence. Very encouraging indications were obtained, the radiations measured were beyond the full scale of the instrument. The observed rate of counts was more than 30 times the background (Fig. 2). Based on the data obtained from the traverses and taking into account counts at least two times the background, a radioactive zone extending about 100 m. in the strike direction with a width of 80 m. could be demarcated. A vertical force torsion magnetometer was used to study the magnetic response of the mineral and its associates, but no significant indication was obtained.

A number of traverses were observed in the Kansa area. On the same considerations as at Bivangaon, it was possible to delineate a broad zone of radiation measuring 300 m. by 60 m. including isolated points of high radiation. In this locality, however, a relatively lower rate of counts, having a maximum of about 11 times the background (Fig. 2), was obtained, as compared to that at Bivangaon. Observations taken inside the village Kansa also indicated a rate of radiation much above the background.

Fig. 1 shows a traverse extending over 5 km. between Bivangaon and Kansa over which radiometric observations were taken. An examination of the profile unfolds two distinctly separate areas of interest, one each at the Bivangaon and Kansa ends. Each of these shows a number of localized radiation maxima. In the Bivangaon end, two such points A and B are seen, with a possibility of two additional points C and D. Similarly, in the Kansa area, three distinct maxima can be seen at G, H and I, with a probability of two additional centres of interest at E and F.

Near Jampodor, at point B in Fig. 1, small pieces of allanite are seen scattered on the surface, from which it appears that the actual body may lie at a shallow depth. In fact, the entire zone extending from Bivangaon to beyond Jampodor for a distance of about 1·5 km. may be considered as a promising zone meriting further intensive exploration. At the other end a zone of over 1·5 km. extending north-westwards from the occurrence at Kansa constitutes the second zone of interest for detailed exploration work. It is likely, that in the intervening areas, low radiometric values have been obtained, because of the presence of a relatively thick soil cover.

Mineralogical Studies

A few samples of allanite were examined in the Central Petrological Laboratory of the Geological Survey of India. Ore microscopic studies show

that the bulk of the material comprises allanite. Veins of calcite, platy allanite and crystals of fluorite are also found. Traces of graphite are also

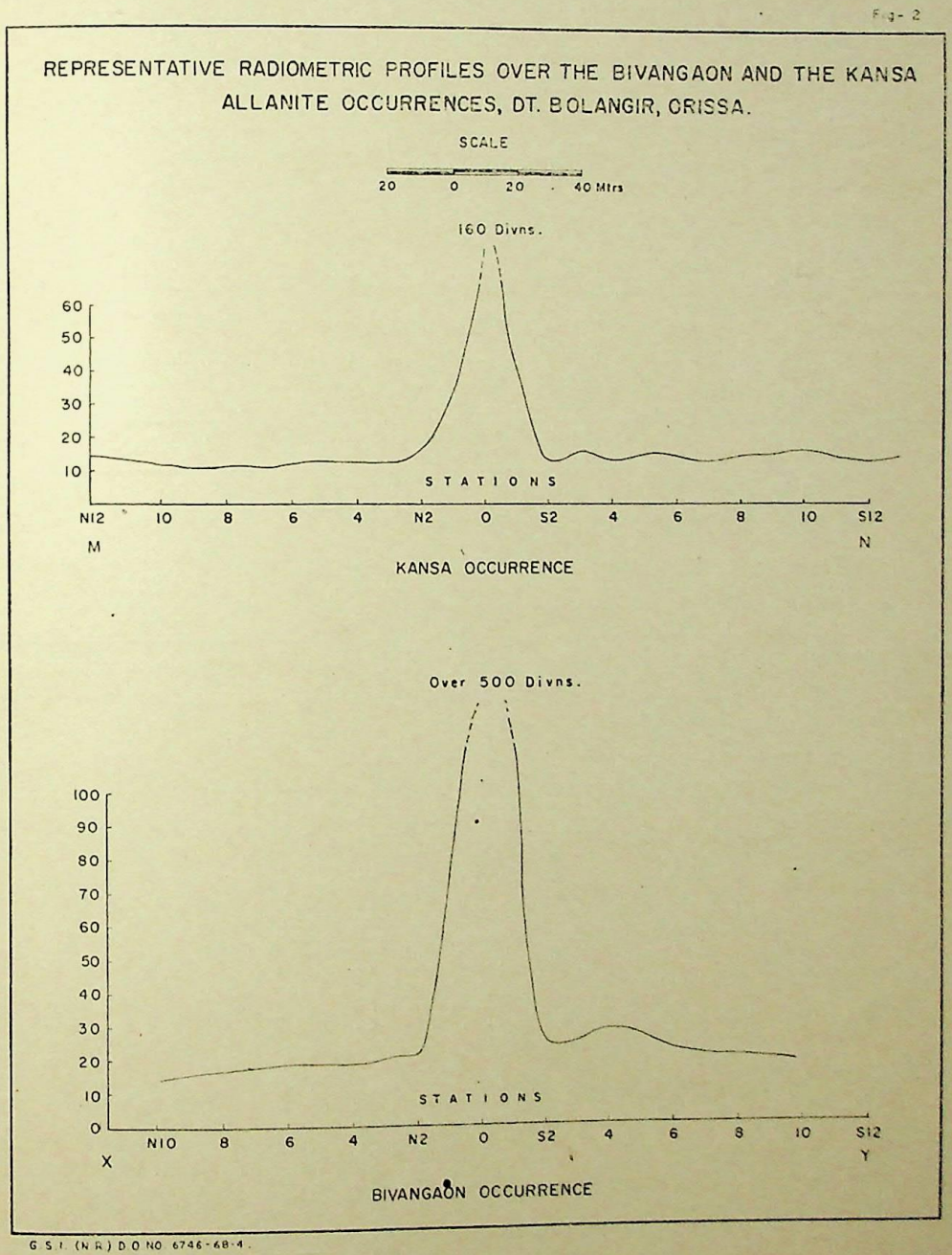

FIG. 2

seen. The specific gravity of the bulk sample is 3·35 and that of the pure allanite 3·455. It shows distinct radioactivity, which was measured as 300 counts per second at 1,360 volts in the contamination monitor. Autoradiograph shows positive indications of radioactivity.

Under the microscope, the mineral shows euhedral habit occurring in the form of elongated crystals. Occasional twinning is observed; one set of imperfect cleavage can be seen. Pleochroism is observed as follows:

X = pale greenish yellow
Y = pale greenish brown
Z = brown
$X \wedge c = 40°$

The mineral gelatinizes with moderately strong HCl.

Chemical Analysis

Percentages of uranium and ThO_2 as determined in five samples of allanite are as follows:

Sample No.	Locality	% Uranium	% ThO_2
1 B	Bivangaon	0·06	Trace
2 B	,,	0·04	0·10
3 B	,,	0·06	0·26
1 K	Kansa	0·05	0·35
2 K	,,	0·03	0·28

The allanite from Bivangaon has possibly a higher uranium content whereas the samples from Kansa have a higher ThO_2 content.

The results of complete chemical analysis of one sample of allanite from Kansa are presented below:

SiO_2	32·60
TiO_2	0·94
Al_2O_3	18·91
FeO	9·71
Fe_2O_3	3·58
MnO	Tr.
CaO	10·69
MgO	1·66
K_2O	0·58
Na_2O	0·01
ThO_2	0·40
Ce_2O_3	3·35
Rare earth oxides less ceria	13·84
P_2O_5	Tr.
Loss on ignition	2·90
	99·17

(The chemical analyses were carried out in the Chemical Laboratory of the Geological Survey of India, Calcutta)—U_3O_8 not estimated.

Conclusion

In the light of the findings of the preliminary radiometric survey it appears likely that all the occurrences and indications obtained between villages Bivangaon and Kansa belong to one belt. It is significant that the allanite contains 0·03 to 0·06 per cent of uranium.

It will be worth while to carry out detailed exploration work to determine the extent of allanite mineralization in the area. It is necessary to assess the actual grade of the ores to study the possibility of commercially exploiting the deposits for uranium and thorium.

Acknowledgements

The authors are thankful to Shri P. C. Hazra and Shri C. Karunakaran, Deputy Director Generals, Geological Survey of India, for their encouragement in this work. Their thanks are due to Dr. G. Basu Chowdhury of the Chemical Division, G.S.I., for the chemical analyses of the samples. The authors are also thankful to the Director General, Geological Survey of India, for his kind permission to publish the paper.

Reference

Jayaram, B. N. (1959). A note on the preliminary investigations of the reported occurrences of lead ores in the Saintala Thana area, Bolangir-Patna district, Orissa (unpublished report of the Geological Survey of India).